Simulating the thermal regime and ice mass balance in blocky terrain in mountain environments

Cas Renette

Thesis submitted for the degree of
Master in Hydrology and Glaciology
60 credits

Department of Geosciences
Faculty of mathematics and natural sciences

UNIVERSITY OF OSLO

Spring 2022

Simulating the thermal regime and ice mass balance in blocky terrain in mountain environments

Cas Renette

Simulating the thermal regime and ice mass balance in blocky terrain in mountain environments

http://www.duo.uio.no/

Printed: Reprosentralen, University of Oslo

Abstract

Ground temperatures in coarse, blocky deposits such as in mountain blockfields and rock glaciers have long been observed to be lower in comparison with other (sub)surface material. One of the reasons for this negative temperature anomaly is the lower soil moisture content in blocky terrain, which decreases the duration of the zero curtain in autumn and can introduce a zero curtain in spring. Many permafrost modelling studies did not include varying water and ice contents. In this thesis, the CryoGrid community model is used to simulate the effect of drainage in blocky terrain on the ground thermal regime and ground ice at two Norwegian mountain permafrost sites and at three ancillary sites in the global permafrost extent. Three idealized stratigraphies are used to investigate thermal anomalies under different amounts of snowfall. The stratigraphies are labeled *blocks only, blocks with sediment* and *sediment only* and are either *drained* or *undrained* of water, resulting six 'scenarios'. The model setup features a surface energy balance, heat conduction and advection, a bucket water scheme with a lateral drainage component and (an adaptation of) the CROCUS snow scheme.

The results show markedly lower ground temperatures in the *blocks only, drained* scenario compared to all five other scenarios. A sensitivity analysis to snowfall results in a thermal anomaly is up to 1.5 °C at the sites in Norway for scenarios with relatively high snowfall amounts and up to 3.5 °C at a continental site in northern Siberia. The effect almost vanishes when no persistent ground ice is present. Stable permafrost conditions are simulated at the location of a rock glacier in northern Norway with a mean annual ground surface temperature (MAGST) of 2.0-2.5 °C in the *blocks only, drained* scenario. Other scenarios under the same climate forcing feature positive ground temperatures. At the location of a blockfield in southern Norway, it is shown that stable permafrost can be present in the *blocks only, drained* scenario even under an extremely thick snowpack. Under (semi-) arid conditions, the rate and timing of subsurface drainage is also strongly affected by the ground stratigraphy. The drainage starts earlier in summer, continues longer in autumn and is of higher magnitude in the *blocks only* stratigraphy, compared to *blocks with sediment* stratigraphy. Finally, transient simulations at the rock glacier site in northern Norway showed a complete or partial lowering of the ground ice table since 1951 for all scenarios except for the *blocks only, drained* scenario.

The drainage effect that was simulated herein helps explain the occurrence of permafrost in coarse, blocky terrain below the assumed elevational limit of permafrost. It is thus important to consider this effect in future permafrost distribution mapping and thermal modelling. An accurate prediction of the evolution of the ground ice table in a future climate has implications for slope stability as well as water sources in arid environments.

Acknowledgements

Fist, I would like to thank my supervisor Sebastian Westermann for the help on all aspects of this thesis. You gave the initial idea for the research and helped me become a (somewhat) independent user of CryoGrid. All our meetings, mostly on Zoom, were extremely useful and always gave me plenty to think about and work on. It was great to be part of the ITCH in November 2021, though unfortunately it was online.

Thanks also to Juditha Aga for all the (MATLAB) tips and for having me as field assistant in northern Norway. As I was unable to plan fieldwork for my own thesis, it was great to get a sense of the mountain permafrost environment as field assistant.

Furthermore, big thanks to Kristoffer Aalstad for spending many hours, especially at the start of my thesis, on helping me request, download, merge, downscale and convert climate data so I could start the modelling work. Also thanks for being a talented teammate during the few times I joined Geo-Football.

I also want to thank my parents, who treated me like a hotel guest during my visit in the latter stages of my thesis to make sure I could focus on reaching the finish line.

Finally, the biggest thanks to Anna, who at all times supported me with planning, structuring, putting everything in perspective and just being the best distraction when needed. You can be proud of all the colours I put in the figures!

Contents

1 Introduction

1.1 Permafrost in the global context

Permafrost is defined as ground that remains at or below 0 °C for two or more consecutive years (French 2007). Permafrost is overlain by the active layer – the zone of soil which thaws during the summer and refreezes during the winter. Permafrost underlays 24% of the landmass in the Northern Hemisphere and is therefore a key element in the cryosphere (T. Zhang et al. 2000). Permafrost is associated with cold climates and is common in high-latitude and high-altitude environments. Different zones are classified based on the aerial extent of permafrost presence. These regions are: continuous, discontinuous, sporadic and isolated, where the surface in underlain by permafrost in more than 90%, 50-90%, 10-50% and less than 10% of the land area respectively (Smith and Riseborough 2002).

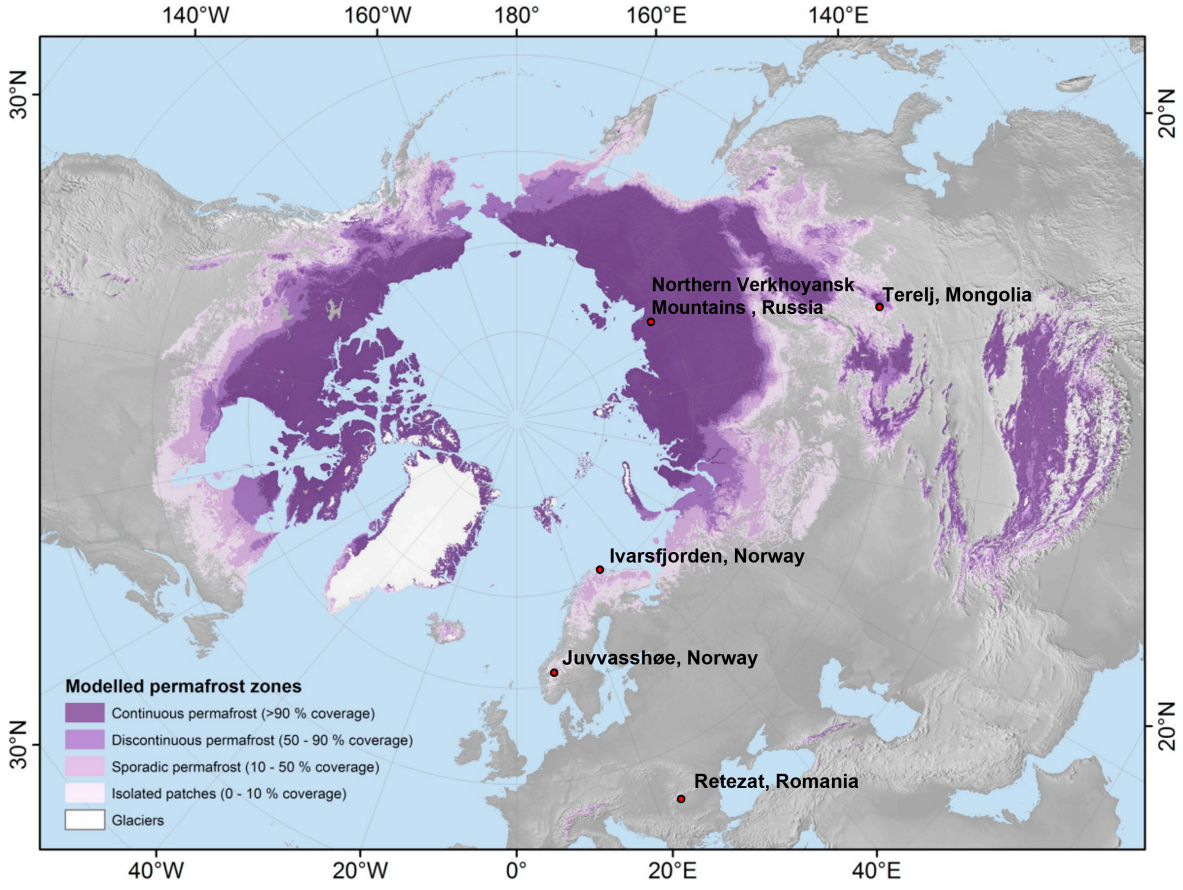

Figure 1: Circum-polar permafrost zonation from Obu et al. (2019). Indicated by the red markers are the study sites in this thesis.

Degradation of permafrost and ground ice affects fresh water availability (Jones et al. 2019), influences regional permafrost limits and raises concerns and uncertainties about the stability of infrastructure, buildings and natural slopes (e.g. Nelson et al. 2001). Additionally, thawing permafrost could lead to additional release of methane and carbon dioxide and thus act as a positive feedback for future climate change (Michaelson et al.

1996). Permafrost is ultimately a function of climate and is sensitive to climate change. Biskaborn et al. (2019) assembled a global temperature data set in 123 permafrost boreholes from 2007 to 2016. On average, they report that mountain permafrost warmed by 0.19 ±0.05 °C/decade. The greatest warming from 2008-2009 to 2016 occured in northwestern Siberia (Marre Sale, at 10 m depth) of 0.93 °C and northeastern Siberia (Samoylov Island, at 20.75 m depth) of 0.90 °C. The latter is close to one of the ancillary sites in this thesis.

1.2 Permafrost in Norway and Scandinavia

Permafrost underlays ca. 6 % of the Norwegian mainland (Gisnås et al. 2013). The warming of mountain permafrost in Norway as a result of climate change has been reported extensively. In 1998, the PACE (Permafrost and Climate in Europe) project was initiated in order to increase the knowledge of permafrost distribution in mountain areas, the thermal state of permafrost and the response of permafrost in the light of climate change (Harris et al. 2001). In the Nordics, this led to the establishment of deep permafrost boreholes on Janssonhaugen (Svalbard/Norway, 78°N), Tarfalaryggen (Sweden, 68°N) and at Juvvasshøe (Norway, 62°N). The latter is one of the main study sites in this thesis. Isaksen et al. (2007) described warming rates at the top of the permafrost in these boreholes of 0.4 °to 0.7 °C/decade. Etzelmüller et al. (2020a) reported a consistent warming in all three boreholes in the 20 years since the onset of measurements. The average temperature at the ground surface increased by 0.9 °C/decade at Janssonhaugen, 0.2 °C/decade at Tarfalaryggen and 0.7 °C/decade at Juvvasshøe. 12 additional boreholes in southern and eastern Norway were drilled by Farbrot et al. (2011) in order to investigate the variability of ground temperatures in this region with regards to location and sediment cover. Local factors are extremely important in governing the presence or absence of permafrost. A characteristic of mountain permafrost environments (excluding large plateaus) is the large spatial variability in slope, aspect, (sub)surface material, water availability, snow distribution and vegetation. This variability can result in a heterogenic distribution of permafrost and ground ice on a small spatial scale. Farbrot et al. (2011) described the variability related to e.g. sediment cover as important knowledge for the application of spatial permafrost models.

1.3 Permafrost modelling

Numerous modelling studies aim to map the permafrost distribution and predict future permafrost degradation in Norway. Westermann et al. (2013) mapped climate change impact on permafrost in southern Norway between 1960 and 2009 with a transient permafrost model. They report a relatively constant permafrost area until 1990, though between 1990 and 2009 the area with negative ground temperatures at 2 m depth decreased by 40%. Hipp et al. (2012) modelled the response of mountain permafrost at boreholes in southern Norway to climate warming from 1860 to 2100, following future climate scenarios. They report that mountain permafrost would degrade at most locations below 1800 m.a.s.l. and likely to degrade (55-75% probability) at the location of the PACE borehole at Juvvasshøe. They found an increase of 1.5 °C at 10 m depth at

Juvvasshøe between 1960 and 2009, with the highest warming rates from 1990 to 2009. Gisnås et al. (2013) used a spatial equilibrium model for permafrost distribution in Norway. They took variations in snow cover, vegetation and ground properties into account. They found an area corresponding to 6.1 - 6.4 % of the Norwegian mainland area to be underlain by permafrost in the period 1981-2010 opposed to 10.0 - 10.8 % in the normal period 1961-1990. They describe 21% of this area to be in blockfields.

A blockfield is a surface that is covered by coarse rocks of boulder or block size. Blockfields are common in mountain areas in Norway (Gisnås et al. 2013). Permafrost landforms that, similar to blockfields, also features a coarse surface cover, are rock glaciers. In mainland Norway, rock glaciers are mostly located in the north (Lilleøren and Etzelmüller 2011). The active permafrost landforms at the lowest elevation in discontinuous mountain permafrost regions often consist of coarse, blocky material (Harris and Pedersen 1998). In fact, landforms such as rock glaciers are found below the assumed elevational permafrost limit (Lilleøren and Etzelmüller 2011).

These landforms feature lower ground temperatures than surrounding terrain in the same general climatic setting. This difference will be referred to as a 'negative thermal anomaly' (as in Delaloye et al. 2003) and has been measured in Norway by Juliussen and Humlum (2008). Studies in other regions have also described this thermal anomaly in e.g. rock glaciers in Greenland (Humlum 1997), in the Alps (Hanson and Hoelzle 2004), Romania (Popescu et al. 2017) and beneath blocky slopes in Canada and China (Harris and Pedersen 1998). This effect is explained to result from air movement processes and evaporation of water and sublimation of ice in the summer (Harris and Pedersen 1998). Juliussen and Humlum (2008) hypothesised that rocks protruding through the snow cover and thereby affecting the thermal conductivity of the subsurface play a role in lowering the ground temperature. Finally, they describe the effect of a low soil moisture content. The freezing of water results in a release of latent heat. If less water is present in the ground when temperatures drop in autumn, less latent heat is liberated and the ground temperature decreases more rapidly. Porous, blocky material is easily drained of water, especially when on a slope (Haeberli et al. 2006). During the snow melt period, water can infiltrate and refreeze at the base of this blocky layer. The process of varying water and ice contents in blocky terrain is the focus of this thesis.

Since a coarse, blocky surface cover often features significantly lower ground temperatures than surrounding terrain, it is important to assess how this is accounted for in permafrost models. Most modelling studies did not include this thermal anomaly for blockfields, neither did they include varying moisture contents. For example, Obu et al. (2019), who produced a circum-polar permafrost distribution map (figure 1), have no mention of blockfields. They used low soil moisture contents in soil-free mountain areas but the water content does not vary over time. Westermann et al. (2013) used constant stratigraphies, meaning that the total water/ice contents do not change. Instead, a zone of low soil moisture is assigned to the upper meters of the blockfield stratigraphy. In order to represent the effect of blocks protruding through the snow cover in a phenomenological way, Westermann et al. (2013) reduced incoming snow by a constant 0.5 m. Finally, Hipp et al. (2012) used a one-dimensional heat flow model where the volumetric water content is considered as a constant to produce their projections.

This raises the question if blocky mountain terrain is correctly represented in these models.

Soil water contents that are considered constant are a major limitation in environments where the soil moisture conditions change strongly (Martin et al. 2019). Martin et al. (2019) simulated ground temperatures in peat plateaus in northern Norway and did include a drainage effect for soil water contents. They found differences up to 2 °C between well drained and undrained conditions. Juliussen and Humlum (2008), who investigated thermal anomalies in blockfields in eastern Norway, observed accumulation of ice in the pores between blocks in winter and hypothesised that this changing ice table is a factor responsible for the thermal anomaly in the blockfield.

1.4 Objectives and structure of the thesis

The goal of this thesis is to investigate one of the processes that is responsible for lower ground temperatures in coarse, blocky deposits. Namely, the effect of lateral drainage which reduces soil moisture and ground ice contents in the active layer. The previous section established that the use of constant soil moisture contents is a shortcoming in many modelling studies in mountain terrain. The development of the CryoGrid community model (Westermann et al. 2022 subm.) now offers a tool to include a subsurface drainage component in a heat conduction model. Therefore it is possible to investigate the effect of a variable soil moisture content in blocky terrain on ground ice and ground temperatures. The focus will be on two locations in Norway: a blockfield site at high elevation in southern Norway and a rock glacier site close to sea level in northern Norway. Additionally, three ancillary sites are used to apply the model setup and investigate thermal anomalies in vastly different climates and serve as model experiments. These sites are: 1) blockfields in the northern Verkhoyansk Mountains in Siberia, Russia, 2) a blockfield near the Terelj valley, northern Mongolia and 3) a rock glacier in the Retezat Mountains in the Southern Carpathians, Romania.

The main objectives of the thesis are to:

- Use a novel method within the CryoGrid community model framework to simulate lateral subsurface drainage and its effect on ground ice and ground temperatures in three idealized ground stratigraphies.
- Quantify thermal anomalies between well drained and poorly drained blocky deposits for different amounts of snowfall in different climatic settings.
- Evaluate the evolution of permafrost and the ground ice table at the rock glacier in Ivarsfjorden, northern Norway for different idealized stratigraphies since 1951.
- Explore the effect of blocky terrain on the zero curtain, subsurface drainage regimes and on ground ice formation.

An overview of the state of the art in the research field has been given in this chapter. Chapter 2 contains relevant scientific background about permafrost processes, zooming in on mountain environments which contain blockfields and rock glaciers. Finally, permafrost models are treated, zooming in from general classes of permafrost models to the CryoGrid community model. The study regions are presented in Chapter 3, where the focus in on

Norway. The three ancillary study sites are briefly presented. Chapter 4 explains the model setup within the CryoGrid framework. Focus is on how blocky terrain is represented and how lateral subsurface drainage is included in the model. Additionally, the procedure of how the meteorological forcing data for the model is generated is explained. Model results, in Chapter 5, are first compared to measurements for the two sites in Norway. Then, the general effect of the different model scenarios on the ground ice and ground temperatures is addressed, after which ground temperatures in different scenarios are presented per site. The transient response to climate warming is simulated only for the two sites in Norway, and the focus here is on the rock glacier in northern Norway. Results at the three ancillary sites are each presented, supporting the overall findings of this thesis. Finally, three aspects that relate to the interplay between ground temperatures and the water and ice balance are presented. These include an analysis of the zero curtain, subsurface drainage at two site and the effect of blocky terrain on permafrost aggradation. In Chapter 6, first the model performance and limitations of the model setup are discussed. This is followed by a discussion of the found thermal anomalies and results are compared with findings in other studies. The findings of the thesis are put in the larger research context, where existing modelling studies are discussed and recommendations for future studies are made. Finally, the main conclusions of the thesis are given in Chapter 7.

2 Background

2.1 The thermal regime of permafrost

Permafrost is defined as ground that remains at or below 0 °C for two or more consecutive years (Everdingen 1998). This definition is solely based on temperature and thus does not require the presence of ice in the ground. The layer of ground that overlays the permafrost is called the active layer. This is the ground that undergoes annual thawing and freezing. The definition of the active layer, opposed to that of permafrost, is based on ground state (frozen or unfrozen) and thus not on temperature. It is therefore possible that the top of the permafrost, while remaining at or below 0 °C, is also part of the active layer when the freezing point is depressed (Everdingen 1998). The active layer is the zone of most biological, hydrological, ecological and geomorphological activity, making it important to have knowledge of the active layer thickness (ALT) in permafrost environments (Hinzman et al. 1991). Ground temperatures and ALT are a result of multiple factors including present and past climate, atmospheric conditions, terrain snow cover, vegetation, ground properties and water content. As a result of these many factors influencing the ground thermal regime, ground temperatures vary spatially on a small scale. These factors will be discussed in the section 2.2.1.

Ground temperature data are often presented in a diagram that shows minimum, maximum and average temperatures at depth, called a 'trumpet curve' (figure 2). The time period is not predefined, but often one hydrological year is used. The top of the permafrost is approximated at the depth where the maximum temperature line crosses the 0 °C isotherm. The depth below the ground surface where minimum and maximum ground temperatures differ 0.1 °C or less is called the depth of zero annual amplitude, typically at 10 to 20 m depth (Everdingen 1998). Below this depth the temperature is mostly constant throughout the year as seasonality plays no more role. As a result of the geothermal heat flux, temperatures at depth increase and cross the 0 °C isotherm at the base of the permafrost.

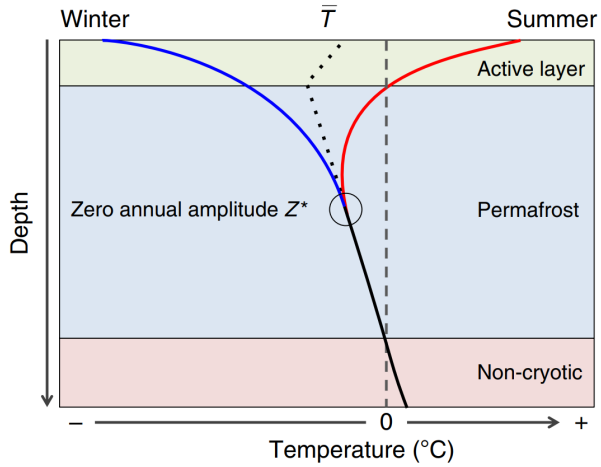

Figure 2: Thermal regime of permafrost with the minimum (blue), maximum (red) and mean (black, dotted) ground temperature. Compiled guided by French 2007 (Biskaborn et al. 2019).

Figure 3 shows an idealized profile of mean annual temperatures in the first several meters below the surface. Lachenbruch (1988) described the climate-permafrost relation, which can be represented by ground temperatures at three levels: 1) The mean annual air temperature (MAAT), 2) the mean annual ground surface temperature (MAGST) and 3) the temperature at the top of the permafrost (TTOP). The difference between the MAAT and the MAGST is called the surface offset. The surface offset reflects the influence of the buffer layer, consisting of snow and/or vegetation on top of the ground surface. Also topographic properties and soil moisture have an effect on the surface offset. The thermal offset is the difference between the MAGST and the TTOP. The thermal offset thus reflects the thermal properties of the active layer.

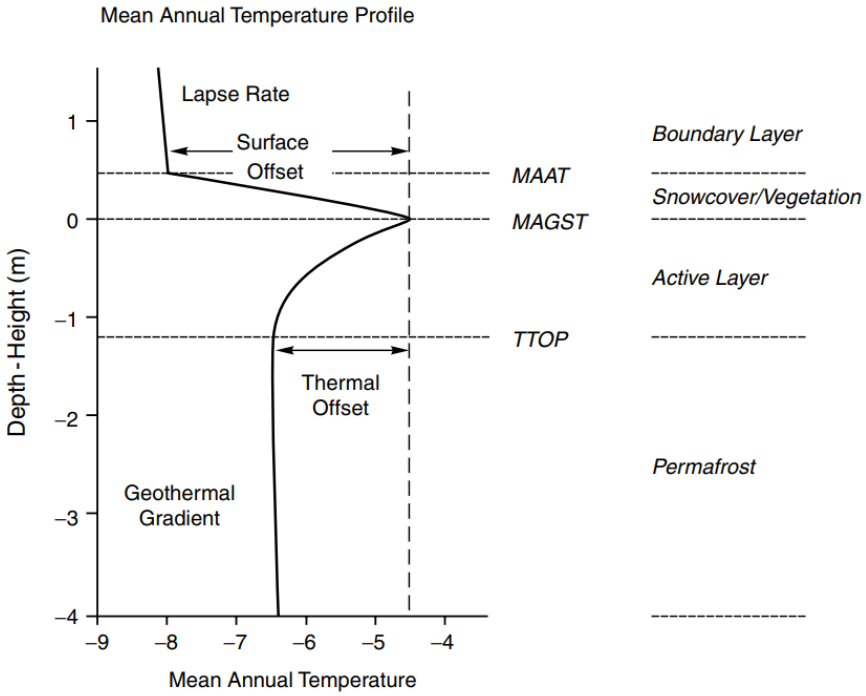

Figure 3: Schematic mean annual temperature profile in the surface boundary layer, active layer and permafrost (Smith and Riseborough 2002).

2.1.1 Factors controlling ground surface temperatures

As mentioned in the previous section, many factors affect temperatures at the ground surface, resulting in a non-linear relationship between air and ground temperature. Adding to the complexity are the fine-scale spatial heterogeneity and interactions between these variables.

Snow. The thickness and timing of the seasonal snow cover in permafrost environments is a major driver of ground temperatures. Snow is an insulator and thus prevents heat loss from the ground during the snow covered period to a certain degree. This results in ground mean ground temperatures that are higher in snow covered sites than in snow free sites in the same climate. In cold regions, the mean annual ground temperature (MAGT) can be several degrees higher then the MAAT (Gold 1963). Several physical principles are

responsible for the thermal effect of snow on the ground (Zhang 2005): First, snow, and especially fresh dry snow, has a thermal conductivity that can be 5 to 20 times lower than the thermal conductivity of a mineral soil. This creates the insulating and warming effect by preventing heat loss from the ground in winter. Next, snow has a higher albedo than the ground, which leads to an increase in reflected shortwave radiation. This property has a cooling effect on the underlying ground. Latent heat absorption during snowmelt delays the warming of the soil and thus acts as a cooling factor. Conversely, refreezing meltwater in the snowpack releases latent heat and hence warms the snow and underlying ground. The net effect that snow has on the ground thermal regime depends on the timing, duration and local characteristics, but in most cases a snow cover induces net warming on the ground.

Vegetation. The interactions between permafrost and vegetation are complex. Different types of vegetation cause differences in soil and heat convection and conduction. The vegetation type and cover therefore influence the thaw-freeze cycle and thermal regime of the ground (Hinzman et al. 2005, Genxu et al. 2012). Trees shade the ground from direct solar radiation. They intercept both fresh snowfall at the canopy and windblown snow at the trunks. Trees also affect the composition of the ground and the soil moisture regime. Ground surface temperatures may be increases or decreased depending on canopy density and vegetation type. In continental discontinuous permafrost regions like Alaska and Mongolia, permafrost might be restricted to forested areas as a consequence of shading from solar radiation. In Scandinavia and the European Alps, permafrost is not present in forested areas. Here, the shading effect is thus of less importance. More important are effects that the generally low vegetation has on snow distribution, by acting as a snow fence and therefore insulating the ground underneath. The snow and vegetation cover are often described together as the 'buffer layer' between the atmosphere and the active layer (Riseborough et al. 2008).

Topography. The topography influences temperatures at the ground surface in various ways. On a large scale, it determines weather patterns and thus the air temperature and precipitation and wind patterns. Locally, the effect of topography on ground temperatures can be divided in direct and indirect processes. Fiddes and Gruber (2014) stated that gradients of meteorological variables related to topography (elevation, aspect, slope, etc.) are often larger over topography (i.e. vertical) gradients than horizontal gradients. The direct effects concerns the amount of long- and shortwave radiation that hits the ground. Incoming shortwave radiation is (on the northern hemisphere) reduced for north-facing slopes compared to south-facing slopes, depending on the slope angle. Shading by surrounding topography also affects incoming longwave radiation from the terrain. In rugged topography, the variation of the surface energy balance with a changing aspect strongly affects the distribution of surface temperatures (Mittaz et al. 2000). The topography also affects the snow and vegetation cover, thus indirectly influencing ground surface temperatures. Wind patterns (both wind speed and direction) are influenced by topography, affecting snow distribution and turbulent heat fluxes. Drainage patterns are governed by topography, affecting soil moisture. Soil moisture has a large effect on ground temperatures related to latent heat effects and thermal conductivity.

2.2 Permafrost in mountain environments

Mountain permafrost is simply defined as permafrost existing at high altitudes in high, middle, and low latitudes (Everdingen 1998). It is a relatively young research field that got more attention during the past decades (Etzelmüller 2013). The growth in interest is mostly a result of the effect that permafrost degradation has on geohazards in mountain areas. Examples are Gruber and Haeberli (2007), who described how permafrost degradation in steep bedrock slopes can cause slope instability and Helgason et al. (2018) who described the role of ground ice thaw on loose material landslides on Iceland.

The main characteristic of mountain permafrost (excluding large plateaus) is the large spatial variability in topographic parameters, subsurface material, water availability, snow distribution and vegetation. The presence of micro-climates is a result of this variability and complicates permafrost distribution mapping in mountain areas. This is further complicated by the high costs and difficult logistics that accompany field studies in mountain areas, leading to sparse data availability (Haeberli et al. 2010). The lowest active permafrost landforms in discontinuous mountain permafrost are frequently found in coarse, blocky terrain Harris and Pedersen (1998). Two landforms that consist of coarse deposits and are relevant for this study will be addressed: blockfields and rock glaciers.

2.2.1 Blockfields

A blockfield is a surface that is covered by coarse rocks of boulder or block size. Their formation is associated with frost weathering and are therefore present in periglacial environments. Blockfields are often divided into *autochthonous* blockfields which originate from in situ weathering of bedrock and into *allochthonous* blockfields that form from blocks or boulders with another origin such as glacial deposits (Ballantyne and Harris 1994). White (1976) stated that blockfields often contain no fine sediments in the upper 1.5 - 3 meter of the ground. Kleman (1994) presented a review study and concluded that landforms including blockfields have been preserved despite being overridden by ice. The locations of preserved landforms match well with locations where ice during the last glaciation was continuously frozen to the bed. Ives (1957) documented early ideas that blockfields could have been preserved after being overridden by an ice-sheet. Talus slopes and screes slopes are also periglacial landforms with that consist of course blocky material, but their formation is linked with mass movement processes (Rea 2007). Blockfields are present in large areas in southern Norway and affect the ground thermal regime and periglacial processes such as frost weathering (Heggem et al. 2005).

A striking feature of blockfields is that they have ground temperatures that are lower than other, finer mineral, soils under the same climate. A so-called negative temperature anomaly in coarse, blocky material has long been recognized. Harris and Pedersen (1998) found a negative temperature anomaly of 4 - 7 °C in blocky terrain opposed to adjacent mineral sediment was measured in mountains in Canada and China. Juliussen and Humlum (2008) found blockfields in Norwegian mountain sites that produced a negative temperature anomaly of 1.3 - 2.0 °C. Mean ground temperatures at 2.5 - 4.0 °C below mean annual air temperatures are reported in Central Asia (Gorbunov et al. 2004). A negative thermal anomaly in blocky surface deposits in also observed in the Swiss Alps

(Rödder and Kneisel 2012). Harris and Pedersen (1998) summarized 4 hypotheses that explain negative thermal anomalies in blocky terrain:

The Balch effect. First described by Balch (1900) and is a result of density differences between cold and warm air. Warmer air in the pore spaces of blocks gets replaced by colder air from the atmosphere and thus a thermal filter is created. This occurs when the snow cover in winter is limited and when there are large connecting spaces between the blocks, allowing for convection. The displacement of warm air by cold air does not occur in sediment covers where no air can circulate. The effect therefore causes an anomaly in comparison with those sediment covers.

The chimney effect. Also based on density differences of cold and warm air, but assuming a larger snow cover, sloped terrain and lateral air flow. Cold air replaces warm air by entering wherever holes in the snow cover are present. When the terrain is sloped, warm air rises through the voids between the blocks and escapes via these holes in the snow cover. The colder air can escape the deposit at the bottom of the slope. Evidence has been found where the lower area of a blocky slope is 1 - 2 °C colder than the 100 - 200 m higher upper part of similar surface cover (Gorbunov et al. 2004).

Evaporation of water and sublimation of ice in the summer. Evaporation of water and sublimation of ice in the summer cools the blocky debris due to the removal of latent heat. This process is expected to be most effective in areas with low humidity in summer.

Continuous air exchange with the atmosphere. An extension to the chimney effect in areas that lack a continuous snow cover in the winter. In this case, continuous air exchange in between the blocks and atmosphere is possible, resulting in a rapid response in temperature changes. This is most effective at steep and windy locations.

The relative importance of these cooling mechanisms is difficult to asses, but a consideration of factors like slope, snow cover and wind can help giving a qualitative estimation.

Juliussen and Humlum (2008) studied the thermal regime of blockfields on mountains in Central-eastern Norway and found a negative temperature anomaly of 1.3 - 2.0 °C compared to till and bedrock sites. They emphasized the need of understanding these systems in order to be included in permafrost models. They issued that convection in the blockfields was of low importance in creating the anomaly. Ice accumulation in the pore volume will have reduced the permeability of the blockfield in winter. Instead they issued that the negative anomalies are mainly a result of blocks that protrude into and through the snow cover. This leads to a higher effective thermal conductivity of the snow cover. Additionally, the accumulation of ice in the pores between blocks leads to a higher thermal conductivity in winter compared to summer, which promotes cooling. Finally, a last important factor is the soil moisture content. A lower soil moisture content in permeable blocky debris leads to more rapid freezing by liberating less latent heat compared to e.g. till with a higher soil moisture content. Therefore, well drained sites will, when the ability to hold water against gravity (field capacity) is low, promote lower ground temperatures and thus the presence of permafrost. This thesis aims to simulate this effect.

Gruber and Hoelze (2008) presented a simple model that simulates the conductive effect

of blocks protruding through the snow cover. Their model did not include phase changes, advective heat transport or convection processes that are described by Harris and Pedersen (1998). However, results showed that the mean annual ground temperature can be reduced as a result of a lower thermal conductivity of a blocky layer. If the thermal conductivity below the surface is reduced, the relative importance of heat transfer through the snow will increase. As a result, the temperature at the ground surface responds more to the cold atmospheric forcing in the winter.

2.2.2 Rock glaciers

Rock glaciers form when ice-cemented ground creeps due to gravity and the plastic properties of ice (Haeberli 1985). Rock glaciers, in addition to palsas, ice-cored moraines and ice-wedge polygons, are a landform indicative of present or former permafrost conditions (Lilleøren and Etzelmüller 2011). The definition and nomenclature of rock glaciers is a topic of discussion among geomorphologists (e.g. Hamilton and Whalley 1995; Berthling 2011). Essentially, two types of definitions have been given to rock glaciers. Descriptive definitions are based on observable geomorphological characterises (e.g. Haeberli 1985) and genetic definitions are based on the processes that formed the rock glacier (Potter Jr 1972). Humlum (1988) distinguished the genesis of rock glaciers between 'glacier-derived rock glaciers' and 'talus-derived rock glaciers'. Berthling (2011) argued that the morphological definition should be abandoned as a whole and proposed the following definition for an active rock glacier: 'the visible expression of cumulative deformation by long-term creep of ice/debris mixtures under permafrost conditions'. He regards rock glaciers as cryo-conditioned landforms, where the origin of the ice can be both glacial or periglacial.

Rock glaciers can be subdivided in terms of activity and presence of ice. Active rock glaciers contain ice and move, while inactive rock glaciers contain ice but do no longer move. Both types are found in areas that contain permafrost in the present-day. The velocity of active rock glaciers is often in the range of centimeters to meters per year and increases exponentially with higher temperatures (Kääb et al. 2007). Relict rock glaciers belong to areas where permafrost is no longer present (Lilleøren and Etzelmüller 2011). These relict landforms show no movement and no, or a small, ice content. Due to the lack of movement, the vegetation cover is often extensive (Lilleøren and Etzelmüller 2011). Active rock glaciers are commonly shaped as lobe or tongue with a steep front. Pressure ridges and furrows can be found both parallel and orthogonal to the flow direction (Wahrhaftig and Cox 1959; Humlum 1996). The surface of a rock glacier consists of coarse blocks or boulders (Hanson and Hoelzle 2004; Humlum 1997) and therefore similar thermal properties as described section 2.2.1. can be expected at rock glaciers. In active rock glaciers, weathering products can be moved towards the tongue and so develop a high porosity instead of accumulating at the base of the blocky surface layer and filling voids between blocks. The latter can be expected in blockfields that are not located on a slope. The cooling effect of a rock glacier surface means that the persistence of subsurface ice is possible in areas and elevations where the MAAT is well above 0 °C (e.g. Popescu et al. 2017) and are thus outside the assumed altitudinal permafrost limit. Since rock glaciers are therefore seen as delimiting the lower permafrost limit, they are of special significance (Humlum 1997).

The zero curtain is defined as the persistence of an almost constant temperature close to the freezing point during freezing or thawing of the active layer and is a result of the change of phase of water (Everdingen 1998). In fine sediments with a high soil moisture content, the decrease of ground temperatures in autumn is therefore delayed compared to air temperatures. Latent heat is released during the freezing of pore water and retards the freezing front. In coarse blocks, as on rock glaciers and in blockfields, the drainage of water makes that this process is minimal to nonexistent (Hanson and Hoelzle 2004). In fact, an almost opposite effect in spring has been observed where percolating melt-water refreezes at the bottom of the blocky surface layer (e.g. Hoelzle et al. 2003; Humlum 1997; Hanson and Hoelzle 2004). This way, a layer of superimposed ice can be formed which has to be melted before the ground can start to warm. In these instances, the zero curtain covers a longer time span in spring than in autumn.

Rock glaciers play an important role in the hydrological cycle, especially in arid regions such as the Andes. Jones et al. (2019) emphasized the non-negligible importance of rock glacier water storage. The open debris structure can act as a trap for snow and a rock glacier can store a significant quantity of ice or liquid water. Rock glaciers studied in Argentina are an important water resource as they release water mainly during periods of drought (Croce and Milana 2002). Water storage in rock glaciers occurs in the form of liquid water, snow and ice at short- intermediate- and long-term timescales respectively (Jones et al. 2019). The global (excluding Antarctica and Greenland) ratio of rock glacier to glacier water volume equivalent (WVEQ) is estimated at 1:456 and is increasing due to differential warming of rock glaciers as compared to glaciers. However, in (semi-)arid regions this value is much higher and thus implying a more significant role for rock glaciers as water source (Jones et al. 2019). For example, Azócar and Brenning (2010) found that rock glaciers are a more significant storage of water than glaciers in the Chilean Andes between 29°S and 32°S.

2.3 Permafrost modelling

2.3.1 General classes of permafrost models

The IPCC (The Intergovernmental Panel on Climate Change, 1990) reported that the climate-permafrost relationship is a subject that research should be directed towards (Riseborough et al. 2008). This includes the effect of changes in climate forcing, snow, vegetation, surficial sediment and bedrock. In this light, a large number of models have been developed and applied in permafrost studies. Many of these models are made in order to make predictions about the effect of climate change on the spatial distribution of permafrost. The two main types of permafrost model approaches used in mountain areas are empirical-statistical models and physically based models (Riseborough et al. 2008). Harris et al. (2009) described that the preferred modelling approach in European mountains changed from stochastic and empirical to more numerical models.

Empirical-statistical permafrost models relate the locations of observed permafrost to topographic-climatic factors. In mountain areas, these factors are solar radiation, elevation, slope, aspect and MAAT (e.g. Etzelmüller et al. 2001; Heggem et al. 2005; Etzelmüller et al. 2007). Etzelmüller et al. (2007) showed that a MAAT of -3 °C is a good

estimate for the altitudinal limit of regional permafrost, though the thermal anomaly in blocky terrain is then not considered. Permafrost occurrence is often determined via bottom temperature of snow (BTS) measurements. Measurements of BTS that are associated with the presence (or absence) of permafrost are coupled to measured MAATs. These models neglect important feedback mechanisms between the atmosphere, snow and ground and transient conditions at depth which occur on a timescale of decades to centuries (Harris et al. 2009). A common model model used in permafrost distribution studies is the TTOP-model (Smith and Riseborough 1996). The TTOP-model calculates the MAGST based on the MAAT and uses semi-empirical adjustments for the thermal offset and thus makes use of the schematic profile in figure 3. It has for example been used to determine the controlling factors of permafrost limits and continuity in Canada (Smith and Riseborough 2002). CryoGrid 1, a previous version of the model that is used in this thesis, also employed a TTOP-model and will be described in the next section. The advantage of empirical-statistical models is that these can be applied easily and perform well if correctly calibrated.

Physically based (or process based) models solve the surface energy balance and determine the thermal regime of the ground. Since permafrost is a largely invisible phenomenon, modelling based on process understanding is the best approach in the estimation of permafrost distribution (Harris et al. 2009). They are better suited to study the sensitivity of permafrost systems to climate change. However, the higher detail of processes included in physically based models, the more input data and computing power is required. Riseborough et al. (2008) categorised these type of models based on temporal, thermal and spatial criteria. Temporally, models can be divided in equilibrium (or steady state) models that determine the conditions of permafrost for a single annual regime and in transient models that calculate how these conditions change over a longer time period. The latter requires a suitable initialization. Thermally, simple models determine the presence or absence of permafrost, MAGT or ALT and include a empirical-statistical component of transfer functions between the atmosphere and the ground. More complex, numerical models may calculate the evolution of the entire ground profile and solve the complete energy balance. Models based on heat conduction are a proven tool to describe the ground thermal regime (e.g. Y. Zhang et al. 2003; Romanovsky et al. 1997). Spatially, conditions can be modelled at a single point, along a transect or in an area. Many distribution studies do not include lateral heat flow and thus do not consider some of the small scale variability which is important in mountain permafrost environments.

2.3.2 The CryoGrid community model

The CryoGrid community model (Westermann et al. 2022 subm.) is a simulation toolbox that can calculate ground temperatures and volumetric water and ice content in permafrost environments. It builds on the well-established CryoGrid 1, 2 and 3. CryoGrid 1 is an equilibrium model, meaning it does not include the evolution of the ground thermal regime with time. This is a TTOP model, meaning it can be used to infer presence or absence of permafrost. CryoGrid 1 has been used in fine-scale studies (Gisnås et al. 2014; Gisnås et al. 2016) and for large-scale permafrost mapping studies (Gisnås et al. 2017; Westermann et al. 2015; Obu et al. 2019). Obu et al. (2019), who produced a circum-polar permafrost distribution map (figure 1) obtained soil moisture classes from remote-sensing

products and assigned low soil moisture contents to mountainous and soil-free locations, though these water contents are static. CryoGrid 2 is a transient model, making it suitable to asses the impacts of climate change. It uses conductive heat transfer in the snow and subsurface to calculate ground temperatures. The movement of water and water vapor is not included in the model (Westermann et al. 2013). It has been used for mapping the impacts of climate change in Norway (Westermann et al. 2013), Siberia (Westermann et al. 2017) and Iceland (Czekirda et al. 2019). It has further been used for paleo-permafrost evolution (Etzelmüller et al. 2020b; Overduin et al. 2019) and salt effects on permafrost (e.g. Angelopoulos et al. 2021). CryoGrid 3 is designed to to simulate landscape changes due to e.g. thermokarst (Westermann et al. 2016). It features a more sophisticated snow scheme, a surface energy balance boundary condition, a bucket hydrology scheme, lateral water and snow transport, an excess ice module and a sophisticated vegetation scheme. CryoGrid 3 has been used in peat plateaus and palsas (Martin et al. 2019), ice-wedge polygons (Nitzbon et al. 2019) and boreal forests (Stuenzi et al. 2021). The CryoGrid community model accommodates a broad range of applications thanks to model structure that builds on classes (representations or parameterizations of different processes). The model structure and setup of the CryoGrid community model that is used in this thesis will be discussed in chapter 4. In the remainder of the thesis, the CryoGrid community model is referred to as 'CryoGrid' for simplicity.

3 Study regions

The main work in this thesis is focused on two sites in Norway. Hence, this chapter covers the regional background of Norway. The study sites in Russia, Mongolia and Romania are ancillary and are included to support the findings and to test the model setup in different climates.

3.1 Geography and Climate of Norway

Norway is located on the Scandinavian peninsula in northern Europe and the mainland ranges from 58°N to 71°N and from 5°E to 31°E. A mountain range, the Scandinavian Mountains, runs through Norway and parts of Sweden with the highest point, Galdhøppigen at 2469 m.a.s.l., in Jotunheimen, southern Norway. The present-day topography and landscape are mostly a result of Pleistocene glaciations during the past 3 million years (Mangerud et al. 2011). The LGM (Last Glacial Maximum) was from ca. 17-21 kyr BP (kiloyears before present) and occurred during the Late Weichselian. The LGM denotes the maximum ice sheet extent in a certain area. Several studies concluded that during the period 30-18 kyr BP, there have been fluctuations of the ice sheet margin (e.g. Olsen et al. 2001; Mangerud et al. 2010). The deglaciation history of Norway is subdivided into three periods (Mangerud et al. 2011). First, after the LGM, the ice margin retreats until the start of the Younger Dryas. The Younger Dryas was a cool period that disrupted the general warming trend in the Northern Hemisphere between ca. 12.9 and 11.6 kyr BP (Reimer et al. 2009). The continental shelf became free of ice during this period and so did parts of the coast of Norway. During the Younger Dryas, the ice margin advanced again in some parts, stayed the same in some and retreated in other areas. The final period is the Early Holocene when the ice sheet retreated during 1000-1500 years (Mangerud et al. 2011). Norway was most likely fully deglaciated about 8.5 kyr BP (Andersen 1980). Currently, the land is rising due to isostatic uplift since the end of the last glaciation.

The surface material in high mountain areas consist of bedrock, till, regolith or coarse blockfields. These blockfields typically occur on mountain plateaus and can be several meters thick (Nesje et al. 1988). Figure 4 shows the map of blockfields in Norway from Gisnås et al. (2013) based on Landsat images. Blockfields have been used to map the upper elevation of the LGM ice sheet as the ice sheet advance during the Late Weichselian removed most of the older sediments in Norway (Mangerud et al. 2011). However, Kleman (1994) has shown that these blockfields could persist under the cold ice of the ice sheet. The survival of blockfields under ice sheets, means that these could be old landforms that predate the deglaciation. Rock glaciers on the other hand are unlikely to be preserved under ice sheets and are landforms formed after the deglaciation. The oldest rock glaciers are the ones that exist down to sea level in areas that deglaciated first (Lilleøren and Etzelmüller 2011).

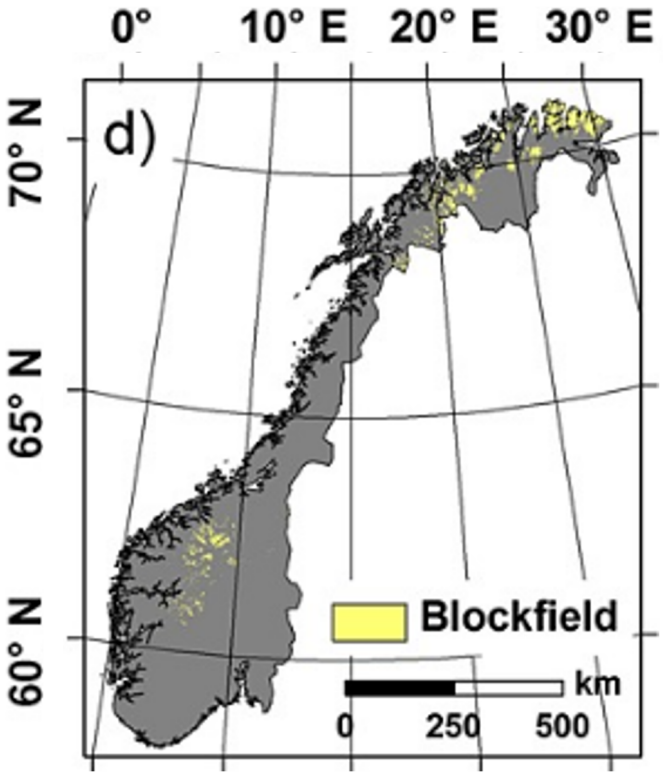

Figure 4: Blockfield map of Norway, produced with Landsat images (Gisnås et al. 2013).

The climate of Norway is heavily governed by the North Atlantic Current, which extents into the Norwegian Current, resulting in mild mean annual air temperatures around 7 °C at the west coast. The prevailing wind direction is from the south-west. The Scandinavian Mountains provide an orographic barrier where these air masses rise and cause a high mean annual precipitation of 2250 mm. The MAAT in the high mountain areas can be below -5 °C. Eastern Norway is partly sheltered by the mountains and features a more continental climate and thus larger diurnal variation in air temperatures. The mean annual precipitation in the east is around 750 mm. In Finnmark, northern Norway, mean annual precipitation can be below 500 mm.

3.2 Permafrost in Norway

Permafrost is present in large areas in the mountains of Norway. Ca. 6 % of the Norwegian main land mass is underlain by permafrost (Gisnås et al. 2013). Figure 5 shows the latest permafrost map of Norway, Sweden and Finland, modelled with CryoGrid 1 (Gisnås et al. 2017). It is important to understand the distribution and development of permafrost during the Holocene in order understand the formation of permafrost landforms (Lilleøren et al. 2012). The largest permafrost extent during the Holocene occurred during the Little Ice Age (LIA), a thermal minimum between the 15th and 19th century. Permafrost in northern Norway is more sensitive to climate change because of the lower relief in areas around the permafrost limit (Lilleøren et al. 2012). Lilleøren et al. (2012) identified two major periods where permafrost degraded during the Holocene. First, during the Holocene

Thermal Maximum, the warmest period during the Holocene, and then after the LIA.

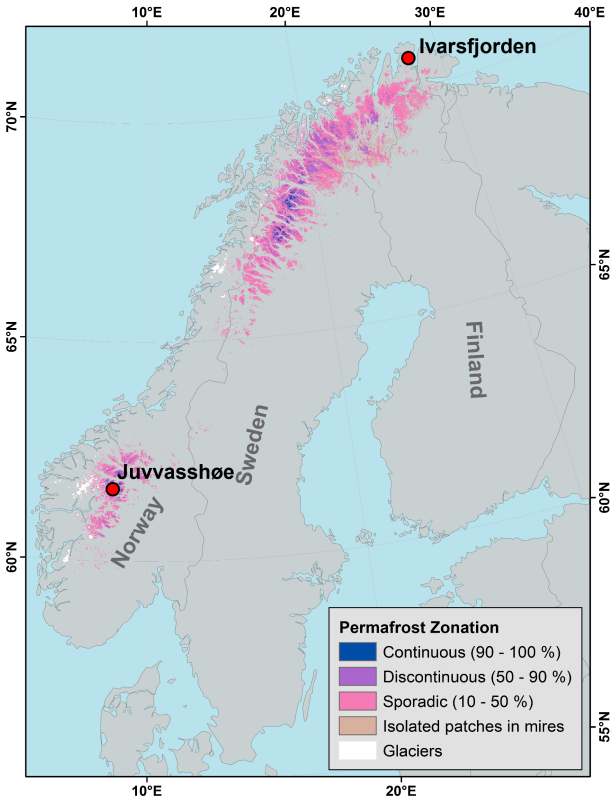

Figure 5: Permafrost map of the Scandinavian peninsula, modelled with CryoGrid 1 (Gisnås et al. 2017). Marked are the two study sites in Norway.

In southern Norway, permafrost underlies large parts of areas above 1500 m.a.s.l.. The altitudinal permafrost limit decreases from above 1600 m.a.s.l. in the west to about 1100 m.a.s.l. in the eastern, more continental areas (Etzelmüller et al. 2003). The southernmost observation of permafrost in Norway is on Gaustatoppen at 59.9°N (Etzelmüller et al. 2003).

In northern Norway, the limit is around 800-1000 m.a.s.l. in the west and decreases towards the east. An inventory of Norwegian rock glaciers based on aerial imagery was published in 2011 (Lilleøren and Etzelmüller 2011). They found no active permafrost landforms below 400 m.a.s.l.. The amount of rock glaciers in Norway is lower than in other mountain permafrost areas which they attributed to a lack of bedrock competence and debris availability and to the lack of alpine topography above the permafrost limit. However, Lilleøren et al. (2022) described rock glaciers near sea level in the area of Hopsfjorden, northern Norway, that have a limited ice body and are in transition from active to relict. One of these, the Ivarsfjorden rock glacier, is a study site in this thesis. Warming of Norwegian mountain permafrost (Etzelmüller et al. 2020a) is expected to continue in the 21st century (Hipp et al. 2012), which likely results in further degradation of these ice bodies and an upward shift of the lower permafrost limit.

3.3 Study sites in Norway

3.3.1 Juvvasshøe

Juvvasshøe (61°40 N, 08°22 E, 1894 m.a.s.l.) is a site located in the southern Norwegian mountains, Jotunheiemen well above the treeline (figure 6). The superficial sediment map from the Norwegian Geological Survey describes Juvvasshøe as moraine deposits, however it has been described as blockfields in several studies (e.g. Isaksen et al. 2003). A 129 m deep borehole has been present since August 1999 and was drilled for the PACE (Permafrost and Climate in Europe) project (Harris et al. 2001). Data from this PACE borehole is available with the exception of a gap between 21 December 2011 to 24 April 2014. The site is located in an extensive blockfield on a mountain plateau with sparse vegetation cover. The bedrock is located at 5 m depth, the first meter consists of large stones and boulders and the ground below are mainly cobbles (Isaksen et al. 2003).

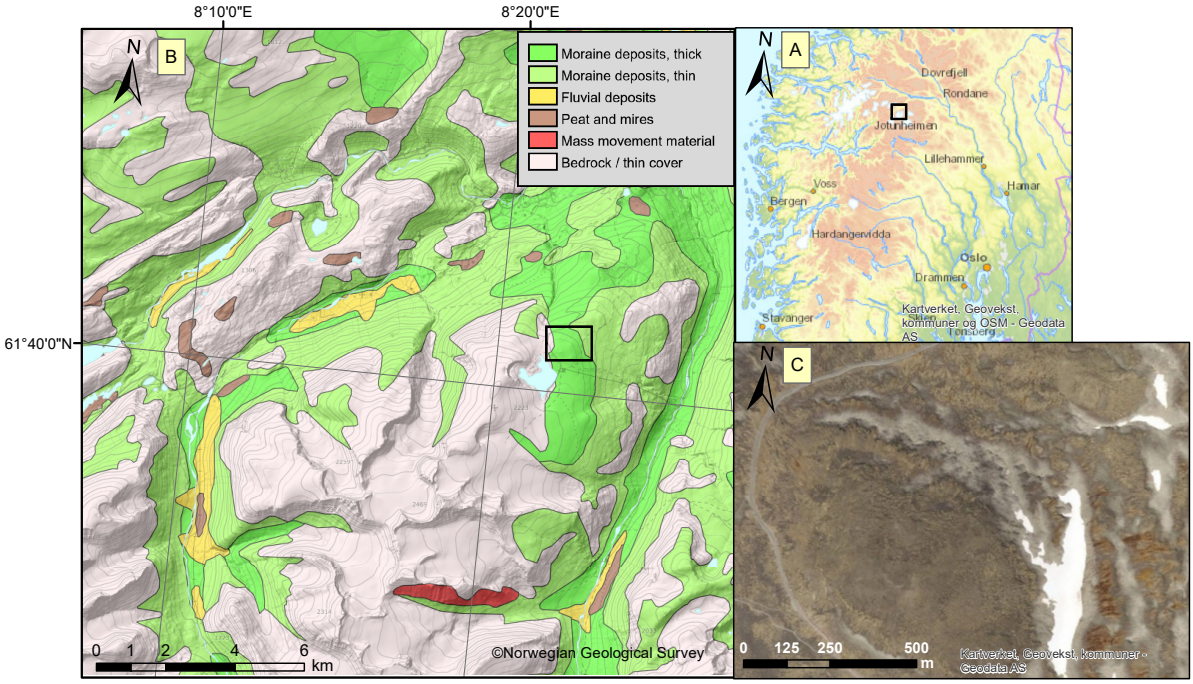

Figure 6: A: Overview map of southern Norway, with the location of map B indicated by the small black box. B: Superficial sediment map of the area around Juvvasshøe, with the location of the satellite photo in figure C indicated by black box (© Norwegian Geological Survey). C: Blockfield at Juvvasshøe. All topographical background maps are the owned by the Norwegian Mapping Authority, Kartverket.

Between 2000 and 2004, Isaksen et al. (2007) measured a mean annual air temperature (MAAT) at 2 m height of -3.3 °C. The mean ground temperature at 2.5 m below the surface during this period was -2.5 °C. The mean annual precipitation was estimated to 800 to 1000 mm. The site is extremely exposed, resulting in a very low snow thickness due to wind distribution. Hipp et al. (2012) described a snow cover of less than 20 cm, while the snow thickness in surrounding, lower and less exposed sites, can be up to 140 cm. The permafrost thickness at the PACE borehole was estimated to approximately 380

m (Isaksen et al. 2001), with the lower permafrost limited at ca. 1450 m.a.s.l. (Farbrot et al. 2011). A low geothermal heat flux could, together with high thermal conductivity, explain the deep permafrost (Isaksen et al. 2001). A short zero curtain suggests a low water content in the active layer (Isaksen et al. 2007). A warming of 0.2 °C/decade and 0.7 °C/decade in surface air temperature and ground surface temperature respectively occurred between 2000 and 2019 (Etzelmüller et al. 2020a). The measured ground temperatures at four depths between 2010 and 2020 are shown in figure 7.

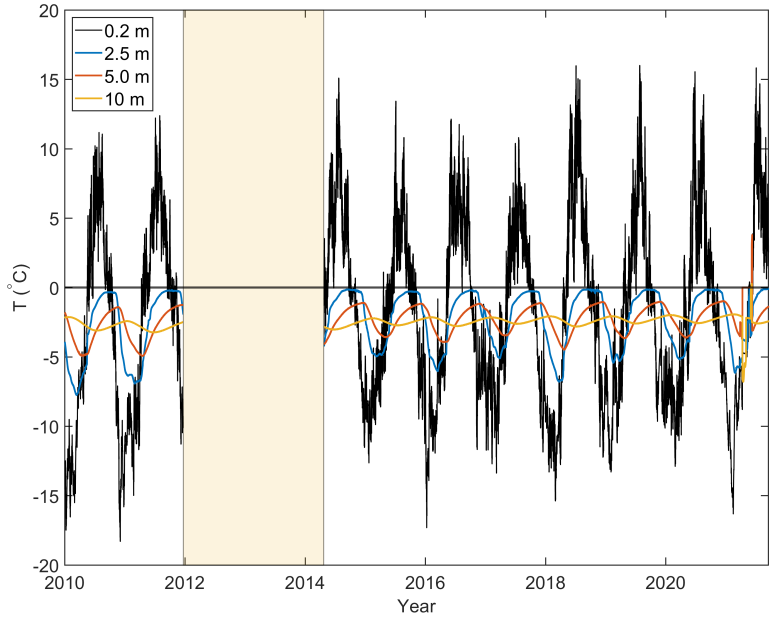

Figure 7: Ground temperatures at different depths at Juvvasshøe between 2010 and 2020, measured by the PACE borehole (provided by K. Isaksen). The shaded area indicates the period where no borehole data is available.

3.3.2 Ivarsfjorden rock glacier

Ivarsfjorden is a small fjord arm of the larger Hopsfjorden, located on the Nordkinn peninsula in the Troms and Finnmark county in northern Norway (figure 8). This county has a relatively low elevation in comparison to the rest of Norway, with areas above 1000 m.a.s.l. restricted to the western part. The Nordkinn peninsula is dominated by flat plateaus of exposed bedrock, in situ weathered material or coarse grained till (Lilleøren et al. 2022), which feature steep slopes towards the sea. Several rock glaciers are located around Hopsfjorden (Lilleøren et al. 2022). The rock glacier of interest lies in a southwest-northeast trending valley that extends from the fjord and has an elevation extent of roughly 60 to 160 m.a.s.l.. The rock glacier is northwest facing and has previously been interpreted as relict (Lilleøren and Etzelmüller 2011), but a detailed analysis showed that a limited ice core might still be present (Lilleøren et al. 2022). Lilleøren et al. (2022) made a geomorphological map of the area and identified two fresh rock glacier surfaces and a larger relict rock glacier surface (figure 8B). Their study also featured ground surface temperature loggers, of which a set with continuous measurements is used in this thesis

(section 4.2). The loggeres were placed in voids close to the surface. The mountain at its east (443 m.a.s.l.) serves as the source area and rockfall debris and coarse talus slopes are common. Sandstones often generate coarse, bouldery material, which is favorable for the formation of rock glaciers (Haeberli et al. 2006). This material is present at the location of the rock glacier in Ivarsfjorden. Lilleøren et al. (2022) describe a MAAT of 1.6 °C between 2010 and 2019. A negative MAAT around 100 to 150 years ago is an indication that rock glaciers in this area were active at the end of the Little Ice Age (LIA). Refraction Seismic Tomography (RST) surveys indicate a porous air-filled stratigraphy such as blocky talus deposits. While observed MAGSTs between 2015 and 2020 are all positive, negative surface temperatures during summer have been observed by a thermal camera at the front slope of the rock glacier. This is likely an indication of the chimney effect and thus of connecting voids that support air flow (Lilleøren et al. 2022).

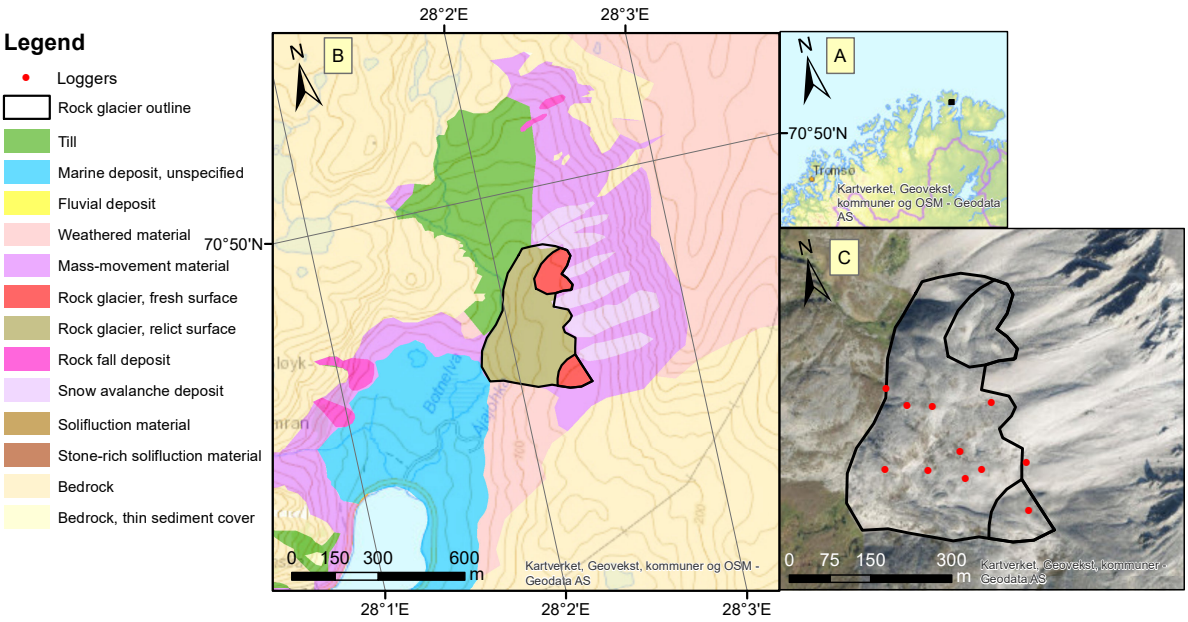

Figure 8: A: Overview map of northern Norway, with the location of map B indicated by the small black square. B: Geomorphological map of Ivarsfjorden (modified after Lilleøren et al. (2022)). C: Ivarsfjorden rock glacier with the location of the ground surface temperature loggers used by Lilleøren et al. (2022). All topographical background maps are the owned by the Norwegian Mapping Authority, Kartverket.

3.4 Ancillary study sites in the global permafrost extent

In addition to the two sites in Norway, three other locations are used in order to investigate ground thermal anomalies in regions with a different climate. The northern Verkhoyansk Mountains, in northeastern Siberia, are situated at a high latitude and feature a continental climate with a low radiation regime. Terelj, in central Mongolia, also has a continental climate, but due to the relatively low latitude, this location features a higher radiation regime and is semi-arid. The Retezat Mountains, in Romania, are located at a similar latitude and thus feature similar solar radiation to Terelj. However, air temperatures are higher and the climate less continental. At the ancillary sites, no ground

temperature measurements are available for a comparison with model results. Also, the climatic forcing data are not strictly validated but represent the broader climate at the sites.

Northern Verkhoyansk Mountains, Russia. The Verkhoyansk Mountains are located in eastern Siberia and are bordered by the Lena River on the west (figure 9). The climatic forcing data for this area are from the Lena River delta (section 4.3), at the northern border of the Verkhoyansk Mountains. There is likely blocky terrain in the mountains located at several hundred km southwest of the Lena River delta, though no specific exposition is modelled. The area features an Arctic continental climate and lies within the continuous permafrost zone. The MAAT is below -12 °C and temperatures range between -45 °C and 25 °C (Nitzbon et al. 2019). Snow thickness at the end of the winter is typically around 0.3 m.

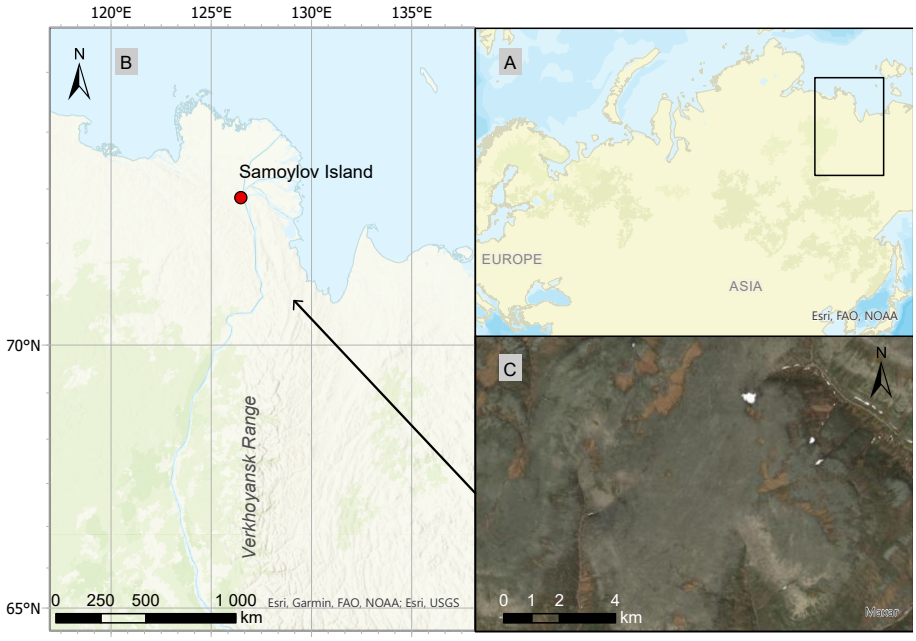

Figure 9: A: Overview map of Asia and parts of Europe (ESRI and World Open Street Map contributors), with the location of map B indicated by the black box. B: Map of the northern part of the Verkhoyansk Mountains, with the location of the climatic forcing data (on Samoylov Island in the Lena River delta) indicated by the red marker. The black arrow indicates the location of the satellite photo in figure C (ESRI and World Topographic Map contributors). C: Example of barren terrain, representing possible blockfields in the northern Verkhoyansk Mountains (ESRI and Maxar World Imagery contributors).

Terelj, Mongolia. The Terelj valley is located in the Gorkhi-Terlej national park at a distance of ca 40 km east of the Mongolian capital, Ulaanbaatar. A blockfield is present at a northwest facing slope at an elevation of ca. 1800 m.a.s.l. (figure 10). South facing slopes are typically sparsely vegetated and feature no permafrost, while north facing slopes are covered by boreal forest and are underlain by discontinuous permafrost (Jambaljav et al. 2008). The climate is continental, with air temperatures ranging from 33 °C in summer to -43 °C in winter. This is a semi-arid site. Jambaljav et al. (2008) measured

air temperatures at a north facing slope on the southern side of the Terelj valley at an elevation of 1656 m.a.s.l. between 2003 and 2007 and found a MAAT of -2.6 °C. They measured ground temperatures at depth are around -1.5 °C to -1.0 °C and low winter snow cover thicknesses around 0.2 m.

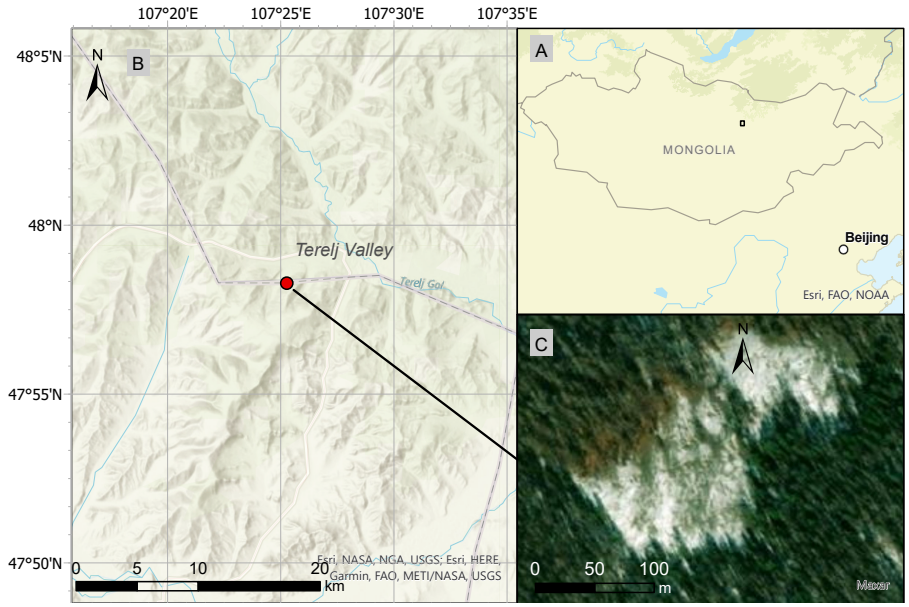

Figure 10: A: Overview map of Mongolia (ESRI and World Open Street Map contributors), with the location of map B indicated by the small black box. B: Map of the Terelj Valley, with the location of the satellite photo in figure C indicated by the red marker (ESRI and World Topographic Map contributors). C: Blockfields in the mountains south of the Terelj Valley (ESRI and Maxar World Imagery contributors).

Retezat, Romania. Information on permafrost and rock glaciers in (south-)eastern Europe is limited, but Ichim (1978) identified the Retezat Mountains, in the southern Carpathians, as area with frequent rock glacier occurrence. Landforms that consist of large blocks (such as blockfields and rock glaciers) usually occur above 1700 m.a.s.l. (Vespremeanu-Stroe et al. 2012). The 0 °C MAAT isotherm is at around 2000 or 2100 m.a.s.l. for north- and south-facing slopes respectively. Air temperatures range between 20°C and -25°C. The average snow cover thicknesses are around 1.5 m at high elevations (Vespremeanu-Stroe et al. 2012). Used as example site is the a rock glacier (figure 11) at an elevation of ca. 2100 m.a.s.l.. The rock glacier site is near the lower edge permafrost extent.

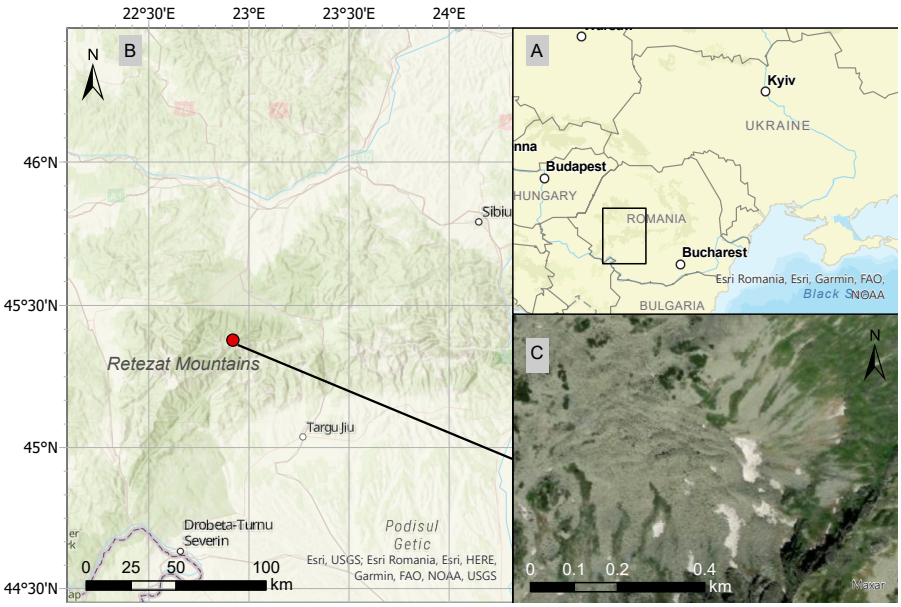

Figure 11: A: Overview map of southeastern Europe (ESRI and Wordl Open Street Map contributors), with the location of map B indicated by the black box. B: Map of the Retezat Mountains, Romania with the location of the satellite photo in figure C indicated by the red marker (ESRI and World Topographic Map contributors). C: Rock glacier and adjacent area (ESRI and Maxar World Imagery contributors).

4 Methods

4.1 CryoGrid

CryoGrid (Westermann et al. 2022 subm.) is a simulation toolbox that can calculate ground temperatures and volumetric water and ice content in permafrost environments. CryoGrid accommodates a broad range of applications thanks to model structure that exists of classes (representations/parameterizations of different processes). Users can therefore use existing or create their own classes that fit their study. A detailed description of the entire model can be found in (Westermann et al. (2022) subm.). In this chapter, key aspects and defining equations of the model setup that are of importance for this thesis will be addressed. In this study, a one-dimensional model setup is used. As climatic forcing data, the model interpolates the surface energy balance. The subsurface stratigraphy features volumetric mineral θ_m, organic θ_o, water θ_w and ice θ_i contents which are specified for each layer of a chosen depth range. The porosity, ϕ is then defined per layer as:

$$\phi = 1 - \theta_m - \theta_o \tag{1}$$

For each layer also a field capacity θ_{fc}, the water content of soil after gravitational drainage, is defined as volumetric fraction of entire volume.

4.1.1 Boundary conditions

The ground thermal regime is mainly determined by the surface energy balance, which serves as the upper boundary in the model setup of this study. The upper boundary condition serves as a coupling to atmospheric forcing data and is used to calculate the energy input to the uppermost grid cell. The surface energy balance is given by the following equation:

$$\frac{\partial H}{\partial t} = S_{in} + S_{out} + L_{in} + L_{out} + Q_h + Q_e + Q_g \tag{2}$$

where $\frac{\partial H}{\partial t}$ is energy input into the uppermost grid cell, S_{in}, S_{out}, L_{in} and L_{out} give the incoming and outgoing short- and longwave radiation fluxes in W/m^2. The sum of the radiation fluxes is the net radiation, which is the most important term of the surface energy balance. Q_h, Q_e and Q_g are the sensible, latent and ground or snow heat flux in W/m^2 respectively. Fluxes are positive if they are towards the surface and negative if they are away from the surface. The required atmospheric forcing data to solve the surface energy balance for the ground heat flux are: Air temperature (°C), rainfall (mm/day), snowfall (mm/day), wind speed (m/sec), incoming short- and longwave radiation (W/m^2), specific humidity (kg water vapor/kg air) and air pressure (Pa). S_{in} and L_{in} are provided directly by the forcing data. S_{out} is derived with the albedo, which depends on the surface cover:

$$S_{out} = -\alpha S_{in}, \tag{3}$$

L_{out} results from Kirchhoff's and Stefan–Boltzmann law:

$$L_{out} = (\epsilon - 1)Lin - \epsilon\sigma(T_{surf} + 273.15)^4, \tag{4}$$

where ϵ is the ground surface emissivity (-), σ the Stefan-Boltzmann constant (W/m^2K^4) and T_{surf} the ground surface temperature (°C). Q_h and Q_e depend on air temperature and humidity gradients:

$$Q_h = -\frac{\rho_a c_p}{r_a^H} \left(T_{air}(h) - T_{surf}\right), \tag{5}$$

$$Q_e = -\frac{\rho_a L_{lg}}{r_a^E} \left(q(h) - q_{surf}\right), \tag{6}$$

where $T_{air}(h)$ and $q(h)$ are the air temperature and specific humidity at height h, provided by the forcing data. q_{surf} is the specific humidity above the surface and results from the surface temperature and the atmospheric pressure. There are several parameters. ρ_a is the density of air (kg/m^3), L_{lg} is the specific latent heat of vaporization, c_p is the specific heat capacity. r_a^H and r_a^E are aerodynamic resistances of the lower atmosphere to turbulent heat transfer. These are calculated depending on atmospheric stability and are calculated from the Monin-Obukhov similarity theory (Monin and Obukhov 1954), see Westermann et al. (2022, subm.) for details. The lower boundary condition is provided by a geothermal heat flux, Q_{geo}, of 0.05 (W/m^2).

4.1.2 Heat transfer and soil freezing

A scheme with heat conduction, following Fourier's law for heat conduction, and heat advection is used for heat transfer and temperature calculation in the subsurface. The rate and amount of heat is determined by the heat transfer equation:

$$\frac{\partial H}{\partial t} = -\frac{\partial}{\partial z}\left(k\frac{\partial T(H)}{\partial z}\right) - c_w\frac{\partial}{\partial z}(j_w T(H)), \tag{7}$$

where k is the thermal conductivity ($W/(mK)$ and c_w is the volumetric heat capacity of water ($J/(Km^3)$ and j_w is the water flux (m/s). k and c are functions of water, ice, mineral, organic and air fractions in the soil (Westermann et al. 2013). The second term describes the heat flux resulting from water advection.

Two types of freezing characteristics of soil moisture are used. In the 'free water' freezing characteristic, water changes state at 0 °C. During this process temperatures are confined at 0 °C. In the 'sand' freezing characteristic, a freeze curve for sand is used, following Dall'Amico et al. (2011). See Westermann et al. (2022, subm.) for details.

4.1.3 Bucket scheme for water balance

For soil hydrology, a bucket water scheme (gravity driven) is used where input from precipitation and condensation infiltrates into the subsurface until the water table. The scheme computes changes in soil moisture contents due to rainfall, evaporation and infiltration.

Rainfall is taken from the forcing data and added to the uppermost cell of the subsurface. The surface energy balance calculations determine how the soil moisture is affected by evaporation. Transpiration plays no part in this study as no vegetated surfaces are involved. The available water in the top of the subsurface determines the latent heat flux, which itself affects soil moisture contents. The potential evaporation is decreased based on the water availability in the soil and the evaporation depth, d_{ev}, which is set to 0.1 m so that evaporation decays exponentially with depth. If the water content in a cell is below the field capacity, θ_{fc}, the water availability, $\sigma(\theta_w)$, is reduced:

$$\sigma(\theta_w) = \begin{cases} 1 & \text{if } \theta_w \geq \theta_{fc} \\ 0.25 \left(1 - cos\left(\pi \frac{\theta_w}{\theta_{fc}}\right)\right)^2 & \text{if } \theta_w < \theta_{fc}. \end{cases} \tag{8}$$

The field capacity is defined for each layer (section 4.3) and is a key factor in determining the results of this thesis. The water flux, for grid cell i, due to evaporation is:

$$j^E_{w,i} = -\frac{\sigma_i}{\sum_i \sigma_i} \frac{Q_e}{\rho_w L_{lg}}, \tag{9}$$

where σ_i is calculated with equation 8. In a frozen soil, the sublimation is set to 0. Water that is in excess of the field capacity infiltrates downwards until either the infiltration limit or a frozen cell is reached. A water table forms if excess water is available and cells are saturated from the bottom upwards. The gravitational flux, j^v_w is described by:

$$j^v_w = \begin{cases} -K_H & \text{if } \theta_w > \theta_{fc} \\ 0 & \text{if } \theta_w \leq \theta_{fc}, \end{cases} \tag{10}$$

where K_H is the hydraulic conductivity. If all grid cells are saturated, excess water is considered as surface runoff.

4.1.4 Lateral drainage

Most studies that used a previous version of CryoGrid (e.g. Westermann et al. 2013; Westermann et al. 2016) considered constant water/ice contents or did not include lateral drainage. This is a major limitation, as varying soil moisture contents strongly affect the ground thermal regime (e.g. Martin et al. 2019). This thesis uses a one-dimensional model and simulates lateral drainage out of the model domain by assuming a seepage face at atmospheric pressure. First, the elevation of the water table is calculated, after which a lateral water flux removes water in grid cells that are below this water table:

$$j^{lat}_{w,i} = -K_H \frac{z_{wt} - z_i}{d^{lat}}, \tag{11}$$

where $j^{lat}_{w,i}$ is the lateral water flux out of cell i, z_{wt} is the elevation of the water table, z_i is the elevation of the cell i and d^{lat} is the lateral distance to the seepage face. The distance

of the model realization to the seepage face can be varied where short distances result in a well drained column and large distances result in a poorly or undrained column. By varying d^{lat}, the strength of drainage can thus be controlled, making it a crucial variable in determining the results of this thesis. Two levels of drainage are used. A distance of 10^4 m is used for *undrained* cases, which emulates conditions at a mostly flat surface, and a distance of 1 m for *drained* cases, which emulates conditions at a slope. The seepage face drains over the entire column depth proportional to the water table.

4.1.5 Snow

The snow scheme used in this thesis is introduced by Zweigel et al. (2021) and is based on the CROCUS snow scheme (Vionnet et al. 2012). It is a one-dimensional physical snow scheme with multiple layers. Snowfall is added on the surface with density and grain properties derived from atmospheric forcing data. The density of fresh snow increases with of wind speed and air temperature. Higher wind speed also result in more rounded snow grains. A key feature of the CROCUS snow scheme is the dynamical evolution of thickness and amount of snow layers in order to best represent natural snow packs.

After deposition, the snow pack undergoes a transient evolution of snow grains and density. It can be described in a phenomenological way by a set of quantitative laws (Vionnet et al. 2012). Both dry and wet metamorphism are described in the scheme. Dry metamorphism depends mostly on the vertical temperature gradient in the snow pack and features a set of empirical laws (Vionnet et al. 2012). Wet metamorphism depends on the volumetric water content in the snow and the angularity of the grains. The effects that result from the metamorphism include a decrease of dendricity over time, rounding of grains when water is present and/or temperature gradients are small, faceting (increase of angularity), when temperature gradients are high and the growth of round grains when conditions are wet (Zweigel et al. 2021).

Several processes give rise to an increase in snow density. Compaction of snow layers as a result of vertical stress from overlying layers raises the density. Next, the physical effect of wind drift on the snowpack is included in the scheme, which breaks up snow grains. Fresh snow is most susceptible to wind drift. Redistribution by wind is not included in the model setup of this thesis. The amount of incoming snow is adjusted by changing the so-called snowfall factor (sf) to phenomenologically represent redistribution of snow by wind. Values above 1 represent net accumulation and values below 1 represent net ablation of snow.

Then, evolution of albedo and transmission of solar radiation are handled. Transmission and reflection are handled on three separate spectral bands, which allows for effects that only affect a small part of the spectrum. Next, surface fluxes are computed. Energy and mass transfer in the snowpack includes heat conduction, percolation of rainfall and percolation of meltwater. The temperature profile within the snow is then resolved and at the bottom of the snowpack, the snow scheme is coupled to the uppermost ground class and features heat conduction into or out of the ground. The temperature and density profile allow for a calculation of the heat content, or enthalpy, of the snowpack, which is compared to the amount of energy needed for melting. Then, either the complete snow

pack or a part of it is melted. Temperature and water content are derived from the heat content and water plus ice content. Water flow happens when the unfrozen water content exceeds the field capacity of snow. Snow sublimation is then handled according to the turbulent vapor fluxes. Finally, the properties of the snowpack are updated in order to ensure coherence between properties and variables. The parameters in the snow scheme are presented in table 1 and are set to default values from Vionnet et al. (2012). The parameters are constant among all simulations in this study.

Table 1: Snow and ground parameters used in all simulations.

Parameter	Value
Ground	
Albedo	0.15
Emissivity	0.99
Roughness length	0.001 m
Hydraulic conductivity	10^{-5} m/s
Snow	
Emissivity	0.99
Roughness length	0.001 m
Hydraulic conductivity	10^{-4} m/s
Field capacity	0.05

4.2 Validation, equilibrium and transient runs

Three types of CryoGrid runs are distinguished, each created to achieve a separate goal: validation runs, equilibrium runs and transient runs. The validation runs are set up to compare modelled ground temperatures with field measurements at the two sites in Norway. At the ancillary sites, no validation data is available, so no comparison with measurements is done. At Juvvasshøe, measurements consist of borehole data from the year 2000 to 2020, allowing a comparison at different depths. The depths that are used for the comparison are 0.2 m and 2.0 m. At the rock glacier in Ivarsfjorden, comparison of model results with in situ measurements can be done with the present ground surface temperature (GST) monitoring network (Lilleøren et al. 2022). The GST is measured from 13 July 2016 to 12 July 2019 at 11 locations (figure 8C).

The equilibrium runs aim to investigate the effect of three idealized stratigraphies under a range of snowfall amounts on the ground thermal regime and ground ice table for a stable climate. These are called equilibrium runs as short periods, 10 years, of relatively stable climate are used and iterated several times (see section 4.5). Each stratigraphy is modelled with both *undrained* and *drained* drainage levels, resulting in six scenarios. Equilibrium runs are performed for all of the sites. This will allow for a comparison of equilibrium ground temperatures between a range of different permafrost climates. In order to investigate the effect of various amounts of lateral drainage, simulations have been performed with a distance to the seepage face, d^{lat}, of 1 m, 10 m, 100 m, 1000 m and 10000 m. This means that each of these steps results in a lateral drainage flux that

is decreased by a factor of 10 (equation 11). This analysis is anchored at the location of the PACE borehole at Juvvasshøe. Additionally, the effect of two different subsurface stratigraphies on the rate and timing of subsurface drainage in Terelj, Mongolia and at Juvvasshøe is examined. This is applied to Terelj since this is a semi-arid site and the mountains around the valley are of importance for the water balance at the nearby settlement (Tuvshinjargal and Saranbaatar 2004). A comparison can then be done with a site that features more precipitation (Juvvasshøe).

The goal of the transient runs is to analyze how the ground temperatures and ground ice table may have developed from 1951 to 2019 under different idealized stratigraphies (section 4.3). These runs are done for the two sites in Norway, as they require long time series of forcing data and validation runs. The rock glacier in Ivarsfjorden is of most interest as only a small remnant of ice is believed to be left (Lilleøren et al. 2022). Another objective of the transient simulations is to investigate warming rates at the different sites. This is done by calculating the difference in mean 2 m ground temperature between the 1951-1960 and 2010-2019 means. For both sites, two snowfall factors are used in order to examine the effect of snowfall amounts on the warming rates. The ground stratigraphy, handling of snow, climatic forcing data and temperature initialization for the three run types are discussed in the following sections.

4.3 Ground stratigraphy and snow

The porosity of the ground and depth of the bedrock are important factors in the ability of ground to hold water. In permafrost regions this thus has a large effect on ice formation and latent heat exchange in the subsurface (Westermann et al. 2013). Three idealized ground stratigraphies are set up in order to effectively investigate the effect of water drainage on the ground thermal regime and ground ice. These will be referred to as the *blocks only*, *blocks with sediment* and *sediment only* stratigraphies (Table 2). Initial water/ice contents are assumed to saturate the pores, though these contents are not static and thus change over the simulation period. In all stratigraphies, bedrock is assumed below 5 m depth. Also, the bedrock properties of 3 % porosity and saturated conditions are kept constant throughout the study, which is in agreement with Hipp et al. (2012) and Farbrot et al. (2011).

The *blocks only* stratigraphy consists of a coarse block layer with 50 % porosity of 5 m thickness on top of bedrock. The coarse blocks have a low field capacity. This idealized column can be realistic on a rock glacier where finer sediments that result from weathering and erosion processes are transported towards the tongue of the rock glacier or on a blockfield at a relatively steep slope (Dahl 1966). The second stratigraphy, *blocks with sediment*, does include the finer sediment fraction that takes up 50% of the pore space between the coarse blocks, resulting in 25 % porosity and a higher field capacity. Finally, the *sediment only* stratigraphy contains sediments with the same porosity as the *blocks only* stratigraphy in order to remain consistent. They are differentiated by a higher field capacity in the *sediment only* stratigraphy.

A changing snow cover is the main source of spatial variability in Norwegian mountains (Gisnås et al. 2016). Following these studies, the sensitivity of the scenarios models

to various amounts of snowfall is analyzed. Between model runs, the snow module is completely unchanged and adjustments are only made in the snowfall factor to create a larger or smaller snowpack.

Table 2: Three idealized sediment stratigraphies. The values indicate the volumetric fractions of the soil constituents. Soil freezing characteristics are explained in section 4.1.2.

Depth (m)	Mineral	Organic	Porosity	Field capacity	Soil freezing
Blocks only					
0-5	0.5	0.0	0.5	0.01	Free water
>5	0.97	0.0	0.03	0.03	Free water
Blocks with sediment					
0-5	0.75	0.0	0.25	0.15	Free water
>5	0.97	0.0	0.03	0.03	Free water
Sediment only					
0-5	0.5	0.0	0.5	0.25	Sand
>5	0.97	0.0	0.03	0.03	Free water

The stratigraphies and snowfall factors that are used in the different types of model runs are discussed below:

Validation runs. For the validation runs with the borehole data in Juvvasshøe, different stratigraphies were tested until a good fit between modelled and measured ground temperatures at 2.0 m and 0.2 m depth was established. The blockfield class from Westermann et al. (2013) (table 3) is used as a starting point. Because of the observations of finer sediments between 1.5 m and 5 m (Isaksen et al. 2003), the mineral content is increased in order to find a better fit. As this site is extremely exposed to wind and snow is blown away, the snowfall factor is given values below 1 to represent the loss of snow. The stratigraphies used for the comparison at the rock glacier in Ivarsfjorden are the *blocks with sediment* and *sediment only* stratigraphies since these are considered most appropriate at this site (see section 5.1.2). In addition, the blockfield stratigraphy that is described in Westermann et al. (2013) is included.

Table 3: Blockfield stratigraphy from Westermann et al. (2013). The values indicate the volumetric fractions of the soil constituents. Soil freezing characteristics are explained in section 4.1.2.

Depth (m)	Mineral	Organic	Porosity	Field capacity	Soil freezing
0-2	0.6	0.0	0.4	00.1	Sand
2-5	0.6	0.0	0.4	0.15	Sand
>5	0.97	0.0	0.03	0.03	Sand

Equilibrium runs. The equilibrium runs simulate the equilibrium ground temperature for the three idealized stratigraphies in both *drained* and *undrained* state. For each scenario CryoGrid is run with snowfall factors of 0.0, 0.25, 0.5, 0.75, 1.0 and 1.5. This approach allows for an estimation of the threshold amount of snow above which permafrost will no longer exist in each of the six scenarios. At values for the snowfall factors larger than 2.0 at Juvvasshøe, snowfall is high enough so that the snowpack can survive the summer and thus a perennial snow patch and eventually a glacier will form. For the ancillary sites, just the *blocks only* and *blocks with sediment* scenario are modelled as the cooling effect of drainage is most significant between these stratigraphies.

Transient runs. All three idealized stratigraphies (table 2 are used to simulate the transient change in ground temperature and ground ice content. The susceptibility to thawing under a warming climate is investigated. For each of the Norwegian sites, the best-fitting snowfall factor from the validation runs is chosen for the transient analysis. Additionally, for both sites the scenarios are modelled with a second snowfall factor in order to analyze their sensitivity to different amounts of snow. A snowfall factor of 0.25 and 0.5 for Juvvasshøe 1.0 and 0.5 for Ivarsfjorden are used.

4.4 Climatic forcing data and downscaling routine

The meteorological data that was used to force CryoGrid at the two sites in Norway was generated by applying a topography-based downscaling routine, TopoSCALE (Fiddes and Gruber 2014), to ERA5 reanalysis data (Hersbach et al. 2020). The forcing data for the sites in Russia, Mongolia and Romania are available from already existing work (discussed in section 4.4.3).

4.4.1 ERA5 reanalysis data

ERA5 is a global atmospheric reanalysis produced by the European Centre for Medium-Range Weather Forecasts (ECMWF) and is part of the Copernicus Climate Change Service. The horizontal resolution of the reanalysis is 0.25°x 0.25°. Outputs are given at both the earth surface level and at pressure levels with a vertical coverage of 1000 hPa to 1 hPa. The output exists of hourly data from 1951 to 2019 and is split in 1951-1979 and 1979-2019 where the former is a preliminary back extension. In this study, the entire period from 1951 to 2019 is considered. Data is taken from the 4 nearest ERA5 grid points to the sites in order to perform a horizontal interpolation.

From the surface level data, the following variables were taken: 2 meter air and dew-point temperature, 10 meter meridional (northward) and zonal (eastward) wind velocity components, surface pressure, constant surface geopotential, incoming longwave radiation, incoming shortwave radiation, and total precipitation. And on the pressure levels: air temperature, specific humidity, zonal and meridional wind velocity components, and dynamic geopotential. A subset of pressure levels was considered, close to the elevatoin of the sites. The ranges are 900 hPa to 700 hPa for Juvvasshøe and 1000 hPa to 900 hPa for Ivarsfjorden were used.

4.4.2 Terrain parameters and downscaling routine

In order to perform the topography-based downscaling to the ERA5 data, terrain parameters derived from a digital elevation model (DEM) are required. TopoSCALE relies on the following terrain parameters: elevation, slope, aspect, sky view factor, and horizon angles. Dozier and Frew (1990) presented post-processing routines to obtain these parameters. ArcticDEM version 3.0 Pan-Arctic (Porter et al. 2018) is generated from Maxar satellite data. A DEM with a spatial resolution of 32 m is used.

TopoSCALE was then used to perform topography-based downscaling. TopoSCALE (Fiddes and Gruber 2014) is developed in order to downscale atmospheric reanalysis data in complex (mountain) terrain. It has been used for e.g. estimating mountain permafrost distribution (Fiddes et al. 2015), snow data assimilation (Aalstad et al. 2018) and the downscaling of regional climate models (Fiddes et al. 2022). The TopoSCALE scheme consists of a sequence of topographic corrections to downscale reanalysis data onto a target grid which is defined by the DEM. The corrections are: (1) horizontal interpolation of the meteorological parameters onto the target grid using inverse distance weighting, (2) linear vertical interpolation of wind speed, humidity, and temperature (3) scaling of the shortwave radiation by accounting for differences in elevation, local illumination geometry, and shading of the the terrain, and finally, (4) adjusting the longwave radiation to account for changes in emissivity and terrain that are blocking the sky hemisphere. After the downscaling, all meteorological variables are provided in order to run CryoGrid. The input variables are described in section 4.1.1.

4.4.3 Forcing data at the ancillary sites

For the three study areas outside Norway, standardized forcing data that were already available from existing work are used. The main objective is to investigate thermal anomalies caused by a well drained, blocky subsurface in contrasting climates. Results from the three ancillary sites are not compared to measurements. However, large scale differences in terms of MAAT, precipitation and continentality, which fits the objective of these simulations, are captured in the forcing data. For the Verkhoyansk Mountains, the data is provided by Nitzbon et al. (2019), which is a study located on Samoylov Island in the Lena River delta. The data is based on in situ measurements from Boike et al. (2019) and gap-filled with ERA5 reanalysis data. No blockfields are present in this delta, but the northern Verkhoyansk Mountains east of the delta feature sparsely vegetated areas with a coarse surface cover. For Terelj, the forcing data is ERA5 reanalysis data at the closest grid cell to the blockfield in figure 10. Finally, forcing data in Retezat is from ERA5 reanalysis data, downscaled with TopoSCALE.

4.5 Model initialization

For the validation runs both at Juvvasshøe and Ivarsfjorden, the model is run for the entire period of available forcing data. At Juvvasshøe the initial ground temperature profile is taken from the borehole data. At Ivarsfjorden the model is initialized to near

equilibrium conditions with the first 10 years of available forcing data. The comparison at Juvvasshøe is done for the years 2010 to 2019 and at Ivarsfjorden for the years 2016 to 2019. This leaves more than 60 years for the model to reach equilibrium with the climate at the depths used for comparison and to be independent of initialization.

In order to reach steady state conditions, a 10 year period chosen and iterated three times until a steady state temperature profile of the upper 5 meters is established. For Juvvasshøe, the period 2000-2010 is selected as the model can be initialized with real-time borehole data. For the Ivarsfjorden equilibrium runs, the period 1960-1970 is selected as this relatively stable period is more likely to be in permafrost conditions than later decades.

The goal of the transient runs is to investigate the warming and possible degradation of permafrost and ground ice from 1951 to 2019 for the different model scenarios. An initialization with a stable ground ice table is required. This is achieved by iterating three times over the coldest 10 year period in the forcing data, from 1962 to 1971, until equilibrium conditions with a stable ice table are present. This is the closest available data to Little Ice Age conditions, when the rock glacier in Ivarsfjorden is hypothesized to have been active (Lilleøren et al. 2022). This initialization period is then followed by the entire forcing data set from 1951 to 2019. Transient runs for Juvvasshøe are set up by the same procedure. As in Ivarsfjorden, the coldest 10 year period in the available data was from 1962 to 1971.

Finally, the model runs that aim to explore the different ways that ground ice forms during permafrost aggradation are initialized with positive ground temperatures, 3 °C warmer than temperatures at the PACE borehole at Juvvasshøe.

5 Results

5.1 Comparison to field measurements

5.1.1 Juvvasshøe

Model results of validation runs at Juvvasshøe are compared with measured ground temperatures at the PACE borehole. The best-fitting stratigraphy is presented in table 4 and the corresponding snowfall factor is 0.25. The model is run for the entire period of available meteorological forcing data, from 1951 to 2019. Figure 12 shows the comparison of measured ground temperatures with modelled temperatures at 2 m and 0.2 m depth for the best-fitting model configuration. No borehole data was available for the period 21 December 2011 to 24 April 2014. The model simulates temperatures at 2 m depth better than at 0.2 m depth as the effect of the extreme variability of the ground surface temperature is dampened. At 2 m depth, a slight cold bias exists for annual maxima close to 0 °C. The snowfall factor for this model setup is 0.25, meaning the model reduces incoming snow by 75% in order to represent wind-blown snow. This resulted in mean annual maximum snow depths of 34 cm. Despite the use of downscaled climatic forcing data, the model can reproduce measured ground temperatures. Model runs that used a freeze curve for sand instead of the free water freezing characteristic, did not feature significant differences to the results that are presented here.

Table 4: Stratigraphy that results in the model that best fits measured ground temperatures at Juvvasshøe with a snowfall factor of 0.25. The values indicate the volumetric fractions of the soil constituents. Soil freezing characteristics are explained in section 4.1.2.

Depth (m)	Mineral	Organic	Porosity	Field capacity	Soil freezing
0-5	0.8	0.0	0.2	0.1	Free water
>5	0.97	0.0	0.03	0.03	Free water

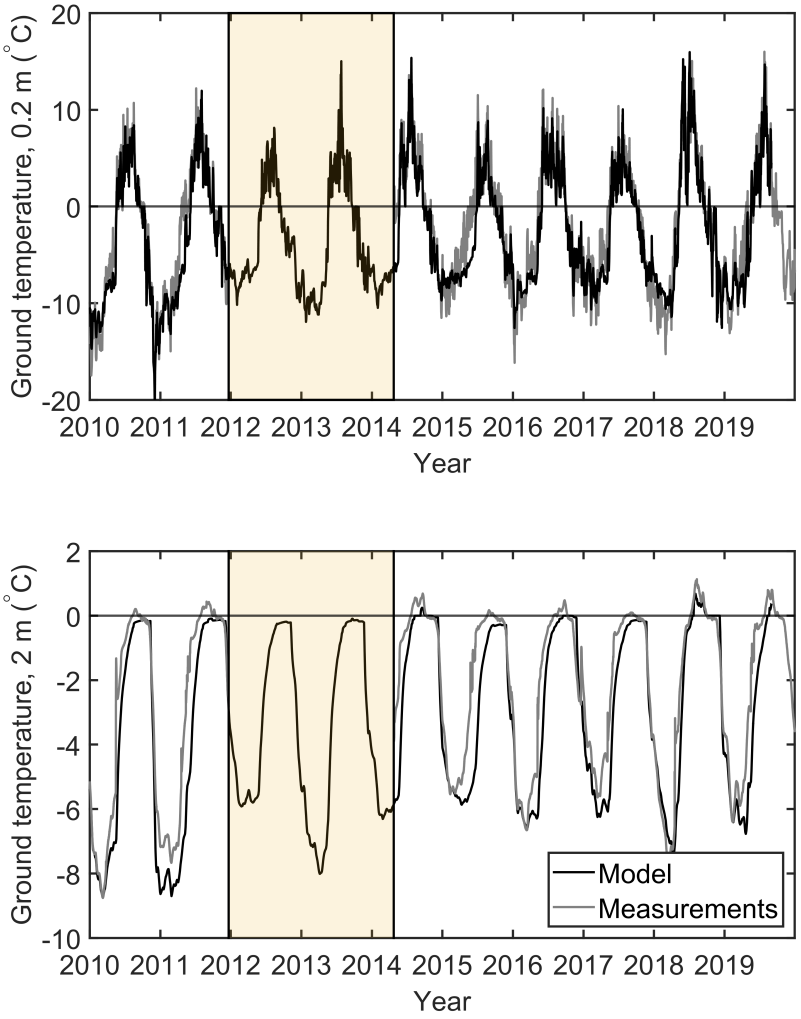

Figure 12: Modelled and measured ground temperature at the PACE borehole in Juvvasshøe at 0.2 m (upper panel) and 2.0 m (lower panel) depth. The shaded area indicates the period where no borehole data is available. The used stratigraphy of is presented in table 4.

5.1.2 Ivarsfjorden rock glacier

At the rock glacier in Ivarsfjorden, no borehole exists. A comparison between modelled and measured temperature is therefore done with data from a ground surface temperature logger network (figure 8). The loggers are located in voids close to the surface (Lilleøren et al. 2022). All loggers except for one are placed on the relict surface of the rock glacier, where the surface does not consists of just coarse blocks, but also contains finer sediment in between. Here, the *blocks with sediment* stratigraphy is considered most appropriate. At depth, also the *sediment only* stratigraphy might be appropriate. The two locations that are termed 'rock glacier, fresh surface' in figure 8 contain larger boulders. However, the temperature logger on the fresh surface did not indicate a significantly lower MAGST

compared to those in the forefield or on the 'relict' surface (Lilleøren et al. 2022). The three years of data at 11 locations on and near the rock glacier are presented together with six model validation runs (figure 13). These consist of the *blocks with sediment* and *sediment only* stratigraphies, as they are considered more appropriate, in addition to the blockfield stratigraphy from Westermann et al. (2013), each in a *drained* and *undrained* configuration. As for the comparison to the borehole data at Juvvasshøe, the model is run for the entire period of available forcing data. Measured MAGST fall between 1.1 °C and 4.1 °C. Modelled MAGST are in the range of 2.0 °C and 2.7 °C. The loggers are spread within the area of the rock glacier where small scale spatial variations in topography, snow accumulation, ground stratigraphy and vegetation play a role. The model results are realized at one point with the same forcing input and therefore show a tighter spread.

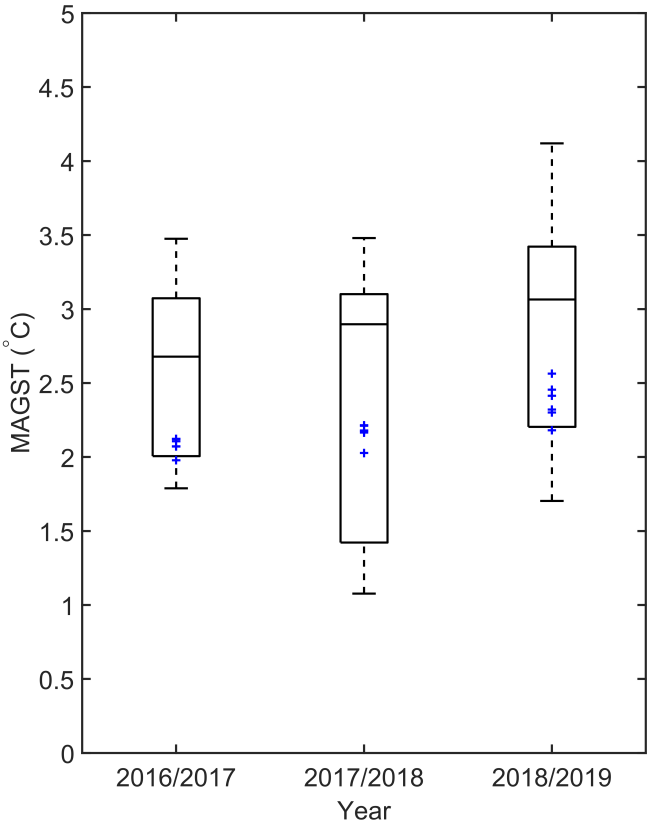

Figure 13: Modelled and measured MAGST in Ivarsfjorden during three years, from 13 July 2016 to 12 July 2019. The bars indicate the 25th and 75th percentile of measured MAGST and the whiskers represent the maximum and minimum temperatures. The blue indicators show modelled MAGST during the same period for three ground stratigraphies, *drained* and *undrained*, for a snowfall factor of 1.0.

5.2 Simulated thermal regime and ground ice in Norway

In this section, the results from the simulations at Juvvasshøe and in Ivarsfjorden will be presented. First, the differences in ground ice content between scenarios is addressed.

Then, the effect of different levels of drainage on the equilibrium ground temperature is shown. Next, differences in equilibrium ground temperatures at various degrees of snowfall are presented for the three idealized stratigraphies (from table 2). This sensitivity analysis is done because differences in snow cover are the main source of spatial variability in Norwegian mountains (Gisnås 2016) and from section 3.3.1 we know that the snow cover at Juvvasshøe is variable and strongly reduced by wind redistribution. Lastly, the transient evolution of ground temperatures and ground ice at the two sites in Norway between 1951 and 2019 for different model scenarios is displayed. The goal of these transient simulations is to compare warming rates between the two sites and to simulate degradation of ground ice at the Ivarsfjorden rock glacier.

Figure 14 shows the volumetric ground ice contents in the upper 2 meters of the ground for the *drained* simulations for the *blocks only* and *blocks with sediment* stratigraphy. The figure applies to one hydrological year at Juvvasshøe and aims to visualize the effect of a subsurface of blocks that is well drained on ground ice contents. The main result is that in the *blocks only, drained* stratigraphy almost no ice is present above the perennial ice table, while in the *blocks with sediment, drained* stratigraphy the complete pore space is filled with ice. In the *blocks only* image, snow melt that infiltrates at the end of spring refreezes at the ice table, resulting in an increasing ice content (indicated by the arrow). The saturated volumetric ice content of 0.5 is a result of the given porosity in this stratigraphy (see table 2). The low field capacity in this stratigraphy results in almost no water being held against gravity. The volumetric ice content in the *blocks with sediment* runs is lower due to the higher mineral content and thus lower porosity of 0.25. The remaining scenarios *(blocks only, undrained; blocks with sediment, undrained; sediment only, drained* and *sediment only, undrained*) all show a similar image to the *blocks with sediment, drained* figure, though volumetric water contents are different depending on the porosity and field capacity. These differences in the ground ice mass balance affect the ground thermal regime, which will be addressed in the next section. The term 'ground ice mass balance' is used for change in ground ice content.

Figure 15 shows the effect of an increasing drainage rate on ground temperatures for the three idealized stratigraphies at Juvvasshøe. Clear is that a low distance to a seepage face, thereby representing a well drained soil column (see section 4.1.4), mainly affects runs with the *blocks only* stratigraphy. By decreasing the distance to a seepage, we can perform a sensitivity analysis towards drainage.

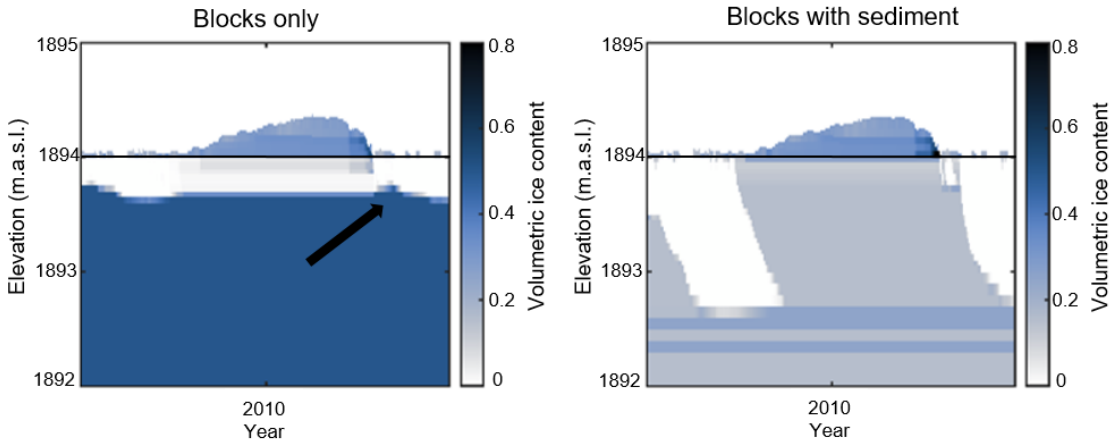

Figure 14: Modelled volumetric ground ice content in the upper 2 meter of the ground for the *blocks only* and *blocks with sediment* stratigraphy, both drained. Shown is one hydrological year at Juvvasshøe. Indicated with the arrow is the ice that builds up after infiltrated snow melt refreezes. The ground surface is at 1894 m.a.s.l., meaning that ice above this elevation is the snow cover. The snowfall factor is 0.25 for all simulations.

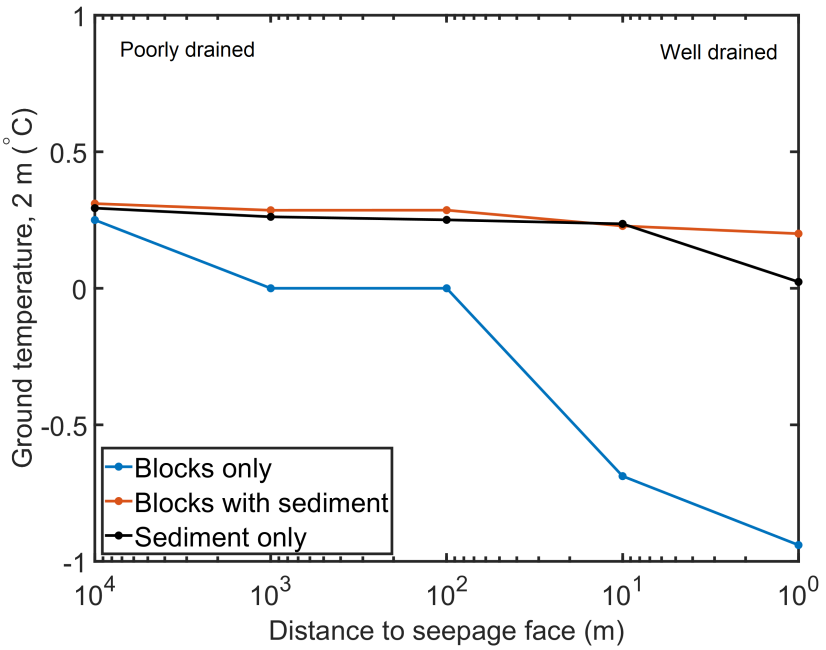

Figure 15: Mean annual ground temperatures at 2 m depth at different distances to the seepage face in the idealized stratigraphies at Juvvasshøe. The magnitude of lateral drainage is inversely proportional to the distance to the seepage face. The snowfall factor is 1.0 for all simulations.

5.2.1 Sensitivity to snowfall

Annual maximum snow depths at a snowfall factor of 1.0 are between 1.5 m and 2.4 m at Juvvasshøe and between 0.4 m and 1.0 m at Ivarsfjorden. Figure 16 shows the equilibrium ground temperature at 2 m below the surface for the three stratigraphies at different snowfall factors at the two sites. For each of the three stratigraphies there is the *drained* and the *undrained* model setup. At both sites there is a clear pattern of lower temperatures in the *blocks only, drained* scenario (solid blue line) compared to all five other scenarios. For snowfall factors of 0.75 and larger, the difference in ground temperature between *blocks only, drained* and the next coldest scenario is in the range of 1.2 °C and 1.4 °C at Juvvasshøe and in the range of 1.1 °C and 1.5 °C at Ivarsfjorden.

At Juvvasshøe, all three *undrained* scenarios feature positive ground temperatures at snowfall factors of 0.75 and above. Temperatures in the *blocks with sediment, drained* and *sediment only, drained* runs are positive from snowfall factor 1.0. The ground temperature in the *blocks only, drained* runs remains below -1.0 °C for all snowfall scenarios. A similar pattern is seen in Ivarsfjorden, though a snowfall factor of 1.5 results in positive temperatures for scenario *blocks only, drained*. Temperatures for the *blocks with sediment* stratigraphy are positive at a snowfall factor of 0.5 and above. This was a snowfall factor of 0.75 for the other scenarios with the exception of the *blocks only, drained* scenario. The increase from a snowfall factor of 0 to 0.25 leads to a slight cooling for the *drained* scenarios as opposed to a slight warming in the *undrained* scenarios. For all other increases in snowfall factor, ground temperature at 2 m depth increases, a result of the insulating effect of snow on the underlying ground.

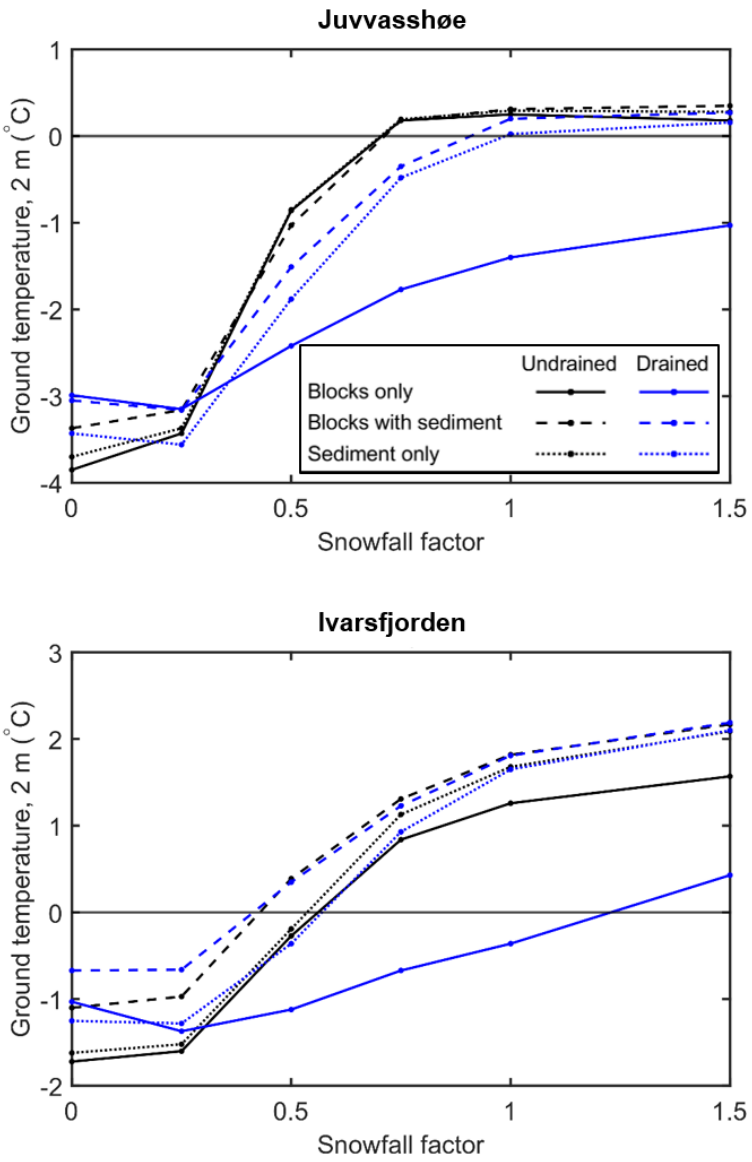

Figure 16: Equilibrium ground temperature at 2 m depth for three idealized stratigraphies (table 2) in *undrained* and *drained* states at Juvvasshøe and the Ivarsfjorden rock glacier.

5.2.2 Transient response of ground temperatures and ice content

The forcing data makes it possible to model the evolution of the ground thermal regime and ground ice content from 1951 to 2019. Figure 17 shows the ground ice content for the scenarios in Ivarsfjorden. In all simulations, a stable ice table has formed during the spin up period, which means that the change from 1951 is a result of the climate and not a remnant of the initialization. The thin vertical lines of ice content represent the seasonally freezing active layer. In the *blocks only, drained* scenario, the ice table does not lower by a significant amount. In all other simulations, the ice table lowers significantly. The saturated volumetric ice content of 0.5 is a result of the porosity in this stratigraphy (table 2). The perennial ice table in the upper 5 m of the *blocks with sediment* stratigraphy disappeared by 1985 and 1975 in the *undrained* and *drained* scenarios respectively.

The saturated volumetric ice content is 0.25. Finally, the *sediment only* simulations show an intermediate effect where the ice table has dropped to approximately half of its initial height by 2019. So we can see three different responses of the ground ice table to atmospheric warming. A full degradation in both the *blocks with sediment* runs, partial degradation in the *blocks only*, *undrained* run and in both *sediment only* runs and finally, no degradation of ground ice in the *blocks only, drained* simulation.

The transient evolution of the ground ice content in in Juvvasshøe is presented in figure 18. A large ice table remains in all scenarios, despite the enforced climatic warming. The saturated volumetric ice content is lower in the *blocks with sediment* simulations, following the given porosity of 0.25. A slight lowering of the ice table happens in these scenarios. Similarly, in the runs with the best-fitting stratigraphy from the validation, a minor decrease of the ice table occurs. This lowering is 0.4 m in the drained case.

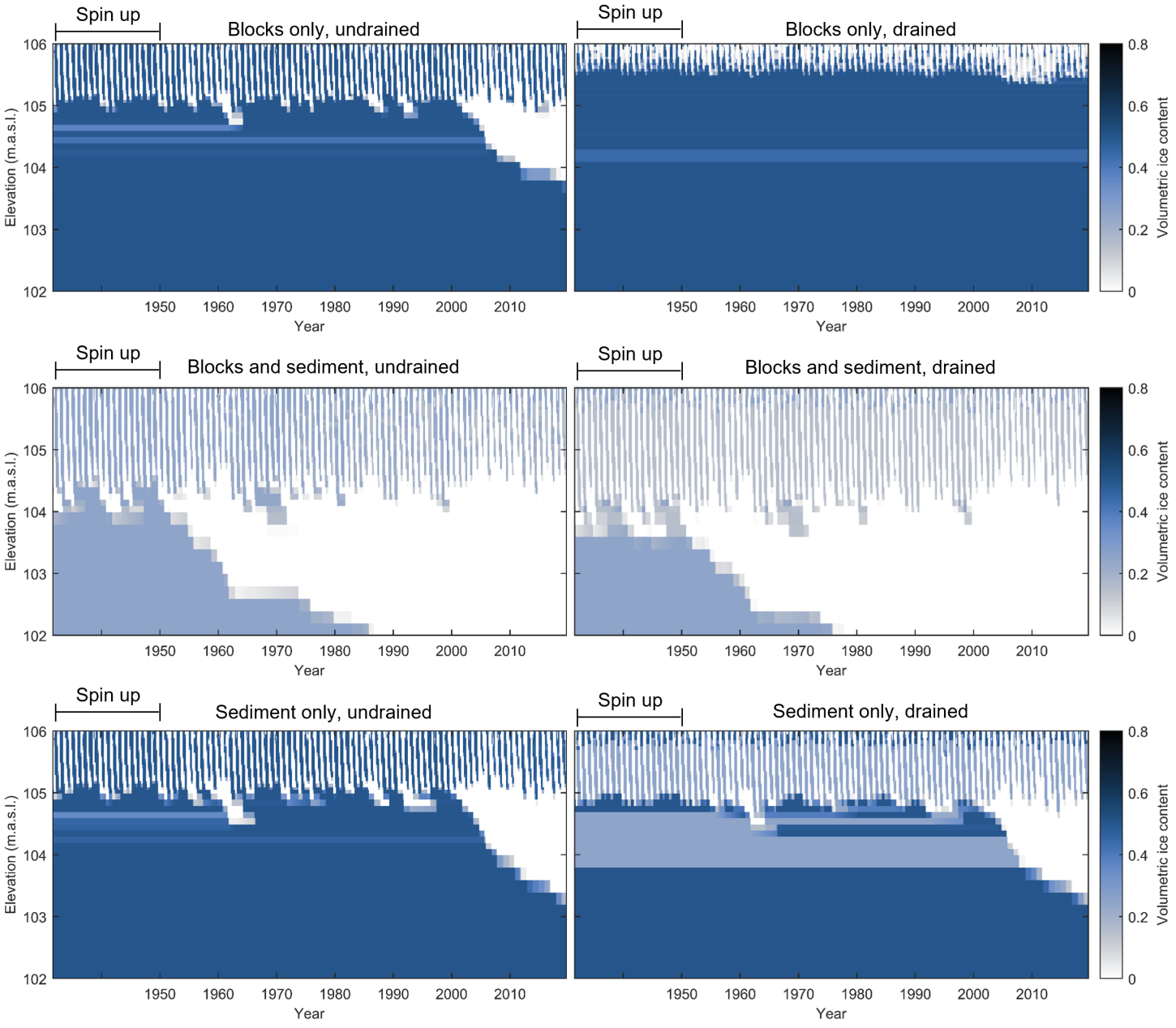

Figure 17: Modelled volumetric ground ice content at Ivarsfjorden for the three idealized stratigraphies in *undrained* and *drained* conditions. The snowfall factor is 1.0 in all simulations.

The change in 2 m ground temperature between 1951-1955 and 2015-2019 is summarized in table 5. A clear difference between the sites is that in all simulations temperatures at Juvvasshøe increased more than in Ivarsfjorden. In the Juvvasshøe simulations, warming is between 0.7 °C and 1.0 °C and in Ivarsfjorden between 0.1 °C and 0.9 °C. The temperature in Ivarsfjorden is higher and thus closer to the freezing point, meaning that relatively more energy is used to melt ground ice as opposed to increasing temperatures. The change in ground ice content can be seen in table 6. At Juvvasshøe, the loss in ground ice is minimal in all scenarios except in the *blocks with sediment, drained* run where 10% of the ground ice below the annually freezing zone has melted. In Ivarsfjorden, ground

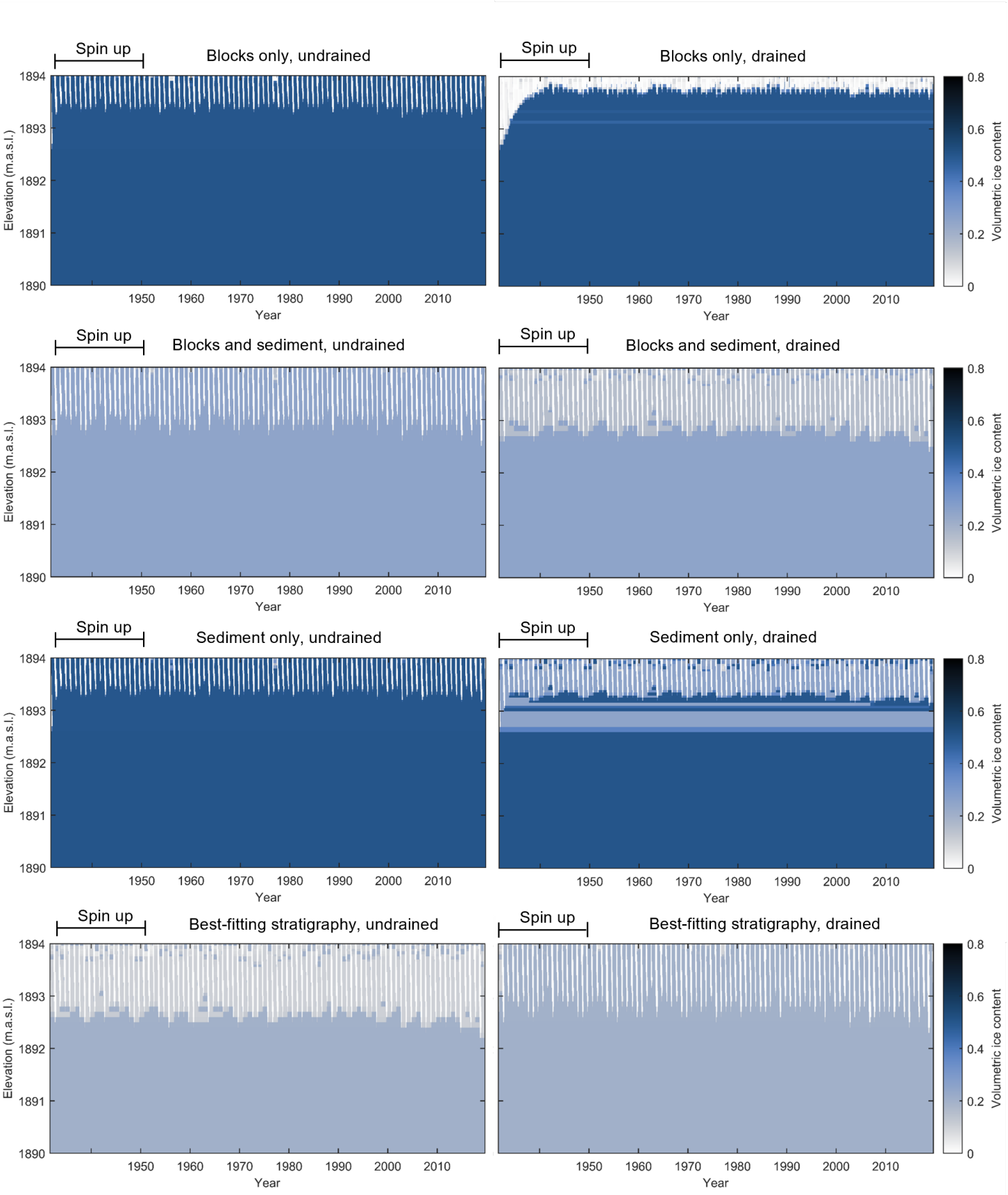

Figure 18: Modelled volumetric ground ice content at Juvvasshøe for the three idealized stratigraphies (upper three rows) and the best-fitting stratigraphy (bottom row) in *undrained* and *drained* conditions. The snowfall factor is 0.25 in all simulations.

ice losses are much higher and in the runs with the *blocks with sediment* stratigraphy and a snowfall factor of 1, all ice below the annually freezing zone has melted. All transient simulations at Ivarsfjorden show significant ice loss except the runs with a *blocks only, drained* setup.

The differences between the two snowfall factors in Juvvasshøe are low. In four of the six scenarios, the warming at 2 m depth is equal, while in the remaining two the warming is 0.1 °C higher in runs with a snowfall factor of 0.25. The scenario *blocks with sediment, drained* is the only scenario where the change in ground ice is significantly different between the two snowfall factors.

The variance in the effect of different snowfall factors is more pronounced at Ivarsfjorden. There is a difference up to 0.5 °C in warming at 2 m depth. Inversely, the decrease in volumetric ice content in the *blocks only, undrained* scenario are 7% and 33% for a snowfall factor of 1.0 and 0.5 respectively. This inverse relationship between changes in temperature and ground ice occurs in several scenarios at Ivarsfjorden. It is explained by the fact that scenarios with a lower steady state temperature require a larger temperature increase in order for ground ice to melt. On the other hand, in a scenario with temperatures close to 0 °C, an increased energy input from the atmosphere leads to the melting of ground ice instead of increasing the temperature. In the runs with a *blocks with sediment* stratigraphy, both the warming and loss of ground ice are high, meaning these scenarios are most susceptible to a change in climate.

Table 5: Change in average 2 m ground temperature between the periods 1951-1960 and 2010-2019 mean. sf: snowfall factor.

		Blocks		Blocks with sediment		Sediment only	
		Undrained	Drained	Undrained	Drained	Undrained	Drained
Juvvasshøe	sf = 0.25	0.3 °C	0.1 °C	0.4 °C	0.4 °C	0.3 °C	0.3 °C
	sf = 0.5	0.5 °C	0.4 °C	0.6 °C	0.6 °C	0.5 °C	0.5 °C
Ivarsfjorden	sf = 1.0	0.1 °C	0.4 °C	0.7 °C	0.7 °C	0.1 °C	0.1 °C
	sf = 0.5	0.6 °C	0.5 °C	0.3 °C	0.3 °C	0.5 °C	0.5 °C

Table 6: Change in ground ice content in the upper 5 m below the annually freezing zone between 1951 and 2019 for two snowfall factors. sf: snowfall factor.

		Blocks		Blocks with sediment		Sediment only	
		Undrained	Drained	Undrained	Drained	Undrained	Drained
Juvvasshøe	sf = 0.25	-1%	-1%	-3%	-10%	0%	-1%
	sf = 0.5	-1%	-1%	-3%	0%	-1%	-1%
Ivarsfjorden	sf = 1.0	-33%	-2%	-100%	-100%	-44%	-37%
	sf = 0.5	-7%	-1%	-92%	-100%	-23%	-26%

The changes in ground temperature are determined by the ground ice table. Figure 19 shows the change in temperatures at 5 m depth for the *drained* scenarios, representing a fully, partially and not lowering ice table at the Ivarsfjorden rock glacier for a snowfall factor of 1.0. The depth of 5 m is chosen here minimize the seasonal variation and to emphasize the long-term warming. The *blocks only* simulation underwent an increase from -0.6 °C to -0.2 °C between the 1951-1960 and 2010-2019 means, not restrained by a take up of latent heat. As the 5 m temperature nears 0 °C, ice degradation will start and the warming will stall. The *sediment only* case experienced minimal warming in this period at 5 m depth, from -0.1 °C to 0.0 °C as the decrease in ice content was not completed. Finally, a complete degradation of the ice table in *blocks with sediment* run resulted in a warming to positive temperatures, from 0.0 °C to 0.6 °C. Ground temperatures at 5 m depth were lower for a snowfall factor of 0.5 and resulted in less ice degradation. Warming between the 1951-1960 and 2010-2019 means were from -0.8 °C to -0.3 °C in the *blocks only* stratigraphy, from -0.5 °C to 0.0 °C in the *sediment only* stratigraphy and from -0.1 °C to 0.1 °C in the *blocks with sediment* stratigraphy.

At Juvvasshøe, for a snowfall factor of 0.25, The *blocks only* simulation underwent an increase from -3.7 °C to -3.5 °C between the 1951-1960 and 2010-2019 means. Warming for the *blocks with sediment* run was from -3.8 °C to -3.4 °C and the *sediment only* run from -4.1 °C to -3.7 °C. At a snowfall factor of 0.5, the change in temperature at 5 m depth in drained scenarios are: from -3.1 °C to -2.6 °C for the *blocks only* stratigraphy, from -2.5 °C to -1.9 °C for the *blocks with sediment* stratigraphy and from -2.9 °C to -2.4 °C for the *sediment only* stratigraphy. The warming rates are more sensitive to changes in the amount of snowfall than to differences in stratigraphy.

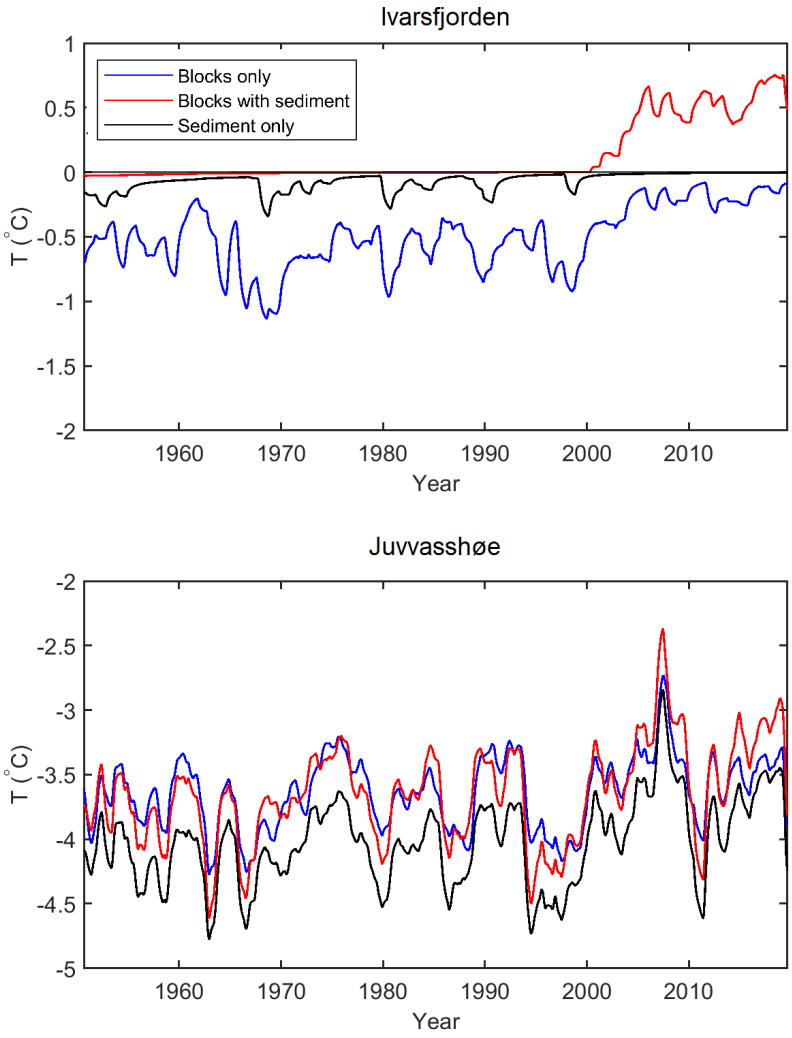

Figure 19: Ground temperature at 5 m depth for the *blocks only*, *blocks with sediment* and *sediment only* stratigraphies under drained conditions. The snowfall factor is 1.0 for Ivarsfjorden and 0.25 for Juvvasshøe.

5.3 Simulated thermal regime at ancillary sites

This section features the ground temperatures and sensitivity analysis to snow at the three ancillary study sites. For each location, the equilibrium ground temperatures at 2 m depth for different snowfall factors are included (similar to figure 16). Only the *blocks only* and *blocks with sediment* stratigraphies are shown as this is where the cooling effect of drainage is most pronounced.

5.3.1 Northern Verkhoyansk Mountains, Russia

The equilibrium ground temperatures for a blockfield in the northern Verkhoyansk Mountains are presented in figure 20. The annual maximum snow thickness at a snowfall factor of 1.0 is between 0.5 m and 0.8 m. As at the Norwegian sites, the *blocks only, drained* scenario clearly features the lowest ground temperatures at higher snowfall factors. All mean 2 m ground temperatures are negative, though close to 0 °C at a snowfall factor of 1.5. The negative thermal anomaly of *blocks only, drained* runs is up to 3.5 °C. A difference up to 12 °C exists between runs with a snowfall factor of 0 compared to runs with a snowfall factor of 1.5, meaning this site is very sensitive to changes in snowfall.

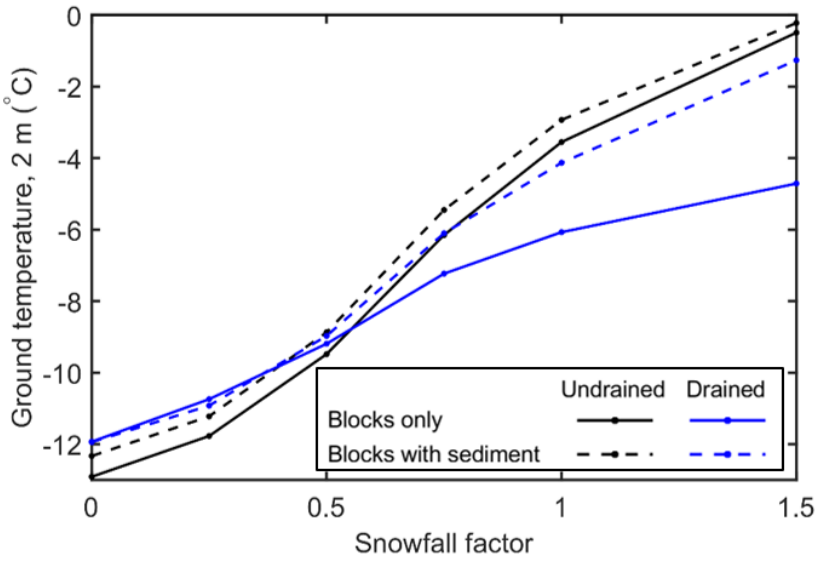

Figure 20: Equilibrium ground temperature at 2 m depth for two idealized stratigraphies (table 2) in *undrained* and *drained* states at a blockfield in the northern Verkhoyansk Mountains, Russia.

5.3.2 Terelj, Mongolia

Figure 21 shows the equilibrium ground temperatures at the blockfield in Terelj for the different snowfall factors. Annual maximum snow depths at a snowfall factor of 1.0 are between 0.2 m and 0.4 m. The difference between the *blocks only, drained* scenario and the next coldest is up to 3 °C and up to 5 °C with the simulations with the *blocks and sediment* stratigraphy. At snowfall factors of 0.75 and higher, the blocks only, drained scenario is the only one with negative mean ground temperatures at 2 m depth. The *blocks only, undrained* simulation also features lower ground temperatures than the simulations with sediment in the pore space. The ground temperatures are less sensitive to an increasing snowfall factor than in the northern Verkhoyansk Mountains.

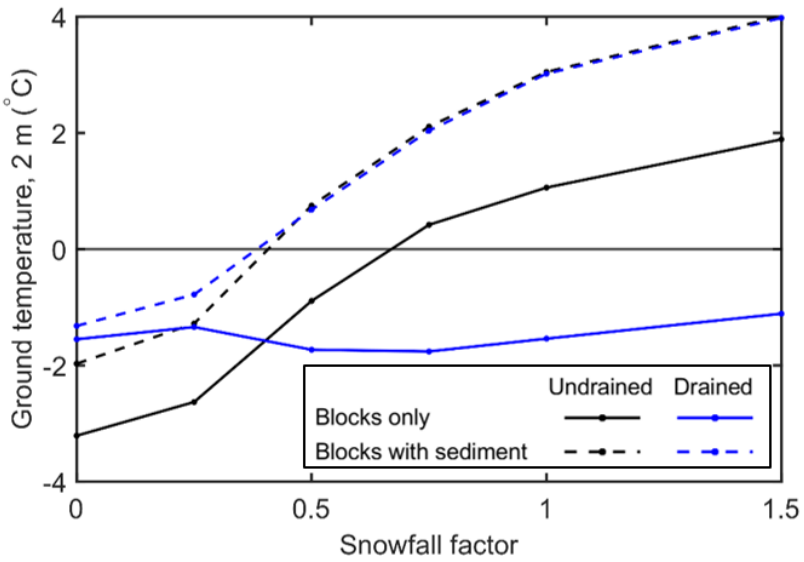

Figure 21: Equilibrium ground temperature at 2 m depth for two idealized stratigraphies (table 2) in *undrained* and *drained* states at a blockfield Terelj, Mongolia.

5.3.3 Retezat, Romania

Figure 22 shows the equilibrium ground temperatures at a rock glacier in Retezat for the different snowfall factors. The annual maximum snow pack thicknesses range from 0.8 m and 1.5 m at a snowfall factor of 1.0. All modelled temperatures are positive and thus no permafrost is present. Compared to the other sites, the simulations with the *blocks only, drained* scenario are not much lower than the other scenarios. At snowfall factors at and below 0.5, there is no clear thermal anomaly. The difference between the *blocks only, drained* scenario and the next coldest scenario for a snowfall factor of 1.0 is 0.4 °C. At a snowfall factor of 1.5, the offset is most clear at 1.0 °C, though still considerably lower than at other sites that do feature permafrost.

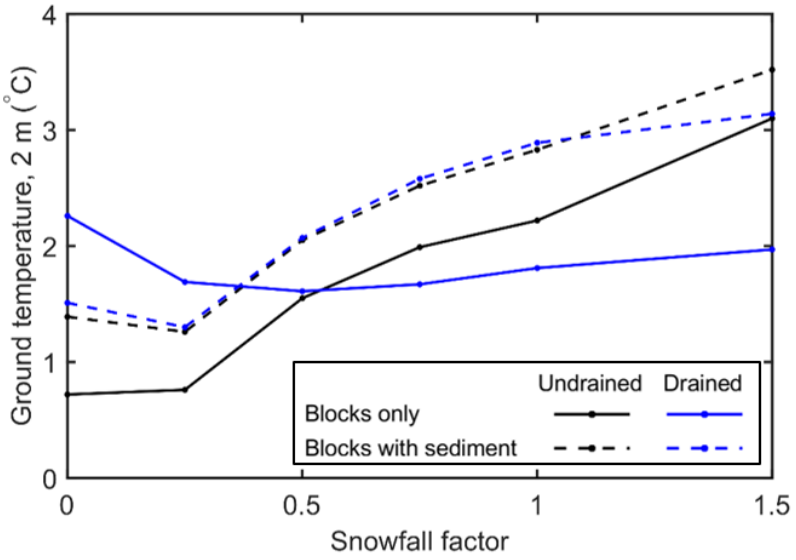

Figure 22: Equilibrium ground temperature at 2 m depth for two idealized stratigraphies (table 2) in *undrained* and *drained* states at the rock glacier in Retezat, Romania.

It has been established in section 5.2 that changes in the ground ice content are a factor in governing changes in ground temperatures. As presented in figure 23, all simulations feature only seasonal freezing and no perennial ice table is present. The *blocks only, drained* simulation has almost no ice in the ground during the winter as all liquid water has been drained. Also, no ice table exists where infiltrating snow melt can accumulate and refreeze as has been the case for simulations with permafrost (figure 14). Another notable result is the timing of the snow. The snow pack builds up late in the winter or early spring, which is considerably later than at e.g. Juvvasshøe (figure 14), where the snow pack build up linearly.

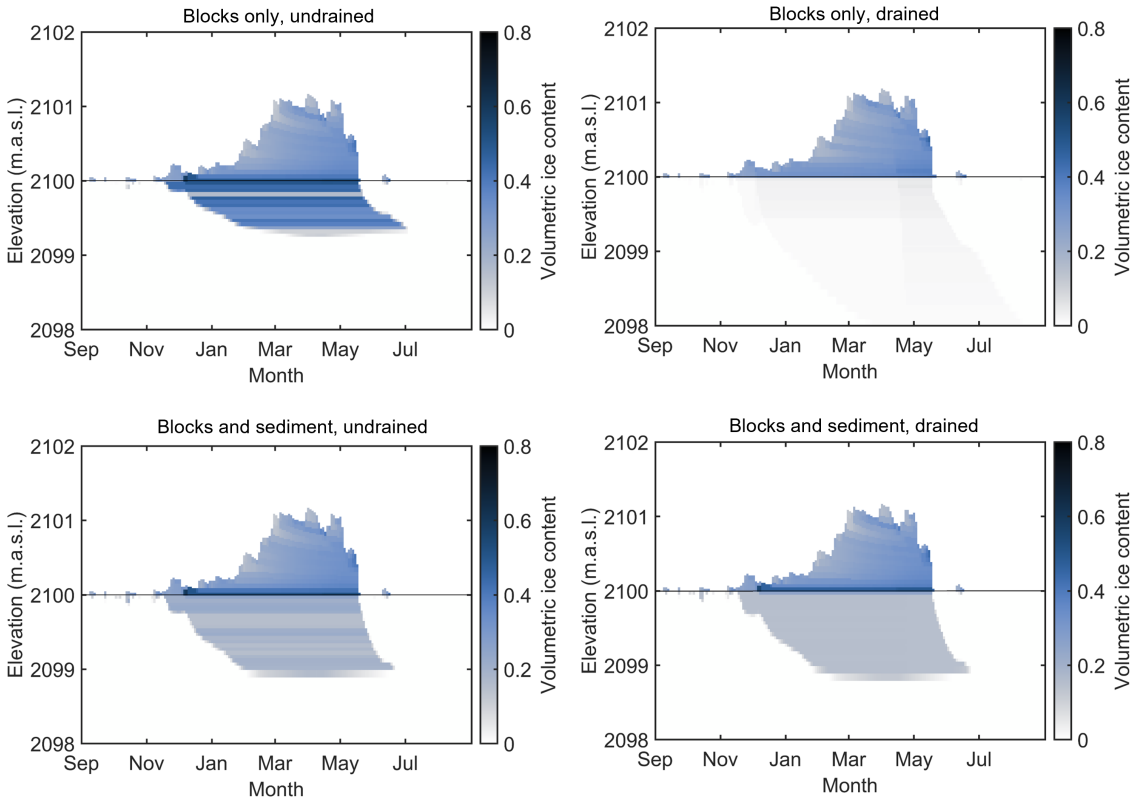

Figure 23: Modelled volumetric ground ice content (below 2100 m.a.s.l.) and snow thickness (above 2100 m.a.s.l.) for equilibrium runs at the rock glacier in Retezat. Shown are the *blocks only* (upper) and *blocks with sediment* (lower) stratigraphies, in the *undrained* (left) and *drained* (right) scenarios for one hydrological year. The snowfall factor is 1.0 for all simulations.

5.4 Connection between the thermal regime and the water/ice balance

In this section, three additional aspects related to the connection between ground temperatures and water or ice in the subsurface are presented. First, the zero curtain in autumn and spring is shown and compared between stratigraphies. This is focused on the site in the northern Verkhoyansk Mountains as the effect is most pronounced here. Then, the subsurface drainage regime is presented at the semi-arid site in Terelj. For comparison with a more wet site, also the subsurface drainage at Juvvasshøe is included. Finally, transient simulations at Juvvasshøe that are initialized for permafrost-free conditions, show ground ice formation during permafrost aggradation in different stratigraphies.

5.4.1 The zero curtain in autumn and spring

In the snowfall sensitivity analysis, it was shown that ground temperatures differ most at high snowfall factors. Hence, this section is split in high and low snowfall factors.

Snowfall factor 1.0. Figure 24 shows the 0.25 m depth ground temperature for the *blocks only*, *drained* and *undrained* scenario in the northern Verkhoyansk Mountains with a snowfall factor of 1.0. The winter temperatures differ greatly between *drained* and *undrained* simulation for the *blocks only* stratigraphy, making this location fit to examine the zero curtain in autumn and spring. The *undrained* curve shows a clear zero curtain of ca. one month in October, when soil water freezes. The *drained* curve does not have this zero curtain and temperatures drop drastically, resulting in winter temperatures up to 8 °C lower than in the *undrained* scenario. In spring, when the snow cover is melting, the opposite happens where a zero curtain of almost one month occurs in the *drained* scenario. Percolating meltwater from the snowpack freezes at the bottom of the blocky layer or on the ice table. A layer of superimposed ice can be formed which has to be melted before the ground can start to warm, and thereby retards the warming of the ground.

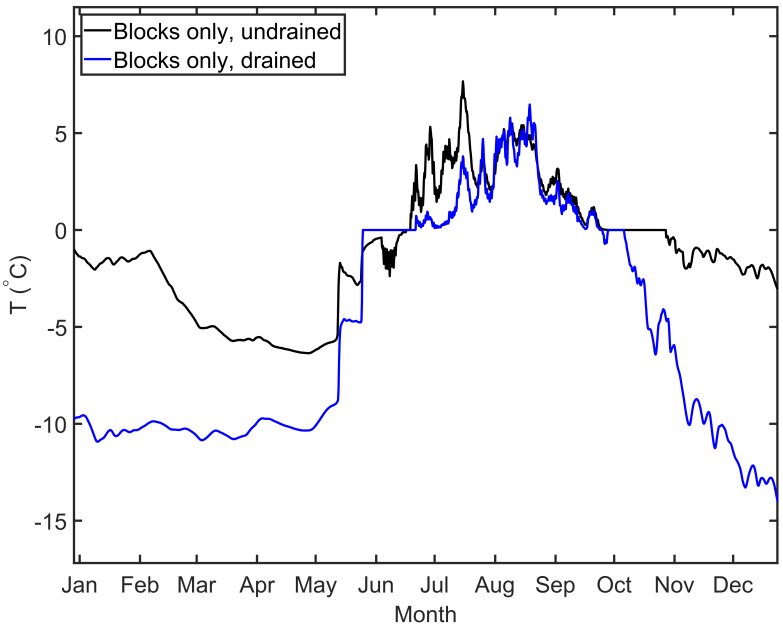

Figure 24: Ground temperature at 0.25 m depth at the northern Verkhoyansk Mountains for a year in the equilibrium results. The snowfall factor is 1.0.

In Ivarsfjorden, which features a similar amount of snowfall, the results are similar to the displayed curves, though absolute temperatures are higher and the difference in winter temperature is smaller. In Juvvasshøe, for a snowfall factor of 1.0, winter temperatures show less amplitude. This is likely a result of the large amounts of snowfall at this site. The zero curtain in autumn and spring are similar to figure 24. In Terelj, the duration of the zero curtain is shorter and differences in winter temperatures are even larger between the *drained* and *undrained* runs, up to 14 °C. Ground temperatures at Retezat did not indicate permafrost in any of the simulations. This means no perennial ice table exists and frost is only seasonal. At a snowfall factor of 1.0, winter temperatures stay just below 0 °C at 0.25 m depth in the *blocks only, undrained* simulation after a zero curtain period in autumn but drop to -6 °C in the *drained* case.

Snowfall factor 0.25. Figure 25 shows the 0.25 m depth ground temperature for the *blocks*

only, drained and *undrained* scenario in the northern Verkhoyansk Mountains at a snowfall factor of 0.25. As this is an extremely cold location, even summer temperatures were close to 0 °C. The effect is largely vanished, compared to figure 24. Winter temperatures are even lower in the *undrained* scenario.

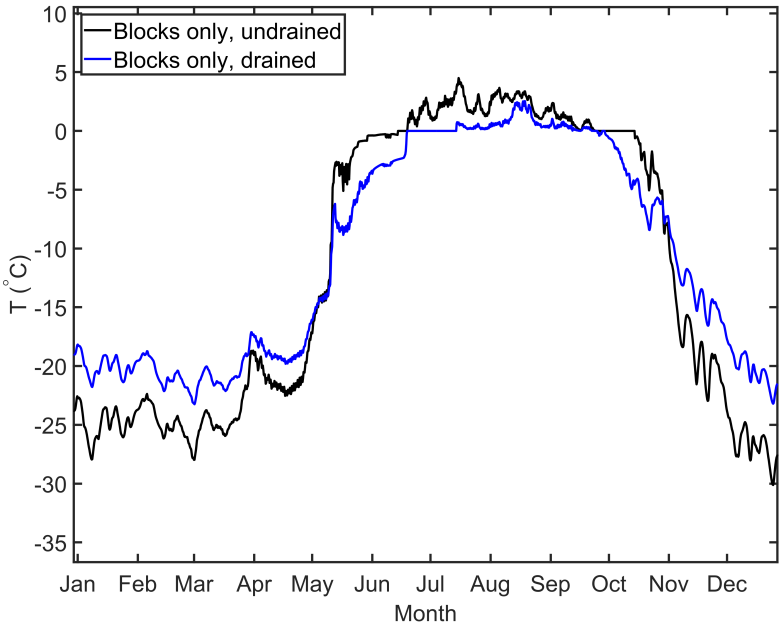

Figure 25: Ground temperature at 0.25 m depth for a blockfield in northern Verkhoyansk mountains for a year in the equilibrium results. The snowfall factor is 0.25.

In Ivarsfjorden, the effect as shown in figure 24 is visible at a snowfall factor of 0.25, but less pronounced. The *drained* scenario here has a short zero curtain in spring and the zero curtain in autumn is slightly longer in the *undrained* scenario than in the *drained* scenario. Winter temperatures are therefore only marginally lower in the *drained* scenario than in the *undrained* scenario. The same general effect occurs in Terelj. The pattern is also similar in Romania, where winter temperatures drop to -12 °C in the *blocks only, drained* scenario. At Juvvasshøe, the image is more similar to figure 24 because absolute snowfall amounts are still relatively impactful for a snowfall factor of 0.25.

5.4.2 Subsurface drainage

It is possible to investigate the timing of subsurface drainage out of the system. Figure 26 displays the drainage for one year in Terelj, Mongolia for two simulations. In addition, the air temperature and rainfall during the same period are presented. The *blocks with sediment* run has drainage only between August and the start of October, while the *blocks only* run features drainage from mid July to mid November. Another difference between the *blocks only* and *blocks with sediment* curve is that the latter has more short drainage events compared to the former. Total drainage is significantly higher in the *blocks only* run. The two drainage peaks in the *blocks with sediment* simulation match with the two strongest rainfall events.

The subsurface drainage, precipitation and air temperature for one year at Juvvasshøe are shown in figure figure 27. Compared to Terelj, the amount of precipitation is higher. Also the absolute values of subsurface drainage are significantly higher, up to 30 mm/day compared to a maximum of 5 mm/day in Terelj. Notably is that the differences between the *blocks only* and *blocks with sediment* stratigraphy are less pronounced at Juvvasshøe at the start of the drainage. The total amount of drainage is more similar between the two stratigraphies at this site. In Terelj, drainage in the *blocks only* run continues one month longer than in the *blocks with sediment* run. For Juvvasshøe this is opposite, likely related to the an earlier frozen active layer in the the *blocks only* run.

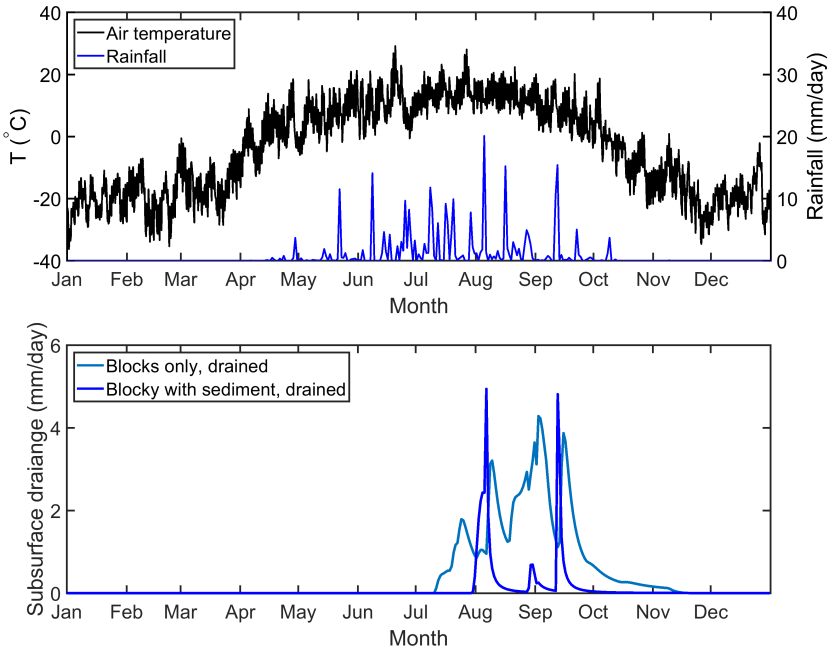

Figure 26: Air temperature and rainfall in 1987 in Terelj, Mongolia (upper panel) and subsurface drainage out of the model realization for the *blocks only* and *blocks with sediment* stratigraphies, both *drained* (lower panel).

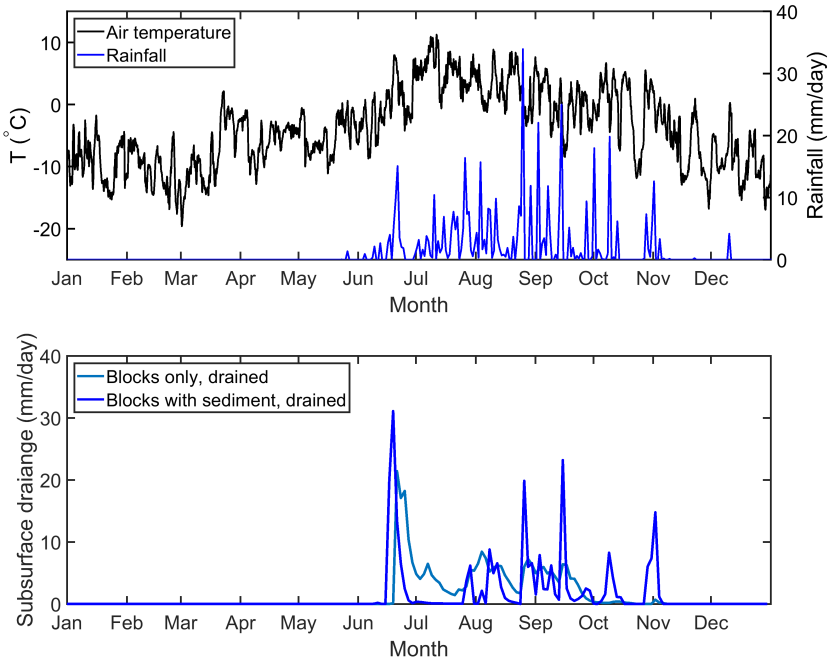

Figure 27: Air temperature and rainfall in 2005 at Juvvasshøe, Norway (upper panel) and subsurface drainage out of the model realization for the *blocks only* and *blocks with sediment* stratigraphies, both *drained* (lower panel).

5.4.3 Ground ice formation

The different stratigraphies also affect how the ice table builds up during the aggradation of permafrost. Figure 28 shows simulations at Juvvasshøe that feature an initial temperature profile that is out of equilibrium with the climate. The initial ground temperatures in 1951 are 3 °C above the measured borehole temperatures in 2000, with the initial temperature at 1890 m.a.s.l. being around 1 °C. There is no ice present at the start, but it forms as the ground cools. The two simulations feature a completely different build up of ice. The *blocks with sediment* run shows a clear downward freezing. In the *blocks only* stratigraphy, the ice table builds up from the bottom upwards. The duration of forming the ice table is longer in this scenario. The higher field capacity in the top figure ensures that water is retained in the subsurface. A downwards progressing freezing front then results in freezing of this water and ground ice formation progresses downwards. The *blocks only* stratigraphy is characterized by a low field capacity, meaning that no water is retained under drained conditions. This means that ice only forms after infiltration and percolation into the subsurface during snowmelt, in the same manner as was presented in the *blocks only, drained* scenario in figure 14. Figure 28 also shows the corresponding ground temperature profiles. The ground in the *blocks only* scenario cools down more than in the *blocks with sediment* scenario. The remaining scenarios also show a downward building of ground ice, similar to that of the *blocks with sediment, drained* simulation.

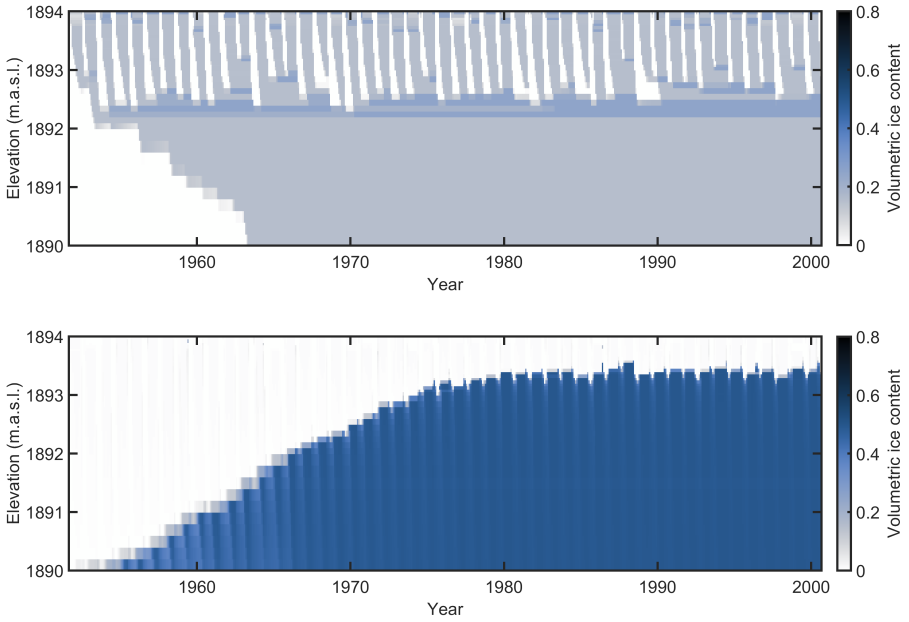

(a) Ground ice formation for the *blocks with sediment, drained* (upper panel) and *blocks only, drained* (lower panel) scenarios.

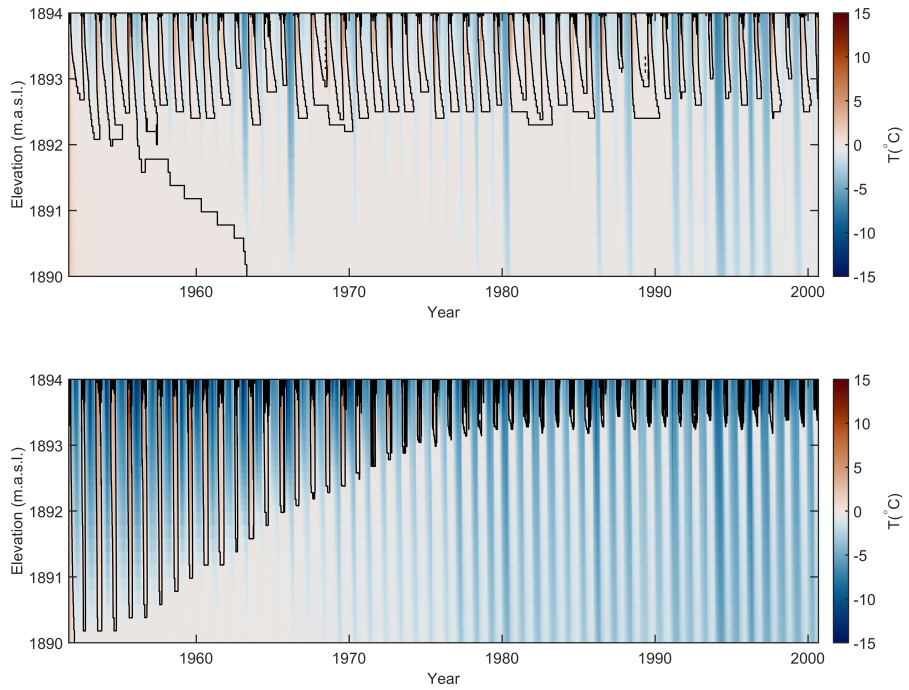

(b) Ground temperature evolution for the *blocks with sediment , drained* (upper panel) and *blocks only, drained* (lower panel) scenarios. The black lines indicate the interpolated 0 °C isotherm.

Figure 28: (a) Ground ice formation and (b) temperature evolution during permafrost formation for two scenarios, anchored in Juvvasshøe. The ground surface is at 1894 m.a.s.l.. The simulations are started in 1951 and are initialized with ground temperatures at 3 °C higher than measurements from the PACE borehole in 2000.

6 Discussion

6.1 Limitations of the model setup

In this study, CryoGrid has been applied to two Norwegian permafrost sites and three locations in the global permafrost extent. The aim of this thesis is to asses the effect of coarse, blocky deposits in combination with a lateral subsurface drainage component on ground ice and ground temperatures. Though the goal was not to represent exact conditions at the sites, the model can satisfactorily reproduce ground temperature measurements from the PACE borehole in Juvvasshøe. The observation of the rock glacier in Ivarsfjorden indicates that permafrost is or has been present in the recent past (Lilleøren et al. 2022). Modelled MAGSTs at the rock glacier fall within the 25th and 75th percentile of measured MAGSTs between July 2016 and July 2019. Modelled MAGSTs are below mean and median measurements, indicating a potential cold bias of the model of approximately 0.5 °C. The implications of this potential cold bias are addressed later in this chapter. The main limitations of the model setup are discussed below:

Unknown parameters and stratigraphy. The model setup contains uncertainties and limitations regarding unknown stratigraphies and parameters at the sites. Exact values of albedo, hydraulic conductivity and roughness length are unknown and default values are used. The freezing characteristic of free water is used in most of the model runs, meaning phase change occurs at 0 °C. Sensitivity tests with a freezing curve based on Dall'Amico et al. (2011) did not show a significant difference in ground temperatures and ground ice content. At Juvvasshøe, the ground stratigraphy was described by Isaksen et al. (2003). The first meter consists of large stones and boulders and the ground below are mainly cobbles and weathered material. The best-fitting stratigraphy (table 4) contained a high volumetric mineral fraction of 0.8, representing a lower porosity then in the idealized stratigraphies (table 2). The best-fitting stratigraphy is similar to the *blocks with sediment* stratigraphy, though the field capacity is lower (0.10 opposed to 0.15). The blockfield stratigraphy from Westermann et al. (2013) (table 3) distinguishes an upper layer of just blocks with a low field capacity of 0.01 in the upper 2 m and a layer with a higher field capacity of 0.15 (and thus a fine sediment fraction) below.

At the rock glacier in Ivarsfjorden, no detailed description of the subsurface stratigraphy is available. Most of the rock glacier surface is described as 'relict' by Lilleøren et al. (2022) (figure 8) and sand and gravel is found in between blocks. The two areas that are described as 'fresh' contain larger blocks, but no description of the amount of finer sediment is available. A subsurface that is similar to the *blocks only* stratigraphy is unlikely to be present in large part of the rock glacier. Lilleøren et al. (2022) described the site as a complex creeping system, meaning that the subsurface is not uniform across the entire rock glacier. Almost all ground surface temperature loggers are located on the relict rock glacier surface (Lilleøren et al. 2022). As the goal of the study is to analyze the difference between idealized stratigraphies for a certain climate, of highest importance is the consistency of parameters between runs. Whether or not the stratigraphies in table 2 accurately represent the blockfield and rock glacier, we cannot say for certain. However, it can be assured that the key values of volumetric mineral content, field capacity and simulated drainage give rise to the response of the ground ice table and ground

temperatures in blocky terrain.

Simplified model setup. Since the model setup is one-dimensional, lateral processes as a result of variable topography, snow cover or stratigraphy are not included. Water in the *drained* scenarios leaves the model domain as subsurface drainage, while in reality water could pond somewhere within the system. The drainage of water via a seepage face, as is in the model setup, is phenomenologically removing water and not capturing real three-dimensional processes. The convective processes, summarized by Harris and Pedersen (1998), that cause a negative thermal anomaly in blocky terrain are not part of the model setup. The same applies to the effect of blocks protruding into and through the snow cover as was described by Juliussen and Humlum (2008). This is a limitation when attempting to simulate the full extent of processes that result in lower ground temperatures in blocky terrain, described by Harris and Pedersen (1998) and Juliussen and Humlum (2008). Wicky and Hauck (2020) stated that the role of convection is often neglected in permafrost modelling and they therefore explicitly modelled air convection in the active layer of rock glaciers. In their study, convection resulted in lower ground temperatures up to 0.93 °C in simulations with a high permeability (and thus with convection) compared to runs with a low permeability (without convection) of the subsurface in two rock glaciers in the Swiss Alps. Suggestions on how future studies can improve the negative thermal anomaly in blocky terrain are done in section 6.3.

Meteorological forcing data. An important factor in deciding the quantitative results and relative differences between sites is the input meteorological forcing data. The ERA5 reanalysis data is a global product and thus has a coarse horizontal scale. Hence, the TopoSCALE downscaling routine (Fiddes and Gruber 2014) is applied. Aalstad et al. (2018) summarized some of the limitations of the scheme. First, no proper atmospheric boundary layer is included, meaning that wind, air temperature and humidity are not adjusted for the stability and roughness length at the surface layer. Next, no significant correction is applied to precipitation other than horizontal interpolation. Thus local effects such as orography are missed. Clouds that are not captured in the ERA5 reanalysis data, will also not be included in the downscaling product, affecting the radiation budget and precipitation. The forcing data that resulted from the downscaling is not validated against measurements and thus presents a source of uncertainty. The meteorological forcing data at the three ancillary sites is compiled in different other projects and used without further consideration. The data for the rock glacier in Retezat is also a product of ERA5 reanalysis data with TopoSCALE and poses the same uncertainties as for the sites in Norway. In Terelj, the ERA5 data is not downscaled, but provided at the closest ERA5 grid cell to the location of the blockfield in figure 10C, at approximately the same elevation. The largest uncertainty is for the site in the northern Verkhoyansk Mountains as the forcing data is from the Lena River delta, provided by Nitzbon et al. (2019), and thus not from the mountain range (figure 9). This data is based on in situ measurements from Boike et al. (2019) and gap-filled with ERA5 reanalysis data. Despite uncertainties regarding forcing data, it can be with confidence stated that continental and regional scale climate characteristics are captured.

Snow. CROCUS is a sophisticated snow scheme (Vionnet et al. 2012; Zweigel et al. 2021) that includes a transient evolution of snow properties. Limitations in the snow scheme regarding parameterizations (of e.g. erodibility) can be found in Zweigel et al. (2021). In order to improve the snow pack representation in the Arctic, a revision of some parameters

has been suggested (Royer et al. 2021), but are not implemented in the model setup at the Arctic sites (Ivarsfjorden and the northern Verkhoyansk Mountains) in this thesis. Zweigel et al. (2021) mention that the capability of the snow scheme depends on the quality of the forcing data and is thus affected by the limitations herein. Further, the inclusion of Richards equation (Richards 1931), representing the movement of water in unsaturated soils, could improve the CROCUS snow scheme. This has been done by D'Amboise et al. (2017) and resulted in higher liquid water contents in the snowpack compared to a simulations with a bucket routine. However, they concluded that the performance was not sufficient for snowpack simulations and first require adaptations in other parts of the CROCUS scheme.

An uncertainty in this study results from the use of a snowfall factor to manipulate incoming snowfall in order to represent snow redistribution by wind. Where adjusting a snowfall factor only changes the amount of incoming snow, snow redistribution by wind creates a more dynamic snowpack in reality (Liston and Sturm 1998). In the model setup, the snowfall factor is static for each run. In reality, especially in mountain areas, large temporal variability of snowfall means that the best representing snowfall factor can change each season or year. The maximum snow depth at Juvvasshøe in the simulation with the best-fitting ground temperatures to the borehole data was 34 cm, while Hipp et al. (2012) reported a thickness of less than 20 cm. Model runs with an even lower snowfall factor result in lower ground temperatures. This means that a possible cold bias in the model setup comes from other sources, such as the simplified stratigraphies or the meteorological forcing data.

6.2 Ground ice mass balance and permafrost thermal regime

By excluding convective processes (Harris and Pedersen 1998) and the effect of blocks protruding through the snow cover (Juliussen and Humlum 2008; Gruber and Hoelze 2008), the effect of a subsurface drainage component is isolated and shown to be significant. Simulations with a *blocks only, drained* setup clearly feature a different ground ice mass balance compared to results from all other simulations (figure 14). Dahl (1966) described a correlation between the absence of a finer sediment fraction between blocks in blockfields in northern Norway and the slope (and drainage amount). This means that on a steeper slope, where drainage is higher, blocks without sediment in the pores (as represented by the *blocks only, drained* scenario) are more common. Since no water is held in the pore space between the blocks, cooling of the ground is not halted by the release of latent heat when the active layer freezes. This effect leads to large differences in winter temperatures and was most clearly seen in simulations at the northern Verkhoyansk Mountains (figure 24).

The effect of lower soil moisture in rock glaciers on the zero curtain in autumn is also described by e.g. Hanson and Hoelzle (2004). Additionally, described an opposing effect in spring, where percolating snow melt refreezes at the bottom of the blocky layer or on the ice table. A layer of superimposed ice has to be melted, which takes up latent heat, before the ground can warm. This process is also successfully modelled and shown in figure 14. The corresponding effect on ground temperatures is displayed in figure 24, where ground temperatures in the *blocks only, drained* run are confined to 0 °C in spring.

In the following sections, the thermal anomalies at the different study sites will be discussed and compared. For the model results at the sites in Norway, also the warming of the ground and degradation of ground ice between 1951 and 2019 is addressed.

6.2.1 Norway

Despite the mentioned limitations of the model setup, the results show a clear negative thermal anomaly. A surface cover of coarse blocks, represented by a high porosity and low field capacity, that is drained of water, results in ground temperatures up to 1.4 °C and 1.5 °C lower than other stratigraphies at the location of the PACE borehole at Juvvasshøe and at the rock glacier in Ivarsfjorden respectively (figure 16). Temperature differences between stratigraphies are comparable between the equilibrium runs and transient runs. In Ivarsfjorden at a snowfall factor of 1.0, the *blocks only, drained* scenario features 2 m temperatures 2.0 °C lower than other *drained* scenarios. In the results from transient simulations, this difference at 5 m depth is up to 1.0 °C. The *blocks with sediment* and *sediment only* runs are losing ice, meaning temperature differences are lower. At Juvvasshøe, for a snowfall factor of 0.25, temperatures at 2 m depth do not show large differences, though in the *sediment only* run, temperatures are 0.5 °C lower than the other stratigraphies. A similar offset is seen in the transient simulations.

The effect of drainage on the ground thermal regime has been successfully modelled in peat plateaus in Northern Norway by Martin et al. (2019), who found 2 °C lower temperatures in drained peat soil compared to undrained peat soil. Their results showed stable permafrost conditions at a MAGST of 2.0-2.5 °C in well drained conditions. While peat plateaus are a completely different landform than those modelled in this thesis, they also feature a varying soil moisture content which is of importance for the ground thermal regime (Martin et al. 2019). Similar results are found in this study, where stable permafrost can exist at a MAGST of 2.0-2.5 °C in the *blocks only, drained* simulations in Ivarsfjorden. Our findings are within the range of the 1.3-2.0 °C lower temperatures that Juliussen and Humlum (2008) found in blockfields compared to till and bedrock in Central-eastern Norway. The results from the equilibrium runs results show that, at Juvvasshøe, stable permafrost occurs in *blocks only, drained* conditions even at a snow cover of more than 2 m thickness.

While the absolute ground temperatures differ greatly between the two sites, warming rates between the 1951-1960 mean and the 2010-2019 mean were similar for the runs that are not affected by latent heat effects of melting ice. The same is true between the different stratigraphies, that all experienced warming between 0.4 °C and 0.6 °C at 2 m depth. An exception is the *blocks only* stratigraphy at Juvvasshøe with a snowfall factor of 0.25, which only warmed 0.2 °C. The warming rates at Juvvasshøe found in this study are lower than was found by Isaksen et al. (2007) and Etzelmüller et al. (2020a). They reported a warming of 0.4 °C to 0.7 °C/decade at the top of the permafrost and a warming at the ground surface in first two decades of this century of 0.7 °C/decade respectively. Warming rates are highest after 1990 (e.g. Hipp et al. 2012; Westermann et al. 2013). The difference in warming rates between these studies and this thesis can be a result of uncertainties in the acquired forcing data or the simplified model setup with idealized stratigraphies. It is again important to note that the model in this study is set up to

compare between scenarios and not with the main goal to reproduce permafrost warming.

The results in figure 17 suggest that the Ivarsfjorden rock glacier underwent different stages of ground ice degradation depending on the subsurface material. A significant ice table remains in the *blocks only* and *sediment only* runs, which does not completely fit the observations from Lilleøren et al. (2022) that only a limited ice core might still be present under certain conditions. As described in section 6.1, a subsurface similar to the *blocks only* stratigraphy is not present at most of the rock glacier. It should be noted that this system is described as 'complex creeping' and that the stratigraphies used in this study are idealized for means of comparison and investigating the effect of drainage in blocky deposits. This system is a degrading lower permafrost limit landform and thus sensitive around 0 °C. The idealized one-dimensional model setup does not cover potential ponding of water or other spatial processes. Following the potential cold bias of our model setup, 0.5 °C higher ground temperatures will lead to more ice loss in the *blocks only* and *sediment only* runs and be more in line with observations from Lilleøren et al. (2022).

6.2.2 Ancillary sites

The model setup has been applied to a multitude of climates. From a relatively mild, wet maritime climate in northern Norway to a more polar alpine climate in southern Norway. An Arctic, continental climate is represented by the site the northern Verkhoyansk Mountains. A lower latitude, semi-arid high mountain continental climate exists in Terelj. The site in Retezat is located at a similar latitude as Terelj, but features higher temperatures, more precipitation and less continentality.

With a thermal anomaly up to 3.5 °C, the cooling effect of a drained, porous subsurface is the most pronounced in the northern Verkhoyansk Mountains. This is mainly a result of an extreme differences in winter temperatures in the ground compared to *undrained* simulations (figure 24) at a relatively high snowfall factor. Juliussen and Humlum (2008) found that the range in ground temperatures is larger in blocky terrain as opposed to till and bedrock, mainly related to lower minimum temperatures in winter. At higher snowfall amounts, the zero curtain in spring in the *drained* runs is higher as more meltwater can infiltrate and ice can build up, which has to be melted before warming of the ground commences. Ground temperatures decrease more rapidly in the *drained* runs because the heat loss through the snow pack takes longer in the scenario that preserves water.

In the mountains south of the Terelj valley, also a very continental site, the thermal anomaly was up to 3 °C. The lower temperatures in the *blocks only, undrained* runs can be explained by the higher thermal conductivity in winter in a ground with a higher pore volume and thus more ice when saturated (Riseborough 2002). At other sites, the higher water content may delay freezing, resulting in a smaller difference. The ground temperatures change less with an increasing snowfall factor than in the northern Verkhoyansk Mountains. The cooling effect of snow, due to its high albedo, is more limited in high latitude regions such as the site in Russia compared to low latitude regions (Zhang 2005). This means that the isulating effect of snow on the ground (section 2.1.2) is relatively greater in colder climates.

Results at the site in Retezat feature no permafrost. While the 2 m ground temperatures

in the *blocks only, drained* simulations are lower than the other scenarios at the higher snowfall factors, the anomaly is smaller than at the other sites (figure 22). The entire effect of superimposed ice building during the annual snow melt is vanished, as was presented in figure 23. The fact that the snow falls late in this region, likely also affects the freezing dynamics. If no, or merely a very small, snow cover is present, the refreezing of the ground will be more efficient as compared to when snow falls at the start of the freezing season. In this case, the difference in freezing duration between a well drained subsurface and a subsurface with a higher soil moisture content will be reduced. The sensitivity to snowfall in the *blocks only, drained* is almost negligible therefore. Lower ground temperatures with increasing amounts of snow can be explained by the insulating effect of snow during spring, which prevent rapid warming of the ground. Also, in low latitude regions and areas with seasonal frost (as opposed to permafrost), snow promotes lower ground temperatures due to its high albedo (Zhang 2005). If this is the case at this site should be investigated in future work.

At the Norwegian sites, the negative thermal anomaly of the *blocks only, drained* model runs is ca. 1.5 °C. In the northern Verkhoyansk Mountains, the anomaly is the most pronounced, up to 3.5 °C. In Terelj, the offset is up to 3 °C with the *blocks only, undrained* scenario. Both sites are extremely continental. The smallest differences between *blocks only, undrained* and other runs is in Retezat (maximum 1 °C), where no permafrost was present, meaning the effect largely vanishes when no persistent ground ice exists.

6.2.3 Simulating subsurface drainage

The subsurface drainage regime, modelled in Terelj, displays large differences between the *blocks only, drained* and *blocks with sediment, drained* scenarios (figure 26). The drainage starts earlier in the summer in the *blocks only* stratigraphy because as soon as ground temperatures are negative, water runs off instead of being held in the pore space (due to the low field capacity). In the *blocks with sediment* stratigraphy, water is held in the pore space and subsurface run off only occurs occasionally, when the, related to precipitation events. The mountains around the valley are important for the water balance of the nearby settlement (Tuvshinjargal and Saranbaatar 2004), which is thus affected by the subsurface stratigraphy. As this is a semi-arid region, the soil moisture content in the active layer is not at field capacity as often as at sites that feature more precipitation. Therefore, the subsurface drainage is lower in the *blocks with sediment* stratigraphy, which features a higher field capacity than the *blocks only* stratigraphy (table 2). Since Juvvasshøe is a site that receives more precipitation, the subsurface is more likely to be saturated and subsurface runoff occurs more regularly in a subsurface with higher field capacity. The drainage regimes differ greatly between the two analyzed sites. Future studies should in detail investigate the quantity and timing of the subsurface runoff in combination with other aspects of the water balance. In order to investigate the exact drainage patterns in blockfields, detailed three dimensional studies, that include field observations are required. A deepening of the active layer is a result of increased subsurface temperatures and affects subsurface drainage (Deline et al. 2015). For that reason, detailed investigations of subsurface drainage should also be performed in transient modelling studies, related to active layer thickening. It is clearly shown that a difference in field capacity strongly affects drainage in blocky terrain, especially in dry regions. Dahl (1966) describe that

blocks without a fine sediment fraction are more common in blockfields on a relatively steep slope (and feature subsurface drainage). Thus, the two factors that together cause the differences in the subsurface drainage regimes, blocky terrain with no sediments in the pores and well drained conditions, are correlated.

6.2.4 Ground ice formation during permafrost aggradation

If no ground ice is present, but the climate is cold enough for permafrost to form, the formation of the ground ice table is vastly different in the *blocks only, drained* simulation compared to the other simulations (figure 28). In reality, this is not the case at any of the study sites in this thesis and no observations regarding this build up of the ice table are available. This section should therefore be considered as a modelling experiment, with potential implications only for specific cases. A situation where it could be of interest are rockfall events near a retreating glacier. Glacier - permafrost interactions are complex and occur on a range of spatial and temporal scales (Harris and Murton 2005), but a glacier foreland that is recently deglaciated often experience permafrost aggradation (Miesen et al. 2021). These environments often contain coarse till and are associated with rockfalls or other slope processes from side walls when a glacier retreats (Miesen et al. 2021; Lukas et al. 2005). In such a setting, the formation of an ice table will be vastly different in deposits that consists of only blocks compared to deposits that feature sediments in the pores and thus have higher field capacity (figure 28).

6.3 Implications for other work

6.3.1 Permafrost models and the lower limit of permafrost

In this thesis it is shown that the inclusion of lateral drainage in porous, blocky deposits with a low field capacity results in a significant negative thermal anomaly in permafrost environments. In order to understand relative effects that cause thermal anomalies in blocky terrain at the lower limit of permafrost, a more sophisticated model setup, that includes convective processes and the effect of blocks protruding through snow, is required. The simulations in this study show the importance of ground ice when assessing the thermal state and evolution of permafrost. In permafrost areas with ground ice around the freezing point, atmospheric warming can lead to significant ground ice loss while temperature increases are limited. This is for example shown in the *blocks with sediment* simulation at the Ivarsfjorden rock glacier.

As was stated in the introduction of this thesis, most modelling studies that aimed to map the distribution of permafrost or warming and degradation rates did not include a lateral subsurface drainage component. (Obu et al. 2019) gave a low soil moisture content to soil-free mountain areas, but have no mention of blockfields. Westermann et al. (2013) included a zone of lower soil moisture in the upper meters for their blockfield stratigraphy, but as permafrost degrades and the active layer deepens, water can pool up at the bottom of the active layer which strongly affects the thermal regime. The one-dimensional heat conduction model by Hipp et al. (2012) also featured constant volumetric water contents.

Martin et al. (2019) already showed that a drainage component can strongly affect ground temperatures and permafrost presence in peat plateaus and palsas in northern Norway. They termed the lack of drainage is a major limitation of aforementioned modelling studies. The findings in this thesis add to this statement, but for blocky mountain terrain. The negative thermal anomaly in this terrain indicates that permafrost might be present in areas that are not included in maps from permafrost distribution studies.

Harris and Pedersen (1998) already stated that the thermal anomaly in blocky terrain complicated the identification of the lower mountain permafrost limit. Thermal anomalies can be translated into elevation differences by assuming a temperature lapse rate, which influences altitudinal permafrost limits. If we assume a temperature lapse rate of 0.5 °C per 100 m (Farbrot et al. 2011), the lower limit of permafrost can be found up to 300 m lower in drained, blocky deposits compared to undrained, blocky deposits. This is a first-order approximation and does not factor in changes in precipitation and other changes with elevation. Gisnås et al. (2017) modelled a lower discontinuous permafrost limit in Finnmark at around 400 m, which is approximately 300 m above the Ivarsfjorden rock glacier.

Future work with CryoGrid can aim to include the effect of air convection (done by e.g. Wicky and Hauck 2020) and blocks protruding through the snow cover (done by e.g. Gruber and Hoelze 2008). While Gruber and Hoelze (2008) used a simple model that uses a lower thermal conductivity for the blocky layer, CryoGrid offers a tool to create a more complex, physically based model setup to represent this effect. A more detailed three dimensional model setup that features subsurface water flow, will lead to a more realistic representation of the ground ice mass balance. Finally, a suggestion for future mapping studies is to include different drainage regimes in grid cells depending on topography and choose a field capacity based on surface material via remote sensing. This would aid in capturing these lower permafrost limit landforms in maps.

6.3.2 Rock glaciers as water resource

While the rock glaciers and blockfields in this study are not actively used as a water resource, rock glaciers in more arid regions are an important source of water for humans (e.g. Croce and Milana 2002). The global ratio of rock glacier-glacier water volume equivalent (WVEQ) is increasing due to differential warming of rock glaciers as compared to glaciers (Jones et al. 2019). Therefore, accurately simulating the transient development of ground ice in rock glaciers will be of value in water resource management. Figure 26 showed a clear difference in subsurface drainage between a stratigraphy with and without a sediment fraction in between blocks at a semi-arid site. The low field capacity in the *blocks only* stratigraphy results in markedly more drainage and longer than in the *blocks with sediment* stratigraphy when the active layer is unfrozen. This means that on blockfields or rock glaciers in (semi-) arid conditions with a stratigraphy similar to the *blocks only* stratigraphy, drainage will be a more direct response to precipitation then if the stratigraphy is more similar to *blocks with sediment*. The interactions of rock glaciers with the catchment are generally poorly understood as field studies on rock glacier hydrology are difficult (Jones et al. 2019). Conceptual models of hydrology in rock glaciers suggest two subsurface flow paths: 'supra-permafrost flow' and 'sub-permafrost flow' (Jones et al.

2019). The 'supra-permafrost flow', in the active layer, is comparable to the drainage that is presented in figure 26. Similar to the findings in this figure, Harrington et al. (2018) report that coarse blocky deposits that form an inactive rock glacier in the Canadian Rockies, allow rapid infiltration and flow of rain and snowmelt.

Further, rock glaciers are sensitive to climate change (Haeberli et al. 2010) and recent studies have linked rock glacier acceleration with increasing air temperatures (e.g. Kääb et al. 2007; Hartl et al. 2016; Eriksen et al. 2018). Permafrost degradation might start a positive feedback of increasing deformation rates related to infiltrating meltwater that accesses the rock glacier interior, resulting in stretching of the permafrost body. Alternatively, rock glaciers that lose ice may increase their active layer thickness and possibly connections between voids or pores (Delaloye and Lambiel 2005). This can improve the air circulation processes that were described by Harris and Pedersen (1998) and retard the warming of the rock glacier. Therefore, the response of rock glaciers to climate warming may be slower compared to glaciers (Jones et al. 2019).

6.3.3 Landforms and slope stability

It was stated in section 3.2.2 that the rock glacier in Ivarsfjorden is located in sandstone, which is common for rock glaciers (Haeberli et al. 2006). Phyllite is the other bedrock type in the region of Ivarsfjorden (Lilleøren et al. 2022), but no rock glaciers are found in this type of rock as it is mechanically weak and forms more fine sediment as opposed to large blocks. Fine grained material is more likely to undergo debris flows or solifluciton (Haeberli et al. 2006). Ikeda and Matsuoka (2006) also described how differences in the geology affect the type of rock glacier that is formed. 'Bouldery rock glaciers', that are matrix-free, form in resistant material and 'pebbly rock glaciers' form in less resistant material. Near the lower limit of mountain permafrost, bouldery rock glaciers have the potential to extend to lower altitudes compared to pebbly rock glaciers, as bouldery or blocky material promotes cooling of the subsurface. It is therefore that rock glaciers in the region of Ivarsfjorden are found almost exclusively in the resistant sandstones (Lilleøren et al. 2022).

Subsurface ice conditions are of great interest to scientists and engineers in mountain areas (Haeberli et al. 2010). Ground ice and ground temperatures play important roles in slope stability in these environments. Ice deformation mechanisms respond strongly to a temperature increase form -5 °C to 0 °C (Haeberli et al. 2010). Results from the transient simulations at Ivarsfjorden and Juvvasshøe showed that rates of warming and ground ice degradation are affected by the stratigraphy of the ground. Degradation of mountain permafrost and ground ice can lead to slope instability (e.g. Gruber and Haeberli 2007; Sæmundsson et al. 2018; Nelson et al. 2001). In bedrock, these mechanisms include: Loss of bonding, ice segregation, expansion, higher hydrostatic pressure and the reduction of shear strength (Gruber and Haeberli 2007). In coarse, blocky terrain, stability problems related to accelerating movement rates (e.g. Kääb et al. 2007) increase and need further studying (Haeberli et al. 2010). Further, an active layer thickening leads to more available loose material for mass movement (Deline et al. 2015).

In addition to long-term warming, the occurrence of single warm summers can strongly

affect the ground ice content in mountain permafrost areas. A study from the Swiss Alps (Hilbich et al. 2008) described how the extremely warm summer of 2003 caused a substantial loss of ground ice which did not recover in following years, while ground temperatures did. This shows the sensitivity of these mountain environments to warming and the vital role of ground ice. An accurate representation of the ground ice mass balance is not only important for blocky mountain terrain. The melting of ground ice has shaped many landscapes, related to excess ice and thaw subsidence (e.g. Schirrmeister et al. 2008) and has been simulated by Westermann et al. (2016). A proper inclusion of the water and ice balance will also be of value for the prediction of thaw subsidence and the formation of thermokarst landforms.

7 Conclusions

In this study, CryoGrid, a heat conduction model, with a bucket scheme for the water balance and a lateral subsurface drainage component was used to simulate the effect of blocky terrain on the ground thermal regime. The main focus is on two permafrost sites in Norway: A blockfield site at high elevation in southern Norway and a rock glacier site close to sea level in northern Norway. Additionally, three ancillary sites in the global permafrost extent are included. Idealized stratigraphies are used to investigate thermal anomalies under different amounts of snowfall. Here, a 'scenario' is referred to a as a setup of the model with a defined subsurface stratigraphy, that is either well drained or poorly drained. From the work in this thesis, the following conclusions can be drawn:

- Markedly lower ground temperatures are found in well drained, blocky deposits (the *blocks only, drained* scenario) compared to other model model scenarios at all permafrost sites. The thermal anomaly is up to 1.5 °C at the sites in Norway and up to 3.5 °C in a continental arctic climate. The anomaly is smallest the simulations that feature no permafrost, meaning that the effect largely vanishes when no persistent ground ice exists. Despite not including convective heat transfer and the effect of blocks protruding through the winter snow cover, the effect of the ground ice mass balance is isolated and shown to be significant.

- The thermal anomaly is largest in simulations with relatively large snowfall amounts. In these cases, the ground temperature drops rapidly in autumn in the *blocks only, drained* scenario, while in other scenarios the temperature is confined at 0 °C for several weeks as freezing pore water releases latent heat. Oppositely, temperatures in the *blocks only, drained* scenario are confined at 0 °C in late spring when a layer of superimposed ice, that is formed due to infiltrating snowmelt melts.

- Stable permafrost can exist in well drained, blocky deposits under a mean annual ground surface temperature (MAGST) of 2.0-2.5 °C at location of the rock glacier in Ivarsfjorden. At the location of the PACE (Permafrost and Climate in Europe) borehole in Juvvasshøe, southern Norway, simulations show stable permafrost for all snowfall amounts in well drained, blocky terrain. All other simulations at this location feature positive ground temperatures at higher snowfall amounts.

- Transient simulations at the Ivarsfjorden rock glacier showed a completely or partially degraded ground ice table since 1951 for all scenarios except the *blocks only, drained* scenario. The melting of ground ice strongly affects the warming rates in the ground due to the uptake of latent heat.

- Subsurface drainage at a semi-arid continental site starts several weeks earlier in summer and continues several weeks longer in autumn in a stratigraphy of only blocks, compared to a stratigraphy that features a fine sediment fraction between blocks (*blocks with sediment* stratigraphy). The latter scenario only has drainage in events related to rainfall, while the former has drainage throughout the entire summer. In a climate with more precipitation, the difference between the scenarios is less pronounced.

This study suggests that the drainage effect can also reproduce the lower altitudinal limit of permafrost in blocky terrain, which has been found in many studies. Additionally, an accurate representation of the evolution of the ground ice table in mountain permafrost environments is important in relation to water resources in (semi-) arid regions, slope stability and future permafrost distribution mapping. The inclusion of the drainage effect is another step towards a better model representation of the complex thermal systems in permafrost environments.

References

Aalstad, K., S. Westermann, T. V. Schuler, J. Boike, and L. Bertino (2018). "Ensemble-based assimilation of fractional snow-covered area satellite retrievals to estimate the snow distribution at Arctic sites". In: *The Cryosphere* 12.1, pp. 247–270. URL: https://doi.org/10.5194/tc-12-247-2018.

Andersen, B. G. (1980). "The deglaciation of Norway after 10,000 BP". In: *Boreas* 9.4, pp. 211–216. URL: https://doi.org/10.1111/j.1502-3885.1980.tb00697.x.

Angelopoulos, M., P. P. Overduin, M. Jenrich, I. Nitze, F. Günther, J. Strauss, S. Westermann, L. Schirrmeister, A. Kholodov, M. Krautblatter, et al. (2021). "Onshore thermokarst primes subsea permafrost degradation". In: *Geophysical Research Letters* 48.20, e2021GL093881. URL: https://doi.org/10.1029/2021GL093881.

Azócar, G. and A. Brenning (2010). "Hydrological and geomorphological significance of rock glaciers in the dry Andes, Chile (27–33 S)". In: *Permafrost and Periglacial Processes* 21.1, pp. 42–53. URL: https://doi.org/10.1002/ppp.669.

Balch, E. S. (1900). *Glacieres or Freezing Caverns.* Philadelphia: Lane and Scott, p. 337. URL: https://doi.org/10.2307/196910.

Ballantyne, C. K. and C. Harris (1994). *The periglaciation of great Britain.* CUP Archive.

Berthling, I. (2011). "Beyond confusion: Rock glaciers as cryo-conditioned landforms". In: *Geomorphology* 131.3-4, pp. 98–106. URL: https://doi.org/10.1016/j.geomorph.2011.05.002.

Biskaborn, B. K., S. L. Smith, J. Noetzli, H. Matthes, G. Vieira, D. A. Streletskiy, P. Schoeneich, V. E. Romanovsky, A. G. Lewkowicz, A. Abramov, et al. (2019). "Permafrost is warming at a global scale". In: *Nature communications* 10.1, pp. 1–11. URL: https://doi.org/10.1038/s41467-018-08240-4.

Boike, J., J. Nitzbon, K. Anders, M. Grigoriev, D. Bolshiyanov, M. Langer, S. Lange, N. Bornemann, A. Morgenstern, P. Schreiber, et al. (2019). "A 16-year record (2002–2017) of permafrost, active-layer, and meteorological conditions at the Samoylov Island Arctic permafrost research site, Lena River delta, northern Siberia: an opportunity to validate remote-sensing data and land surface, snow, and permafrost models". In: *Earth System Science Data* 11.1, pp. 261–299. URL: https://doi.org/10.5194/essd-11-261-2019.

Croce, F. A. and J. P. Milana (2002). "Internal structure and behaviour of a rock glacier in the arid Andes of Argentina". In: *Permafrost and Periglacial Processes* 13.4, pp. 289–299. URL: https://doi.org/10.1002/ppp.431.

Czekirda, J., S. Westermann, B. Etzelmüller, and T. Jóhannesson (2019). "Transient modelling of permafrost distribution in Iceland". In: *Frontiers in Earth Science* 7, p. 130. URL: https://doi.org/10.3389/feart.2019.00130.

D'Amboise, C. J., K. Müller, L. Oxarango, S. Morin, and T. V. Schuler (2017). "Implementation of a physically based water percolation routine in the Crocus/SURFEX (V7. 3) snowpack model". In: *Geoscientific Model Development* 10.9, pp. 3547–3566. URL: https://doi.org/10.5194/gmd-10-3547-2017.

Dahl, R. (1966). "Block fields, weathering pits and tor-like forms in the Narvik Mountains, Nordland, Norway". In: *Geografiska Annaler: Series A, Physical Geography* 48.2, pp. 55–85. URL: https://doi.org/10.1080/04353676.1966.11879730.

Dall'Amico, M., S. Endrizzi, S. Gruber, and R. Rigon (2011). "A robust and energy-conserving model of freezing variably-saturated soil". In: *The Cryosphere* 5.2, pp. 469–484. URL: https://doi.org/10.5194/tc-5-469-2011.

Delaloye, R., E. Reynard, C. Lambiel, L. Marescot, and R. Monnet (2003). "Thermal anomaly in a cold scree slope (Creux du Van, Switzerland)". In: *Proceedings of the 8th International Conference on Permafrost*. Vol. 2125. Balkema: Zurich, pp. 175–180.

Delaloye, R. and C. Lambiel (2005). "Evidence of winter ascending air circulation throughout talus slopes and rock glaciers situated in the lower belt of alpine discontinuous permafrost (Swiss Alps)". In: *Norsk Geografisk Tidsskrift-Norwegian Journal of Geography* 59.2, pp. 194–203. URL: https://doi.org/10.1080/00291950510020673.

Deline, P., S. Gruber, R. Delaloye, L. Fischer, M. Geertsema, M. Giardino, A. Hasler, M. Kirkbride, M. Krautblatter, F. Magnin, et al. (2015). "Ice loss and slope stability in high-mountain regions". In: *Snow and ice-related hazards, risks, and disasters*. Elsevier, pp. 521–561. URL: https://doi.org/10.1016/B978-0-12-394849-6.00015-9.

Dozier, J. and J. Frew (1990). "Rapid calculation of terrain parameters for radiation modeling from digital elevation data". In: *IEEE Transactions on geoscience and remote sensing* 28.5, pp. 963–969. URL: https://doi.org/10.1109/36.58986.

Eriksen, H., L. Rouyet, T. Lauknes, I. Berthling, K. Isaksen, H. Hindberg, Y. Larsen, and G. Corner (2018). "Recent acceleration of a rock glacier complex, Adjet, Norway, documented by 62 years of remote sensing observations". In: *Geophysical Research Letters* 45.16, pp. 8314–8323. URL: https://doi.org/10.1029/2018GL077605.

Etzelmüller, B. (2013). "Recent advances in mountain permafrost research". In: *Permafrost and periglacial Processes* 24.2, pp. 99–107. URL: https://doi.org/10.1002/ppp.1772.

Etzelmüller, B., I. Berthling, and J. L. Sollid (2003). "Aspects and concepts on the geomorphological significance of Holocene permafrost in southern Norway". In: *Geomorphology* 52.1-2, pp. 87–104. URL: https://doi.org/10.1016/S0169-555X(02)00250-7.

Etzelmüller, B., H. Farbrot, Á. Guðmundsson, O. Humlum, O. E. Tveito, and H. Björnsson (2007). "The regional distribution of mountain permafrost in Iceland". In: *Permafrost and Periglacial Processes* 18.2, pp. 185–199. URL: https://doi.org/10.1002/ppp.583.

Etzelmüller, B., M. Guglielmin, C. Hauck, C. Hilbich, M. Hoelzle, K. Isaksen, J. Noetzli, M. Oliva, and M. Ramos (2020a). "Twenty years of European mountain permafrost dynamics—the PACE legacy". In: *Environmental Research Letters* 15.10, p. 104070. URL: https://doi.org/10.1088/1748-9326/abae9d.

Etzelmüller, B., M. Hoelzle, E. S. Flo Heggem, K. Isaksen, C. Mittaz, D. V. Mühll, R. S. Ødegård, W. Haeberli, and J. L. Sollid (2001). "Mapping and modelling the occurrence and distribution of mountain permafrost". In: *Norsk Geografisk Tidsskrift-Norwegian Journal of Geography* 55.4, pp. 186–194. URL: https://doi.org/10.1080/00291950152746513.

Etzelmüller, B., H. Patton, A. Schomacker, J. Czekirda, L. Girod, A. Hubbard, K. S. Lilleøren, and S. Westermann (2020b). "Icelandic permafrost dynamics since the Last Glacial Maximum–model results and geomorphological implications". In: *Quaternary Science Reviews* 233, p. 106236. URL: https://doi.org/10.1016/j.quascirev.2020.106236.

Everdingen, R. O. van (1998). *Multi-language glossary of permafrost and related ground-ice terms*. International Permafrost Association.

Farbrot, H., T. F. Hipp, B. Etzelmüller, K. Isaksen, R. S. Ødegård, T. V. Schuler, and O. Humlum (2011). "Air and ground temperature variations observed along elevation and continentality gradients in Southern Norway". In: *Permafrost and Periglacial Processes* 22.4, pp. 343–360. URL: https://doi.org/10.1002/ppp.733.

Fiddes, J., S. Endrizzi, and S. Gruber (2015). "Large-area land surface simulations in heterogeneous terrain driven by global data sets: application to mountain permafrost". In: *The Cryosphere* 9.1, pp. 411–426. URL: https://doi.org/10.5194/tc-9-411-2015.

Fiddes, J. and S. Gruber (2014). "TopoSCALE v. 1.0: downscaling gridded climate data in complex terrain". In: *Geoscientific Model Development* 7.1, pp. 387–405. URL: https://doi.org/10.5194/gmd-7-387-2014.

Fiddes, J., K. Aalstad, and M. Lehning (2022). "TopoCLIM: rapid topography-based downscaling of regional climate model output in complex terrain v1. 1". In: *Geoscientific Model Development* 15.4, pp. 1753–1768. URL: https://doi.org/10.5194/gmd-15-1753-2022.

French, H. M. (2007). *The periglacial environment*. John Wiley & Sons, pp. 83–115, 456. URL: https://doi.org/10.1002/9781118684931.

Genxu, W., L. Guangsheng, L. Chunjie, and Y. Yan (2012). "The variability of soil thermal and hydrological dynamics with vegetation cover in a permafrost region". In: *Agricultural and Forest Meteorology* 162, pp. 44–57. URL: https://doi.org/10.1016/j.agrformet.2012.04.006.

Gisnås, K., B. Etzelmüller, H. Farbrot, T. Schuler, and S. Westermann (2013). "CryoGRID 1.0: Permafrost distribution in Norway estimated by a spatial numerical model". In: *Permafrost and Periglacial Processes* 24.1, pp. 2–19. URL: https://doi.org/10.1002/ppp.1765.

Gisnås, K. (2016). "Permafrost modelling over different scales in arctic and high-mountain environments". In:

Gisnås, K., B. Etzelmüller, C. Lussana, J. Hjort, A. B. K. Sannel, K. Isaksen, S. Westermann, P. Kuhry, H. H. Christiansen, A. Frampton, et al. (2017). "Permafrost map for Norway, Sweden and Finland". In: *Permafrost and periglacial processes* 28.2, pp. 359–378. URL: https://doi.org/10.1002/ppp.1922.

Gisnås, K., S. Westermann, T. V. Schuler, T. Litherland, K. Isaksen, J. Boike, and B. Etzelmüller (2014). "A statistical approach to represent small-scale variability of permafrost temperatures due to snow cover". In: *The Cryosphere* 8.6, pp. 2063–2074. URL: https://doi.org/10.5194/tc-8-2063-2014.

Gisnås, K., S. Westermann, T. V. Schuler, K. Melvold, and B. Etzelmüller (2016). "Small-scale variation of snow in a regional permafrost model". In: *The Cryosphere* 10.3, pp. 1201–1215. URL: https://doi.org/10.5194/tc-10-1201-2016.

Gold, L. W. (1963). *Influence of the snow cover on the average annual ground temperature at Ottawa, Canada*. National Research Council, Division of Building Research.

Gorbunov, A. P., S. S. Marchenko, and E. V. Seversky (2004). "The thermal environment of blocky materials in the mountains of Central Asia". In: *Permafrost and Periglacial Processes* 15.1, pp. 95–98. URL: https://doi.org/10.1002/ppp.478.

Gruber, S. and W. Haeberli (2007). "Permafrost in steep bedrock slopes and its temperature-related destabilization following climate change". In: *Journal of Geophysical Research: Earth Surface* 112.F2. URL: https://doi.org/10.1029/2006JF000547.

Gruber, S. and M. Hoelze (2008). "The cooling effect of coarse blocks revisited: a modeling study of a purely conductive mechanism". In: *Zurich Open Repository and Archive*.

Haeberli, W. (1985). "Creep of mountain permafrost: internal structure and flow of alpine rock glaciers." In: *Mitteilungen der Versuchsanstalt fur Wasserbau, Hydrologie und Glaziologie an der ETH Zurich* 77.

Haeberli, W., B. Hallet, L. Arenson, R. Elconin, O. Humlum, A. Kääb, V. Kaufmann, B. Ladanyi, N. Matsuoka, S. Springman, et al. (2006). "Permafrost creep and rock glacier dynamics". In: *Permafrost and periglacial processes* 17.3, pp. 189–214. URL: https://doi.org/10.1002/ppp.561.

Haeberli, W., J. Noetzli, L. Arenson, R. Delaloye, I. Gärtner-Roer, S. Gruber, K. Isaksen, C. Kneisel, M. Krautblatter, and M. Phillips (2010). "Mountain permafrost: development and challenges of a young research field". In: *Journal of Glaciology* 56.200, pp. 1043–1058. URL: https://doi.org/10.3189/002214311796406121.

Hamilton, S. J. and W. B. Whalley (1995). "Rock glacier nomenclature: a re-assessment". In: *Geomorphology* 14.1, pp. 73–80. URL: https://doi.org/10.1016/0169-555X(95)00036-5.

Hanson, S. and M. Hoelzle (2004). "The thermal regime of the active layer at the Murtèl rock glacier based on data from 2002". In: *Permafrost and Periglacial Processes* 15.3, pp. 273–282. URL: https://doi.org/10.1002/ppp.499.

Harrington, J. S., A. Mozil, M. Hayashi, and L. R. Bentley (2018). "Groundwater flow and storage processes in an inactive rock glacier". In: *Hydrological Processes* 32.20, pp. 3070–3088. URL: https://doi.org/10.1002/hyp.13248.

Harris, C., L. U. Arenson, H. H. Christiansen, B. Etzelmüller, R. Frauenfelder, S. Gruber, W. Haeberli, C. Hauck, M. Hoelzle, O. Humlum, et al. (2009). "Permafrost and climate in Europe: Monitoring and modelling thermal, geomorphological and geotechnical responses". In: *Earth-Science Reviews* 92.3-4, pp. 117–171. URL: https://doi.org/10.1016/j.earscirev.2008.12.002.

Harris, C., W. Haeberli, D. Vonder Mühll, and L. King (2001). "Permafrost monitoring in the high mountains of Europe: the PACE project in its global context". In: *Permafrost and periglacial processes* 12.1, pp. 3–11. URL: https://doi.org/10.1002/ppp.377.

Harris, C. and J. B. Murton (2005). "Interactions between glaciers and permafrost: an introduction". In: *Geological Society, London, Special Publications* 242.1, pp. 1–9. URL: https://doi.org/10.1144/GSL.SP.2005.242.01.01.

Harris, S. A. and D. E. Pedersen (1998). "Thermal regimes beneath coarse blocky materials". In: *Permafrost and periglacial processes* 9.2, pp. 107–120. URL: https://doi.org/10.1002/(SICI)1099-1530(199804/06)9:2%3C107::AID-PPP277%3E3.0.CO;2-G.

Hartl, L., A. Fischer, M. Stocker-waldhuber, and J. Abermann (2016). "Recent speed-up of an alpine rock glacier: an updated chronology of the kinematics of outer hochebenkar rock glacier based on geodetic measurements". In: *Geografiska Annaler: Series A, Physical Geography* 98.2, pp. 129–141. URL: https://doi.org/10.1111/geoa.12127.

Heggem, E. S., H. Juliussen, and B. Etzelmüller (2005). "Mountain permafrost in central-eastern Norway". In: *Norsk Geografisk Tidsskrift-Norwegian Journal of Geography* 59.2, pp. 94–108. URL: https://doi.org/10.1080/00291950510038377.

Helgason, J. K., C. Morino, S. J. Conway, Þ. Sæmundsson, and M. R. Balme ((2018)). "On the dynamics of permafrost-induced landslides in Iceland". In: EUCOP5.

Hersbach, H., B. Bell, P. Berrisford, S. Hirahara, A. Horányi, J. Muñoz-Sabater, J. Nicolas, C. Peubey, R. Radu, D. Schepers, et al. (2020). "The ERA5 global reanalysis". In: *Quarterly Journal of the Royal Meteorological Society* 146.730, pp. 1999–2049. URL: https://doi.org/10.1002/qj.3803.

Hilbich, C., C. Hauck, M. Hoelzle, M. Scherler, L. Schudel, I. Völksch, D. Vonder Mühll, and R. Mäusbacher (2008). "Monitoring mountain permafrost evolution using electrical resistivity tomography: A 7-year study of seasonal, annual, and long-term variations

at Schilthorn, Swiss Alps". In: *Journal of Geophysical Research: Earth Surface* 113.F1. URL: https://doi.org/10.1029/2007JF000799.

Hinzman, L. D., N. D. Bettez, W. R. Bolton, F. S. Chapin, M. B. Dyurgerov, C. L. Fastie, B. Griffith, R. D. Hollister, A. Hope, H. P. Huntington, et al. (2005). "Evidence and implications of recent climate change in northern Alaska and other arctic regions". In: *Climatic change* 72.3, pp. 251–298. URL: https://doi.org/10.1007/s10584-005-5352-2.

Hinzman, L., D. Kane, R. Gieck, and K. Everett (1991). "Hydrologic and thermal properties of the active layer in the Alaskan Arctic". In: *Cold Regions Science and Technology* 19.2, pp. 95–110. URL: https://doi.org/10.1016/0165-232X(91)90001-W.

Hipp, T., B. Etzelmüller, H. Farbrot, T. Schuler, and S. Westermann (2012). "Modelling borehole temperatures in Southern Norway–insights into permafrost dynamics during the 20th and 21st century". In: *The Cryosphere* 6.3, pp. 553–571. URL: https://doi.org/10.5194/tc-6-553-2012.

Hoelzle, M., W. Haeberli, and C. Stocker-Mittaz (2003). "Miniature ground temperature data logger measurements 2000–2002 in the Murtèl-Corvatsch area, Eastern Swiss Alps". In: *Proceedings of the Eighth International Conference on Permafrost*. Vol. 21. Balkema Lisse, Netherlands, p. 25.

Humlum, O. (1988). "Rock glacier appearance level and rock glacier initiation line altitude: a methodological approach to the study of rock glaciers". In: *Arctic and Alpine Research* 20.2, pp. 160–178. URL: https://doi.org/10.2307/1551495.

— (1996). "Origin of rock glaciers: observations from Mellemfjord, Disko Island, central West Greenland". In: *Permafrost and Periglacial Processes* 7.4, pp. 361–380. URL: https://doi.org/10.1002/(SICI)1099-1530(199610)7:4%3C361::AID-PPP227%3E3.0.CO;2-4.

— (1997). "Active layer thermal regime at three rock glaciers in Greenland". In: *Permafrost and Periglacial Processes* 8.4, pp. 383–408. URL: https://doi.org/10.1002/(SICI)1099-1530(199710/12)8:4%3C383::AID-PPP265%3E3.0.CO;2-V.

Ichim, I. (1978). "Preliminary observations on the rock glacier phenomenon in the Romanian Carpathians". In: *Rev. Roum. Geol. Geophys. Geogr., Geographie* 23.2, pp. 295–299.

Ikeda, A. and N. Matsuoka (2006). "Pebbly versus bouldery rock glaciers: Morphology, structure and processes". In: *Geomorphology* 73.3-4, pp. 279–296. URL: https://doi.org/10.1016/j.geomorph.2005.07.015.

Isaksen, K., E. Heggem, S. Bakkehøi, R. Ødegård, T. Eiken, B. Etzelmüller, and J. Sollid (2003). "Mountain permafrost and energy balance on Juvvasshøe, southern Norway". In: *8th International Conference on Permafrost, Zurich, Switzerland, ISI: 000185049300083*, pp. 467–472.

Isaksen, K., P. Holmlund, J. L. Sollid, and C. Harris (2001). "Three deep alpine-permafrost boreholes in Svalbard and Scandinavia". In: *Permafrost and Periglacial Processes* 12.1, pp. 13–25. URL: https://doi.org/10.1002/ppp.380.

Isaksen, K., J. L. Sollid, P. Holmlund, and C. Harris (2007). "Recent warming of mountain permafrost in Svalbard and Scandinavia". In: *Journal of Geophysical Research: Earth Surface* 112.F2. URL: https://doi.org/10.1029/2006JF000522.

Ives, J. (1957). "Glaciation of the Torngat mountains, northern Labrador". In: *Arctic*, pp. 66–87. URL: https://doi.org/10.14430/arctic3755.

Jambaljav, Y., A. Dashtseren, D. Solongo, D. Saruulzaya, D. Battogtokh, Y. Iijima, M. Ishikawa, Y. Zhang, H. Yabuki, and T. Kadota (2008). "The temperature regime in

boreholes at Nalaikh and Terelj sites, Mongolia". In: *Proceedings of the Ninth International Conference on Permafrost*. Vol. 29, pp. 821–825.

Jones, D. B., S. Harrison, K. Anderson, and W. B. Whalley (2019). "Rock glaciers and mountain hydrology: A review". In: *Earth-Science Reviews* 193, pp. 66–90. URL: https://doi.org/10.1016/j.earscirev.2019.04.001.

Juliussen, H. and O. Humlum (2008). "Thermal regime of openwork block fields on the mountains Elgåhogna and Sølen, central-eastern Norway". In: *Permafrost and Periglacial Processes* 19.1, pp. 1–18. URL: https://doi.org/10.1002/ppp.607.

Kääb, A., R. Frauenfelder, and I. Roer (2007). "On the response of rockglacier creep to surface temperature increase". In: *Global and Planetary Change* 56.1-2, pp. 172–187. URL: https://doi.org/10.1016/j.gloplacha.2006.07.005.

Kleman, J. (1994). "Preservation of landforms under ice sheets and ice caps". In: *Geomorphology* 9.1, pp. 19–32. URL: https://doi.org/10.1016/0169-555X(94)90028-0.

Lachenbruch, A. H. (1988). "Permafrost temperature and the changing climate". In: *1988, Proceedings of the Fifth International Conference on Permafrost, Trondhelm, Norway*. Vol. 3, pp. 9–17.

Lilleøren, K. S. and B. Etzelmüller (2011). "A regional inventory of rock glaciers and ice-cored moraines in Norway". In: *Geografiska Annaler: Series A, Physical Geography* 93.3, pp. 175–191. URL: https://doi.org/10.1111/j.1468-0459.2011.00430.x.

Lilleøren, K. S., B. Etzelmüller, T. V. Schuler, K. Gisnås, and O. Humlum (2012). "The relative age of mountain permafrost—estimation of Holocene permafrost limits in Norway". In: *Global and Planetary Change* 92, pp. 209–223. URL: https://doi.org/10.1016/j.gloplacha.2012.05.016.

Lilleøren, K. S., B. Etzelmüller, L. Rouyet, T. Eiken, and C. Hilbich (2022). "Transitional rock glaciers at sea-level in Northern Norway". In: *Earth Surface Dynamics Discussions*, pp. 1–29. URL: https://doi.org/10.5194/esurf-2022-6.

Liston, G. E. and M. Sturm (1998). "A snow-transport model for complex terrain". In: *Journal of Glaciology* 44.148, pp. 498–516. URL: https://doi.org/10.3189/S0022143000002021.

Lukas, S., L. I. Nicholson, F. H. Ross, and O. Humlum (2005). "Formation, meltout processes and landscape alteration of high-Arctic ice-cored moraines—Examples from Nordenskiold Land, central Spitsbergen". In: *Polar Geography* 29.3, pp. 157–187. URL: https://doi.org/10.1080/789610198.

Mangerud, J., S. Gulliksen, and E. Larsen (2010). "14C-dated fluctuations of the western flank of the Scandinavian Ice Sheet 45–25 kyr BP compared with Bølling–Younger Dryas fluctuations and Dansgaard–Oeschger events in Greenland". In: *Boreas* 39.2, pp. 328–342. URL: https://doi.org/10.1111/j.1502-3885.2009.00127.x.

Mangerud, J., R. Gyllencreutz, Ø. Lohne, and J. I. Svendsen (2011). "Glacial History of Norway". eng. In: *Developments in Quaternary Science*. Vol. 15. Elsevier Science & Technology, pp. 279–298. ISBN: 9780444534477. URL: https://doi.org/10.1016/B978-0-444-53447-7.00022-2.

Martin, L. C. P., J. Nitzbon, K. S. Aas, B. Etzelmüller, H. Kristiansen, and S. Westermann (2019). "Stability conditions of peat plateaus and palsas in northern Norway". In: *Journal of Geophysical Research: Earth Surface* 124.3, pp. 705–719. URL: https://doi.org/10.1029/2018JF004945.

Michaelson, G. J., C. Ping, and J. Kimble (1996). "Carbon storage and distribution in tundra soils of Arctic Alaska, USA". In: *Arctic and Alpine Research* 28.4, pp. 414–424. URL: https://doi.org/10.2307/1551852.

Miesen, F., S. O. Dahl, and L. Schrott (2021). "Evidence of glacier-permafrost interactions associated with hydro-geomorphological processes and landforms at Snøhetta, Dovrefjell, Norway". In: *Geografiska Annaler: Series A, Physical Geography* 103.3, pp. 273–302. URL: https://doi.org/10.1080/04353676.2021.1955539.

Mittaz, C., M. Hoelzle, and W. Haeberli (2000). "First results and interpretation of energy-flux measurements over Alpine permafrost". In: *Annals of Glaciology* 31, pp. 275–280. URL: https://doi.org/10.3189/172756400781820363.

Monin, A. S. and A. M. Obukhov (1954). "Basic laws of turbulent mixing in the surface layer of the atmosphere". In: *Contrib. Geophys. Inst. Acad. Sci. USSR* 151.163, e187.

Nelson, F. E., O. A. Anisimov, and N. I. Shiklomanov (2001). "Subsidence risk from thawing permafrost". In: *Nature* 410.6831, pp. 889–890. URL: https://doi.org/10.1038/35073746.

Nesje, A., S. O. Dahl, E. Anda, and N. Rye (1988). "Block fields in southern Norway: Significance for the Late Weichselian ice sheet". In: *Norsk Geologisk Tidsskrift* 68.3, pp. 149–169. URL: https://njg.geologi.no/images/NJG_articles/NGT_68_3_149-169.pdf.

Nitzbon, J., M. Langer, S. Westermann, L. Martin, K. S. Aas, and J. Boike (2019). "Pathways of ice-wedge degradation in polygonal tundra under different hydrological conditions". In: *The Cryosphere* 13.4, pp. 1089–1123. URL: https://doi.org/10.5194/tc-13-1089-2019.

Obu, J., S. Westermann, A. Bartsch, N. Berdnikov, H. H. Christiansen, A. Dashtseren, R. Delaloye, B. Elberling, B. Etzelmüller, A. Kholodov, et al. (2019). "Northern Hemisphere permafrost map based on TTOP modelling for 2000–2016 at 1 km2 scale". In: *Earth-Science Reviews* 193, pp. 299–316. URL: https://doi.org/10.1016/j.earscirev.2019.04.023.

Olsen, L., H. Sveian, and B. Bergstrøm (2001). "Rapid adjustments of the western part of the Scandinavian lee Sheet during the Mid and late Weichselian-a new model." In: *Norwegian Journal of Geology/Norsk Geologisk Forening* 81.2.

Overduin, P., T. Schneider von Deimling, F. Miesner, M. Grigoriev, C. Ruppel, A. Vasiliev, H. Lantuit, B. Juhls, and S. Westermann (2019). "Submarine permafrost map in the Arctic modeled using 1-D transient heat flux (supermap)". In: *Journal of Geophysical Research: Oceans* 124.6, pp. 3490–3507. URL: https://doi.org/10.1029/2018JC014675.

Popescu, R., A. Vespremeanu-Stroe, A. Onaca, M. Vasile, N. Cruceru, and O. Pop (2017). "Low-altitude permafrost research in an overcooled talus slope–rock glacier system in the Romanian Carpathians (Detunata Goală, Apuseni Mountains)". In: *Geomorphology* 295, pp. 840–854. URL: https://doi.org/10.1016/j.geomorph.2017.07.029.

Porter, C., P. Morin, I. Howat, M. Noh, B. Bates, K. Peterman, S. Keesey, M. Schlenk, J. Gardiner, K. Tomko, et al. (2018). *ArcticDEM, Harvard Dataverse [data set], V1.* URL: https://doi.org/10.7910/DVN/OHHUKH.

Potter Jr, N. (1972). "Ice-cored rock glacier, Galena Creek, northern Absaroka Mountains, Wyoming". In: *Geological Society of America Bulletin* 83.10, pp. 3025–3058. URL: https://doi.org/10.1130/0016-7606(1972)83[3025:IRGGCN]2.0.CO;2.

Rea, B. (2007). "Blockfields (Felsenmeer)". In: *PERIGLACIAL LANDFORMS, ROCK FORMS*. Elsevier. URL: https://doi.org/10.1016/B0-44-452747-8/00110-1.

Reimer, P. J., M. G. Baillie, E. Bard, A. Bayliss, J. W. Beck, P. G. Blackwell, C. B. Ramsey, C. E. Buck, G. S. Burr, R. L. Edwards, et al. (2009). "IntCal09 and Ma-

rine09 radiocarbon age calibration curves, 0–50,000 years cal BP". In: *Radiocarbon* 51.4, pp. 1111–1150. URL: https://doi.org/10.1017/S0033822200034202.

Richards, L. A. (1931). "Capillary conduction of liquids through porous mediums". In: *Physics* 1.5, pp. 318–333. URL: https://doi.org/10.1063/1.1745010.

Riseborough, D., N. Shiklomanov, B. Etzelmüller, S. Gruber, and S. Marchenko (2008). "Recent advances in permafrost modelling". In: *Permafrost and Periglacial Processes* 19.2, pp. 137–156. URL: https://doi.org/10.1002/ppp.615.

Riseborough, D. (2002). "The mean annual temperature at the top of permafrost, the TTOP model, and the effect of unfrozen water". In: *Permafrost and Periglacial Processes* 13.2, pp. 137–143. URL: https://doi.org/10.1002/ppp.418.

Rödder, T. and C. Kneisel (2012). "Influence of snow cover and grain size on the ground thermal regime in the discontinuous permafrost zone, Swiss Alps". In: *Geomorphology* 175, pp. 176–189. URL: https://doi.org/10.1016/j.geomorph.2012.07.008.

Romanovsky, V., T. Osterkamp, and N. Duxbury (1997). "An evaluation of three numerical models used in simulations of the active layer and permafrost temperature regimes". In: *Cold Regions Science and Technology* 26.3, pp. 195–203. URL: https://doi.org/10.1016/S0165-232X(97)00016-5.

Royer, A., G. Picard, C. Vargel, A. Langlois, I. Gouttevin, and M. Dumont (2021). "Improved Simulation of Arctic Circumpolar Land Area Snow Properties and Soil Temperatures". In: *Frontiers in Earth Science* 9, p. 515. URL: https://doi.org/10.3389/feart.2021.685140.

Sæmundsson, Þ., C. Morino, J. K. Helgason, S. J. Conway, and H. G. Pétursson (2018). "The triggering factors of the Móafellshyrna debris slide in northern Iceland: Intense precipitation, earthquake activity and thawing of mountain permafrost". In: *Science of the total environment* 621, pp. 1163–1175. URL: https://doi.org/10.1016/j.scitotenv.2017.10.111.

Schirrmeister, L., G. Grosse, V. Kunitsky, D. Magens, H. Meyer, A. Dereviagin, T. Kuznetsova, A. Andreev, O. Babiy, F. Kienast, et al. (2008). "Periglacial landscape evolution and environmental changes of Arctic lowland areas for the last 60 000 years (western Laptev Sea coast, Cape Mamontov Klyk)". In: *Polar Research* 27.2, pp. 249–272. URL: https://doi.org/10.1111/j.1751-8369.2008.00067.x.

Smith, M. and D. Riseborough (1996). "Permafrost monitoring and detection of climate change". In: *Permafrost and periglacial processes* 7.4, pp. 301–309. URL: https://onlinelibrary.wiley.com/doi/10.1002/(SICI)1099-1530(199610)7:4%3C301::AID-PPP231%3E3.0.CO;2-R.

— (2002). "Climate and the limits of permafrost: a zonal analysis". In: *Permafrost and Periglacial Processes* 13.1, pp. 1–15. URL: https://doi.org/10.1002/ppp.410.

Stuenzi, S. M., J. Boike, W. Cable, U. Herzschuh, S. Kruse, L. A. Pestryakova, T. Schneider von Deimling, S. Westermann, E. S. Zakharov, and M. Langer (2021). "Variability of the surface energy balance in permafrost-underlain boreal forest". In: *Biogeosciences* 18.2, pp. 343–365. URL: https://doi.org/10.5194/bg-18-343-2021.

Tuvshinjargal, D. and L. Saranbaatar (2004). "Thermal balance features in the Terelj valley (Mongolia)". In: *proceedings of the 3rd International Workshop on Terrestrial Change in Mongolia*.

Vespremeanu-Stroe, A., P. Urdea, R. Popescu, and M. Vasile (2012). "Rock glacier activity in the Retezat mountains, Southern Carpathians, Romania". In: *Permafrost and Periglacial Processes* 23.2, pp. 127–137. URL: https://doi.org/10.1002/ppp.1736.

Vionnet, V., E. Brun, S. Morin, A. Boone, S. Faroux, P. Le Moigne, E. Martin, and J.-M. Willemet (2012). "The detailed snowpack scheme Crocus and its implementation in SURFEX v7. 2". In: *Geoscientific Model Development* 5.3, pp. 773–791. URL: https://doi.org/10.5194/gmd-5-773-2012.

Wahrhaftig, C. and A. Cox (1959). "Rock glaciers in the Alaska Range". In: *Geological Society of America Bulletin* 70.4, pp. 383–436. URL: https://doi.org/10.1130/0016-7606(1959)70[383:RGITAR]2.0.CO;2.

Westermann, S., T. Østby, K. Gisnås, T. Schuler, and B. Etzelmüller (2015). "A ground temperature map of the North Atlantic permafrost region based on remote sensing and reanalysis data". In: *The Cryosphere* 9.3, pp. 1303–1319. URL: https://doi.org/10.5194/tc-9-1303-2015.

Westermann, S., T. Ingeman-Nielsen, J. Scheer, K. Aalstad, J. Aga, N. Chaudhary, B. Etzelmüller, S. Filhol, A. Kääb, C. Renette, L. S. Schmidt, T. V. Schuler, R. B. Zweigel, L. Martin, S. Morard, M. Ben-Asher, M. Angelopoulos, J. Boike, B. Groenke, F. Miesner, J. Nitzbon, P. Overduin, S. M. Stuenzi, and M. Langer (2022). *The CryoGrid community model - a multi-physics toolbox for climate-driven simulations in the terrestrial cryosphere*. submitted to Geoscientific Model Development.

Westermann, S., M. Langer, J. Boike, M. Heikenfeld, M. Peter, B. Etzelmüller, and G. Krinner (2016). "Simulating the thermal regime and thaw processes of ice-rich permafrost ground with the land-surface model CryoGrid 3". In: *Geoscientific Model Development* 9.2, pp. 523–546. URL: https://doi.org/10.5194/gmd-9-523-2016.

Westermann, S., M. Peter, M. Langer, G. Schwamborn, L. Schirrmeister, B. Etzelmüller, and J. Boike (2017). "Transient modeling of the ground thermal conditions using satellite data in the Lena River delta, Siberia". In: *The Cryosphere* 11.3, pp. 1441–1463. URL: https://doi.org/10.5194/tc-11-1441-2017.

Westermann, S., T. Schuler, K. Gisnås, and B. Etzelmüller (2013). "Transient thermal modeling of permafrost conditions in Southern Norway". In: *The Cryosphere* 7.2, pp. 719–739. URL: https://doi.org/10.5194/tc-7-719-2013.

White, S. E. (1976). "Rock glaciers and block fields, review and new data". In: *Quaternary Research* 6.1, pp. 77–97. URL: https://doi.org/10.1016/0033-5894(76)90041-7.

Wicky, J. and C. Hauck (2020). "Air convection in the active layer of rock glaciers". In: *Frontiers in Earth Science*, p. 335. URL: https://doi.org/10.3389/feart.2020.00335.

Zhang, T., J. Heginbottom, R. G. Barry, and J. Brown (2000). "Further statistics on the distribution of permafrost and ground ice in the Northern Hemisphere". In: *Polar geography* 24.2, pp. 126–131. URL: https://doi.org/10.1080/10889370009377692.

Zhang, T. (2005). "Influence of the seasonal snow cover on the ground thermal regime: An overview". In: *Reviews of Geophysics* 43.4. URL: https://doi.org/10.1029/2004RG000157.

Zhang, Y., W. Chen, and J. Cihlar (2003). "A process-based model for quantifying the impact of climate change on permafrost thermal regimes". In: *Journal of Geophysical Research: Atmospheres* 108.D22. URL: https://doi.org/10.4095/219968.

Zweigel, R., S. Westermann, J. Nitzbon, M. Langer, J. Boike, B. Etzelmüller, and T. Vikhamar Schuler (2021). "Simulating snow redistribution and its effect on ground surface temperature at a high-Arctic site on Svalbard". In: *Journal of Geophysical Research: Earth Surface* 126.3, e2020JF005673. URL: https://doi.org/10.1029/2020JF005673.

Appendix

Renette, C., Westermann, S., Aalstad, K., Aga, J., Zweigel, R. B., Etzelmüller, B., Lilleøren, K. S., and Isaksen, K. (2022). *Simulating the effect of subsurface drainage on the thermal regime and ground ice in blocky terrain, Norway.* Manuscript to be submitted to: Earth Surface Dynamics or The Cryosphere.

Simulating the effect of subsurface drainage on the thermal regime and ground ice in blocky terrain, Norway

C. Renette[1], S. Westermann[1], K. Aalstad[1], J. Aga[1], R. B. Zweigel[1], B. Etzelmüller[1], K. S. Lilleøren[1], K. Isaksen[2]

[1]Department of Geosciences, University of Oslo, Oslo, Norway
[2]Norwegian Meteorological Institute, Oslo, Norway

Correspondence to: C. Renette (casr@student.geo.uio.no)

Abstract. Ground temperatures in coarse, blocky deposits such as mountain blockfields and rock glaciers have long been observed to be lower in comparison with other (sub)surface material. One of the reasons for this negative temperature anomaly is the lower soil moisture content in blocky terrain, which decreases the duration of the zero curtain in autumn. Here we used the CryoGrid community model to simulate the effect of drainage in blocky terrain on the ground thermal regime and ground ice at two Norwegian mountain permafrost sites. The model setup features a surface energy balance, heat conduction and advection, a bucket water scheme with a lateral drainage component and (an adaptation of) the CROCUS snow scheme. Idealized stratigraphies were used to investigate thermal anomalies under different amounts of snowfall.

Our results show markedly lower ground temperatures in the scenario with well drained, blocky deposits compared to other scenarios that feature a fine-grained sediment fraction. Here, a 'scenario' is referred to a as a setup of the model with a defined subsurface stratigraphy, that is either well drained or poorly drained. A sensitivity analysis to snowfall results in a negative thermal anomaly is up to 1.5 ◦C for scenarios with relatively high snowfall amounts and is similar between the two sites despite the climatic differences. We simulate stable permafrost conditions at the location of a rock glacier in northern Norway with a mean annual ground surface temperature (MAGST) of 2.0–2.5 ◦C under well drained, blocky deposits. Other scenarios under the same climate forcing feature positive ground temperatures. At the location of a blockfield in southern Norway, we show that stable permafrost can be present in these specific conditions even under an extremely thick snowpack. Finally, transient simulations at the rock glacier site showed a complete or partial lowering of the ground ice table since 1951 for all scenarios except the blocky, well drained stratigraphy.

The drainage effect that was simulated herein helps explain the occurrence of permafrost in coarse blocky terrain below the assumed elevational limit of permafrost. It is thus important to consider this effect in future permafrost distribution mapping. An accurate prediction of the evolution of the ground ice table in a future climate has implications for slope stability as well as water sources in arid environments.

1 Introduction

Permafrost is defined as ground that remains at or below 0 °C for two or more consecutive years (Van Everdingen, 1998) and is a common feature in mountain environments. The lowest active permafrost landforms in discontinuous mountain permafrost are frequently found in coarse, blocky terrain (Harris and Pedersen, 1998). In fact, landforms such as rock glaciers are found below the assumed elevational limit of permafrost (Lilleøren and Etzelmüller 2011).

The occurrence of a negative temperature anomaly in coarse, blocky deposits has long been recognized, e.g. in central eastern Norway by Liestøl (1965). Harris and Pedersen (1998) found a negative temperature anomaly of 4 to 7 ◦C in blocky terrain relative to adjacent mineral sediment in mountains in Canada and China. They summarized 4 hypotheses that explain these anomalies: (a) The Balch effect; (b) chimney effect; (c) evaporation of water and sublimation of ice in the summer and (d) continuous air exchange with the atmosphere when no continuous winter snow cover is present.

Juliussen and Humlum (2008) showed that block fields in the Norwegian mountains featured a negative temperature anomaly of 1.3 to 2.0 ◦C, which is mainly attributed to rocks protruding into and through the snow cover which leads to a higher effective thermal conductivity of the snow cover. Gruber and Hoezle (2008) presented a simple model for the conductive effect of blocks protruding through the snow cover which showed that the mean annual ground temperature is reduced as a result of a lower thermal conductivity of a blocky layer.

Additionally, a lower soil moisture content in permeable blocky debris decreases the duration of the zero-curtain in autumn since less latent heat is liberated compared to soil with higher soil moisture content (Juliussen and Humlum 2008). In spring, the opposite effect is observed where percolating meltwater refreezes at the bottom of the blocky surface layer and confines temperatures at the ice interface to ◦C (e.g. Juliussen and Humlum, 2008; Hanson and Hoelzle, 2004; Humlum, 1997).

Rock glaciers play an important role in the hydrological cycle, especially in arid regions like the Andes, where in some areas more water is stored in rock glaciers than in glaciers (Jones et al., 2019; Azócar and Brenning, 2010). The open debris structure can act as a trap for snow and a rock glacier can store a significant quantity of ice or liquid water. Rock glaciers studied in Argentina are an important water resource as they release water mainly during periods of drought (Croce and Milana 2002). Ground ice melt as a response to climate warming threatens this water source. Additionally, melting of ground ice can lead to slope instability (e.g. Gruber and Haeberli, 2007; Saemundsson et al. 2018; Nelson et al., 2001) and damage to infrastructure (e.g. Arenson et al., 2009).

In southern Norway, permafrost underlies large parts of areas above 1500 m.a.s.l.. The permafrost elevation limit decreases from above 1600 m.a.s.l. in the west to about 1100 m.a.s.l. in the eastern, more continental areas (Etzelmüller et al., 2003). In northern Norway, the limit is around 800–1000 m.a.s.l in the west and decreases towards the east. An inventory of Norwegian rock glaciers based on aerial imagery was published in 2011 (Lilleøren and Etzelmüller, 2011). They found no active permafrost landforms below 400 m.a.s.l.. The amount of rock glaciers in Norway is lower than in other mountain permafrost areas which they attributed to a lack of bedrock competence and debris availability as well as to the relative lack of steep topography above the permafrost limit. However, Lilleøren et al. (2022) described rock glaciers near sea level in the area of Hopsfjorden, northern Norway, that have a limited ice body and are in transition from active to relict. Additionally, Nesje et al. (2022) presented new evidence for active rock glaciers in southern Norway well below the assumed permafrost limit. Warming of Norwegian mountain permafrost (Etzelmüller et al., 2020) is expected to continue in the 21st century (Hipp et al., 2012), resulting in further degradation of these ice bodies and an upward shift of the lower permafrost limit. Hipp et al. (2012) also mentioned the need to address the effect of snow cover and surface material on how ground temperatures respond to climate forcing.

Land surface models that can represent permafrost are vital tools to investigate the sensitivity to climate change and complex environmental conditions. Since permafrost is a largely invisible phenomenon, numerical modelling based on process understanding is the best approach in the estimation of permafrost distribution (Harris et al. 2009). One-dimensional heat flow models have been used in studies to investigate the effect of climate change on permafrost (e.g. Etzelmüller et al., 2011; Hipp et al., 2012) or to model specific processes in mountain permafrost (e.g. Gruber and Hoezle, 2008). However, many such models do not include changes in volumetric water and ice contents (e.g. Etzelmüller et al., 2011; Hipp et al., 2012).

The CryoGrid community model (Westermann et al., 2022 subm.) is a simulation toolbox that can calculate ground temperatures and volumetric water as well as ice content in permafrost environments. It builds on the well-established CryoGrid 1, 2 and 3 (used in e.g. Gisnås et al., 2013; Westermann et al., 2013; Etzelmüller et al., 2020; Martin et al., 2019) and accommodates a broad range of applications. In the remainder of the study, the CryoGrid community model is referred to as “CryoGrid” for simplicity.

In this study we present simulations of ground temperatures and ice content for different idealized subsurface stratigraphies and drainage regimes using CryoGrid, applied at two Norwegian permafrost sites: a blockfield site in southern Norway and a rock glacier in northern Norway. The aim is to simulate one of the processes that is responsible for a negative

thermal anomaly in coarse, blocky deposits. Namely, the effect of lateral drainage which reduces soil moisture and ground ice contents in the active layer. We present how the ground ice mass balance in blocky terrain affects ground temperatures and the occurrence of permafrost.

2 Study sites

2.1 Juvvasshøe, southern Norway

Juvvasshøe (61◦40 N, 08◦22 E, 1894 m a.s.l.) is a site located in the southern Norwegian mountains, Jotunheiemen well above the tree line. A 129 m deep borehole was drilled in August 1999 and was drilled for the PACE (Permafrost and Climate in Europe) project (Harris et al., 2001). Continuous data streams from this PACE borehole are available with the exception of a gap between 21 December 2011 to 24 April 2014. The site is located in an extensive block field on a mountain plateau with sparse vegetation cover. The bedrock is located at 5 m depth, the first meter consists of large stones and boulders and the ground below mainly consists of cobbles (Isaksen et al., 2003). The bedrock consists of crystalline rocks (Farbrot et al., 2011), Between 2000 and 2004, Isaksen et al. (2007) measured a mean annual air temperature (MAAT) at 2 m height of -3.3 ◦C. The mean ground temperature (MGT) at 2.5 m below the surface during this period was -2.5 ◦C. The mean precipitation was estimated to be between 800 and 1000 mm yr^{-1}. The site is extremely exposed, resulting in a very low snow thickness due to wind distribution. Hipp et al. (2012) described a snow depth of less than 20 cm, while the snow thickness in surrounding, lower and less exposed sites, can be up to 140 cm. Isaksen et al. (2011) measured the difference between the MAGST and MAAT (surface offset) at exposed and less exposed sites in this area. At sites with a significant snow cover, the surface offset was up to more than 2 ◦C, while at exposed (including Juvvasshøe) sites this offset is generally below 1 ◦C. The permafrost thickness at the PACE borehole was estimated to be approximately 380 m (Isaksen et al., 2001), with the lower permafrost limited at ca. 1450 m.a.s.l. (Farbrot et al., 2011). A weak zero curtain effect suggests a low water content in the active layer (Isaksen et al., 2007). A warming of 0.2 ◦C per decade and 0.7 ◦C per decade in surface air temperature and ground surface temperature respectively occurred between 2000 and 2019 (Etzelmüller et al., 2020).

2.2 Ivarsfjorden rock glacier, northern Norway

Ivarsfjorden is a small fjord arm of the larger Hopsfjorden, located on the Nordkinn peninsula in the Troms and Finnmark county in northern Norway. The peninsula is dominated by flat mountain plateaus of exposed bedrock, *in situ* weathered material or coarse grained till (Lilleøoren et al., 2022), which feature steep slopes towards the sea. The coastal areas of Finnmark have a wet maritime climate. The mean annual precipitation ranges from 400 mm at the large plateau Finnmarksvidda to 1000 mm at parts of the coast (Saloranta, 2012). Lilleøren et al. (2022) describe a MAAT of 1.6 °C between 2010 and 2019 in the area of the rock glacier. The rock glacier of interest lies in a southwest-northeast trending valley that extends from the fjord and has an elevation extent of roughly 60 to 160 m.a.s.l.. The mountain at its east (443 m.a.s.l.) serves as the source area with rockfall debris and coarse talus slopes being common. The bedrock in Ivarsfjorden consists of sandstones and phyllites (NGU, 2008). Sandstones often generate coarse, bouldery material, which is favorable for the formation of rock glaciers (Haeberli et al. 2006). Finnmark was glaciated several times during the Pleistocene and the Nordkinn peninsula was deglaciated by approximately 14–15 cal kyr BP (Romundset et al., 2011). The rock glacier in Ivarsfjorden is northwest facing and has previously been interpreted as relict (Lilleøren and Etzelmüller, 2011), but a detailed analysis showed that a limited ice core might still be present (Lilleøren et al., 2022). A negative MAAT around 100 to 150 years ago is an indication that rock glaciers in this area were active at the end of the Little Ice Age (LIA). Refraction Seismic Tomography (RST) surveys indicate a porous air-filled stratigraphy such as blocky talus deposits. While observed MAGSTs between 2015

and 2020 are all positive, negative surface temperatures during summer have been observed by a thermal camera at the front slope of the rock glacier. This is likely an indication of the chimney effect and thus of connecting voids that support air flow.

3. Methods

3.1 The CryoGrid community model

CryoGrid is a simulation toolbox that can be applied to a wide range of applications thanks to its modular structure (Westermann et al., 2022 sumb.). Users can use existing classes (representations/parameterizations of different processes) or create their own that fit their study. All stratigraphy classes, which describe subsurface properties, feature volumetric mineral, organic, water and ice content.

In our model setup, the lower boundary condition is provided by a constant geothermal heat flux of 0.05 Wm^{-2}. The upper boundary results from solving the full surface energy balance, including both radiative and turbulent heat fluxes, which gives rise to a ground heat flux. In order to solve the surface energy balance, atmospheric forcing data is required (chapter 3.4). A scheme with heat conduction, following Fourier's law for heat conduction, and heat advection is used for heat transfer and temperature calculation in the subsurface.

For soil hydrology, a gravity driven bucket scheme is used. Rainfall is taken from the forcing data and added to the uppermost cell of the subsurface. The surface energy balance calculations determine how the soil moisture is affected by evaporation. Transpiration plays no part in this study as no organic matter is involved. Water that is in excess of the field capacity infiltrates downwards until either the infiltration limit or a frozen cell is reached. The water table forms if excess water is available and cells are saturated from the bottom upwards. If all grid cells are saturated, excess water is considered as surface runoff.

The freezing characteristic of water in the subsurface can be set to follow a freeze curve depending on the soil type, following Dall'Amico et al. (2011) and used by e.g. Westermann et al. (2013) or set as free water (water changes state at 0 ◦C) which would be more common in porous material.

Studies that used a previous model version (e.g. Westermann et al., 2013; Westermann et al., 2016; Langer et al., 2016) considered constant water/ice contents. This is a major limitation, as varying soil moisture contents strongly affect the ground thermal regime (e.g. Martin et al., 2019). We use a one-dimensional model setup and simulate lateral drainage out of the model domain by assuming a seepage face at atmospheric pressure. First, the elevation of the water table is calculated, after which a lateral water flux removes water in grid cells that are below this water table. The distance of the model realization to the seepage face can be varied where short distances result in a well-drained column and large distances result in a poorly or completely undrained column. In this study only two levels of drainage are used. A distance of 10^4 m is used for *undrained* cases, which emulates conditions at a mostly flat surface, and a distance of 1 m for *drained* cases, which emulates conditions at a slope. The seepage face drains over the entire column depth proportional to the water table. This is but a phenomenological way to simulate drainage, though the exact rate at which it happens is not of interest in this study.

The snow scheme used in this study was introduced by Zweigel et al. (2021) and is based on the CROCUS snow scheme (Vionnet et al. 2012). Snowfall is added on the surface with density and grain properties derived from atmospheric forcing data and then undergoes transient evolution of snow grains and density. The physical effect of wind drift on the snowpack is included in the module as well. Energy and mass transfer in the snowpack includes heat conduction, percolation of rainfall and percolation of meltwater. The incoming snow is adjusted by changing the so-called *snowfall factor, sf,* to phenomenologically represent redistribution of snow by wind and to account for potential biases in the snowfall forcing. Values above 1 represent net accumulation and values below 1 represent net ablation of snow compared to the baseline.

Ground and snow parameters are kept constant in all model runs. For the ground we used an albedo of 0.15, emissivity of 0.99, roughness length of 10^{-3} m and hydraulic conductivity of 10^{-5} m s^{-1}. For snow we used an emissivity of 0.99, roughness

length of 10^{-3} m, hydraulic conductivity of 10^{-4} m s^{-1} and a field capacity of 5%. The snow albedo undergoes a transient evolution in the snow scheme.

3.2 Validation, equilibrium and transient runs

Three types of CryoGrid runs are distinguished, each created to achieve a separate goal: *Validation runs, equilibrium runs* and *transient runs*. The *validation runs* are set up to compare modelled ground temperatures with field measurements at the two sites. At Juvvasshøe, measurements consist of borehole data from 2000 to 2019, allowing a comparison at different depths. At the rock glacier in Ivarsfjorden, comparison of model results with in situ measurements can only be done with the available ground surface temperature monitoring network (Lilleøren et al., 2022). The loggers within the rock glacier outline and with continuous measurements are used in this study. The *equilibrium runs* aim to investigate the effect of three idealized stratigraphies under a range of different amounts of snowfall on the ground thermal regime and ground ice table for a stable climate. Each stratigraphy is modelled with both *undrained* and *drained* drainage levels, resulting in six scenarios. The goal of the *transient runs* is to analyze how the ground temperatures and ground ice table may have developed from 1951 to 2019 under these different model setups. The ground stratigraphy, handling of snow, climatic forcing data and temperature initialization for the three run types are discussed below.

3.3 Ground stratigraphy and snow

The porosity of the ground and thickness of sediment are important factors in the capacity of the ground to hold water. In permafrost regions this thus has a large effect on ice formation and latent heat exchange in the subsurface (Westermann et al., 2013). Three idealized ground stratigraphies are set up in order to effectively investigate the effect of water drainage on the ground thermal regime and ground ice. These will be referred to as the *blocks only*, *blocks with sediment* and *sediment only* stratigraphies (table 1). In all stratigraphies, bedrock is assumed below 5 m depth. Also, the bedrock properties of 3% porosity and saturated conditions are kept constant throughout the study, which is in agreement with Hipp et al. (2012) and Farbrot et al. (2011).

The *blocks only* stratigraphy consists of a coarse block layer with 50% porosity of 5 m thickness on top of bedrock. The coarse blocks have a low field capacity of 1% (table 1). This idealized column can be realistic on an active rock glacier where finer sediments that result from weathering and erosion processes are transported towards the tongue of the rock glacier. Dahl (1966) observed that blockfields on a slope more often do not contain a fine sediment fraction between the blocks in northern Norway. The second stratigraphy, *blocks with sediment*, does include the finer sediment fraction that takes up 50% of the pore space between the course blocks, resulting in 25% porosity and a higher field capacity. Finally, the *sediment only* stratigraphy contains sand with the same porosity as *blocks only* in order to remain consistent. They are differentiated by a higher field capacity in the *sediment only* stratigraphy.

A changing snow cover is the main source of spatial variability in ground temperatures in Norwegian mountains (Gisnås et al., 2016). Following these studies, the sensitivity of the scenarios to various amounts of snowfall is analyzed. Between model runs, the snow module is completely unchanged and adjustments are only made in the snowfall factor to change the thickness of the winter snowpack.

Validation runs. For the validation runs with the borehole data in Juvvasshøe, different stratigraphies were manually tested until a good visual fit between modelled and measured ground temperatures at 2.0 m and 0.2 m depth was established. The *blockfield* stratigraphy from Westermann et al. (2013) is used as a starting point. Because of the observations of finer sediments between 1.5 m and 5 m (Isaksen et al. 2003), the mineral content is increased in order to find a better fit. As this site is extremely exposed to wind and snow is blown away, the snowfall factor is given values below 1 to represent the loss of snow. The stratigraphies used for the comparison at the rock glacier in Ivarsfjorden are the *blocks only, blocks with sediment* and *sediment only* in addition to the *blockfield* stratigraphy described in Westermann et al., (2013).

Equilibrium runs. The equilibrium runs simulate the equilibrium ground temperature for the three idealized stratigraphies in both the drained and undrained state. For each scenario CryoGrid is run with snowfall factors of 0.0, 0.25, 0.5, 0.75, 1.0 and 1.5. This approach allows for an estimation of the threshold amount of snow above which permafrost will no longer exist in each of the 6 scenarios. At values of sf > 2 at Juvvasshøe, snowfall is high enough so that the snowpack can survive the summer and thus a perennial snow patch and eventually a glacier will form.

Transient runs. The same three idealized stratigraphies are used to simulate the transient change in ground temperature and ground ice content. The susceptibility to thawing under a historically warming climate is investigated. For each of the sites, the best fitting snowfall factor from the validation runs is chosen for the transient analysis. Additionally, for both sites the scenarios are modelled with a second snowfall factor in order to analyze their sensitivity to different amounts of snow. This results in sf = 0.25 and sf = 0.5 for Juvvasshøe and sf = 1.0 and sf = 0.5 for Ivarsfjorden.

3.4 Climatic forcing data and downscaling routine

The meteorological data used to force CryoGrid were generated by applying TopoSCALE (Fiddes and Gruber, 2014), a topography-based downscaling routine, to ERA5 reanalysis data (Hersbach et al., 2020). ERA5 outputs are provided as interpolated point values on a regular latitude-longitude grid at a resolution of 0.25° at an hourly frequency both on the surface level, corresponding to Earth's surface as represented in the reanalysis, and at 37 pressure levels in the atmosphere from 1000 to 1 hPa. We considered data for the reanalysis period from 1950 to 2019. From the surface level we obtained: 2 meter air and dewpoint temperature, 10 meter meridional (northward) and zonal (eastward) wind velocity components, surface pressure, constant surface geopotential, incoming longwave radiation, incoming shortwave radiation, and total precipitation. From the pressure levels we acquired: air temperature, specific humidity, zonal and meridional wind velocity components, and dynamic geopotential. For Juvvasshøe at 1894 m a.s.l. we used all levels in the range 900 hPa to 700 hPa, while for the lower elevation Ivarsfjorden rock glacier at 60–160 m a.s.l. we used all levels between 900 hPa and 1000 hPa.

Terrain parameters derived from a digital elevation model (DEM) are needed to apply topography-based downscaling to the ERA5 data. We obtained these parameters by processing the mosaic version of the ArcticDEM (Porter et al., 2018) at the respective sites. Based on the ERA5 data and the DEM-derived parameters we performed a topography-based downscaling to 32 m using the TopoSCALE routine. TopoSCALE was initially developed by Fiddes and Gruber (2014) to downscale atmospheric reanalysis data in complex terrain, and it has since been used in several cryospheric applications including: estimating mountain permafrost distribution (Fiddes et al., 2015), snow data assimilation (Aalstad et al., 2018), hyper-resolution snow reanalysis (Fiddes et al., 2019), and downscaling regional climate model output (Fiddes et al., 2022).

By applying TopoSCALE all the necessary meteorological forcing fields required to run CryoGrid are retrieved: near surface air temperature, specific humidity, wind speed, incoming longwave radiation, incoming shortwave radiation, and total precipitation.

3.5 Model initialization

For the validation runs both at Juvvasshøe and Ivarsfjorden, the model is run for the entire period of available forcing data. At Juvvasshøe the initial ground temperature profile is taken from the borehole data. At Ivarsfjorden the model is initialized to near equilibrium conditions with the first 10 years of available forcing data. The comparison at Juvvasshøe is done for the years 2010 to 2019 and at Ivarsfjorden for the years 2016 to 2019. This leaves > 60 years for the model to reach equilibrium with the climate at the depths used for comparison and to be independent of initialization.

In order to reach steady state conditions, a 10 year period of roughly stable climate is chosen and iterated three times until a steady state temperature profile of the upper 5 meters is established. For Juvvasshøe, the period 2000–2010 is selected as the model can be initialized with real-time borehole data. For the Ivarsfjorden steady-state runs the period 1960–1970 is selected as this relatively stable period is more likely to be in permafrost conditions than later decades.

The goal of the transient runs is to investigate the warming and possible degradation of permafrost and ground ice melt from the second half of the 20th century until present for the different model scenarios and compare warming rates. An initialization with a stable ground ice table is required. This is achieved by iterating three times over the coldest 10 year period in the forcing data, from 1962 to 1971, until equilibrium conditions with a stable ice table are present. This is the closest available data to Little Ice Age conditions, when the rock glacier Ivarsfjorden is hypothesized to have been active (Lilleøren et al., 2022). This initialization period is then followed by the entire forcing dataset from 1951 to 2019. Transient runs for Juvvasshøe are set up by the same procedure. As in Ivarsfjorden, the coldest 10 year period in the available data was from 1962 to 1971.

4. Results

4.1 Comparison to borehole data for Juvvasshøe

Model results of validation runs at Juvvasshøe are compared with measured ground temperatures at the PACE borehole. The model is run for the entire period of available meteorological forcing data, from 1951 to 2019. Table 2 contains the best fitting stratigraphy and the corresponding snowfall factor is 0.25. Figure 2 shows the comparison of measured ground temperatures with modelled temperatures at 2 m and 0.2 m depth for the best fitting model configuration. No borehole data was available for the period 21 December 2011 to 24 April 2014. The model simulates temperatures at 2 m depth better than at 0.2 m depth as the effect of the extreme variability of the ground surface temperature is dampened. At 2 m depth, a slight cold bias exists for annual maxima close to 0 ◦C. The snowfall factor for this model setup is 0.25, meaning the model reduces incoming snow by 75% in order to represent windblown snow. This resulted in mean annual maximum snow depths of 34 cm. Despite the use of downscaled climatic forcing data, the model can reproduce measured ground temperatures.

4.2 Comparison to ground surface temperature data for Ivarsfjorden

At the rock glacier in Ivarsfjorden, no borehole exists. A comparison between modelled and measured temperature is therefore done with data from a ground surface temperature logger network. The three years of data at 11 locations on and near the rock glacier are presented together with seven model validation runs (Fig. 3). These consist of the three idealized stratigraphies plus the *blockfield* stratigraphy from (Westermann et al., 2013), each in a *drained* and *undrained* setup. The *blocks only, drained* simulation is excluded as MAGSTs are considerably lower than observed MAGSTs. As for the comparison to the borehole data at Juvvasshøe, the runs cover the entire period of available forcing data.

Measured MAGST fall between 1.1 ◦C and 4.1 ◦C. Modelled MAGST are in the range of 2.0 ◦C and 2.7 ◦C. The loggers are spread within the area of the rock glacier where small scale spatial variations in topography, snow accumulation, ground stratigraphy and vegetation play a role. The model results are realized at one point with the same forcing input and therefore show a tighter spread. For all years combined, the measured mean is 2.7 ◦C, opposed to a 2.2 ◦C modelled mean.

4.3 Equilibrium ground temperatures and sensitivity to snow

Annual maximum snow depths at a snowfall factor of 1.0 are between 1.5 m and 2.4 m at Juvvasshøe and between 0.4 m and 1.0 m at Ivarsfjorden. Figure 4 shows the equilibrium ground temperature at 2 m below the surface for the three stratigraphies at different snowfall factors at both sites. For each of the three stratigraphies there is the drained and the undrained model setup. At both sites there is a clear pattern of lower temperatures in the *blocks only, drained* scenario (solid blue line) compared to all 5 other scenarios. For snowfall factors of 0.75 and larger, the difference in ground temperature between *blocks only, drained* and the next coldest scenario is in the range of 1.2 ◦C and 1.4 ◦C at Juvvasshøe and in the range of 1.1 ◦C and 1.5 ◦C at Ivarsfjorden.

At Juvvasshøe, all 3 undrained scenarios feature positive ground temperatures at snowfall factors of 0.75 and above. Temperatures in the *blocks with sediment, drained* and *sediment only, drained* runs are positive from snowfall factor 1.0. The ground temperature in the *blocks only, drained* runs remains below -1.0 ◦C for all snowfall scenarios. A similar pattern is seen in Ivarsfjorden, though a snowfall factor of 1.5 results in positive temperatures for scenario *blocks only, drained*. Temperatures for the *blocks with sediment* stratigraphy are positive at sf = 0.5 and above. This was sf = 0.75 for the other scenarios with the exception of the *blocks only, drained* scenario. The increase from a snowfall factor of 0 to 0.25 leads to a slight cooling for the *drained* scenarios as opposed to a slight warming in the *undrained* scenarios. The large increase in albedo when going from no snow to a limited amount of snow might outweigh the insulating effect of snow, resulting in this cooling. For all other increases in snowfall factor, ground temperature at 2 m depth increases, a result of the insulating effect of snow on the underlying ground.

4.4 Transient response of ground temperatures and ice content

The ERA5 reanalysis dataset allows us to model the evolution of the ground thermal regime and ground ice content from 1950 to 2020. Figure 5 shows the ground ice content for the scenarios in Ivarsfjorden. In all simulations, a stable ice table has formed during the spin up period, which means that the change from 1950 is a result of the climate and not a remnant of the initialization. In the *blocks only, drained* scenario, the ice table does not lower by a significant amount. In all other simulations, the ice table lowers significantly. The saturated volumetric ice content of 0.5 is a result of the natural porosity in this stratigraphy (table 1). The perennial ice table in the upper 5 m of the *blocks with sediment* stratigraphy disappeared by 1985 and 1975 in the *undrained* and *drained* scenarios respectively. The saturated volumetric ice content is 0.25. Finally, the *sediment only* simulations show an intermediate effect where the ice table has dropped to approximately half of its initial height by 2020. So we can see three different responses of the ground ice table to atmospheric warming. A full degradation in both the *blocks with sediment* runs, partial degradation in the *blocks only, undrained* run and in both *sediment only* runs and finally, no degradation of ground ice in the *blocks only, drained* simulation. At Juvvasshøe, the ice table persists in all simulations. A slight lowering happens in the *blocks with sediment* scenarios.

The changes in ground temperature are determined by the ground ice table. Figure 6 shows the change in temperatures at 5 m depth for the *drained* scenarios, representing a full, partial and not lowering of the ice table at the Ivarsfjorden rock glacier for sf = 1.0. The depth of 5 m is chosen here minimize the seasonal variation and to emphasize the long-term warming. The *blocks only* simulation underwent an increase from -0.6 ◦C to -0.2 ◦C between the 1951–1960 and 2010–2019 means, not restrained by a take up of latent heat. As the 5 m temperature nears 0 ◦C, ice degradation will start and the warming will stall. The *sediment only* case experienced minimal warming in this period at 5 m depth, from -0.1 ◦C to 0.0 ◦C as the decrease in ice content was not completed. Finally, a complete degradation of the ice table in *blocks with sediment* run resulted in a warming to positive temperatures, from 0.0 ◦C to 0.6 ◦C. Ground temperatures at 5 m depth were lower for sf = 0.5 and resulted in less ice degradation. Warming between the 1951–1960 and 2010–2019 means were from -0.8 ◦C to -0.3 ◦C in the *blocks only* stratigraphy, from -0.5 ◦C to 0.0 ◦C in the *sediment only* stratigraphy and from -0.1 ◦C to 0.1 ◦C in the *blocks with sediment* stratigraphy.

At Juvvasshøe, for sf = 0.25, The *blocks only* simulation underwent an increase from -3.7 ◦C to -3.5 ◦C between the 1951–1960 and 2010–2019 means. Warming for the *blocks with sediment* run was from -3.8 ◦C to -3.4 ◦C and the *sediment only* run from -4.1 ◦C to -3.7 ◦C. For sf = 0.5, the change in temperature at 5 m depth in *drained* scenarios are: from -3.1 ◦C to -2.6 ◦C for the *blocks only* stratigraphy, from -2.5 ◦C to -1.9 ◦C for the *blocks with sediment* stratigraphy and from -2.9 ◦C to -2.4 ◦C for the *sediment only* stratigraphy. The warming rates are more sensitive to changes in the amount of snowfall than to differences in stratigraphy.

5. Discussion

5.1 Limitations of the model setup

In this study, CryoGrid has been applied to two Norwegian permafrost sites in order to show how the ground ice mass balance in blocky terrain affects ground temperatures and the occurrence of permafrost. The model can satisfactorily reproduce ground temperature measurements from the PACE borehole in Juvvasshøe. The observation of the rock glacier in Ivarsfjorden indicates that permafrost is or has been present in the recent past (Lilleøren et al., 2022). Modelled MAGSTs at the rock glacier fall within the 25th and 75th percentile of measured MAGSTs between July 2016 and July 2019. Modelled MAGSTs are below mean and median measurements, indicating a potential cold bias of the model of approximately 0.5 ◦C.

The model setup contains uncertainties and limitations regarding unknown stratigraphies and parameters at the sites. Exact values of albedo, hydraulic conductivity and roughness length are unknown. The freezing characteristic of free water is used in most of the model runs, meaning phase change occurs at 0 ◦C. Sensitivity tests with a freezing curve based on Dall'Amico et al. (2011) and used by e.g. Westermann et al. (2013; 2016) did not show a significant difference in ground temperatures and ground ice content.

At Juvvasshøe, the ground stratigraphy was described by Isaksen et al. (2003). At the rock glacier in Ivarsfjorden, no description of the subsurface stratigraphy is available. Lilleøren et al. (2022) described the site as a complex creeping system, meaning that the subsurface is likely not uniform across the entire rock glacier. As the goal of the study is to analyze the difference between idealized stratigraphies for a certain climate, of highest importance is the consistency of parameters between runs. Whether or not the stratigraphies in table 1 accurately represent the blockfield and rock glacier, we cannot say for certain as no data is available. However, we are confident that the key values of volumetric mineral content, field capacity and simulated drainage give rise to the response of the ground ice table and ground temperatures. in blocky terrain.

Since our model setup is one dimensional, lateral processes as a result of variable topography, snow cover or stratigraphy are not included. Water in the *drained* scenarios leaves the model domain, while in reality water could pond somewhere within the system. The drainage of water via a seepage face, as is in the model setup, is phenomenologically removing water and not capturing real three-dimensional processes. The convective processes, summarized by Harris and Pedersen (1998), that cause a negative thermal anomaly in blocky terrain are not part of the model setup. The same applies to the effect of rocks protruding into and through the snow cover as was described by Juliussen and Humlum (2008).

The ERA5 reanalysis data is a global product and thus has a coarse horizontal scale. Hence, the TopoSCALE downscaling routine (Fiddes and Gruber 2014) is applied. Aalstad et al., (2018) summarized key limitations of the scheme. First, no proper atmospheric boundary layer is included, meaning that wind, air temperature and humidity are not adjusted for the stability and roughness length at the surface layer. Next, no significant correction is applied to precipitation other than horizontal interpolation. Thus local effects such as orography are missed. Clouds that are not captured in the ERA5 reanalysis data, will also not be included in the downscaling product, affecting the radiation budget and precipitation. Despite uncertainties regarding forcing data, it can be with confidence stated that continental and regional scale climate characteristics are captured.

CROCUS is a sophisticated snow scheme (Vionnet et al. 2012; Zweigel et al., 2021) that includes a transient evolution of snow properties. An uncertainty in this study results from the use of a *snowfall factor* to manipulate incoming snowfall in order to represent snow redistribution by wind. Where adjusting a snowfall factor only changes the amount of incoming snow, snow redistribution by wind creates a more dynamic snowpack in reality (Liston & Sturm, 1998). In our model setup, the snowfall factor is static for each run. In reality, especially in mountain areas, large temporal variability of snowfall means that the best representing snowfall factor can change each season or year.

5.2 The effect of the ground ice mass balance on ground temperatures

Despite the mentioned limitations of the model setup, our results show a clear thermal anomaly. A surface cover of coarse blocks, represented by a high porosity and low field capacity, that is drained of water, results in equilibrium ground temperatures up to 1.4 ◦C and 1.5 ◦C lower than other stratigraphies at the location of the PACE borehole at Juvvasshøe and at the rock glacier in Ivarsfjorden respectively. Temperature differences between stratigraphies are comparable between the equilibrium runs and transient runs. In Ivarsfjorden at sf = 1.0, the *blocks only, drained* scenario features 2 m temperatures 2.0 ◦C lower than other drained scenarios. In the results from transient simulations, this difference at 5 m depth is up to 1.0 ◦C. The *blocks with sediment* and *sediment only* runs are losing ice and are not in equilibrium with the climate, meaning temperature differences are lower. At Juvvasshøe for sf = 0.25, equilibrium 2 m temperatures do not show large differences, though in the *sediment only* run, temperatures are 0.5 ◦C lower than the other stratigraphies. A similar offset is seen in the transient simulations.

By excluding convective processes (Harris and Pedersen, 1998) and the effect of blocks protruding through the snow cover (Juliussen and Humlum, 2008; Gruber Hoelzle, 2008), the effect of a ground ice mass balance is isolated and shown to be significant. The effect of drainage on the ground thermal regime has been successfully modelled in peat plateaus in Northern Norway by Martin et al. (2019), who found 2 ◦C lower temperatures in drained soil compared to undrained soil. Their results showed stable permafrost conditions at a MAGST of 2.0–2.5 ◦C in well drained conditions. While peat plateaus are a completely different landform, they also feature a varying soil moisture content which is of importance for the ground thermal regime (Martin et al. 2019) We find similar results where stable permafrost can exist at a MAGST of 2.0–2.5 ◦C in the *blocks only, drained* simulations in Ivarsfjorden.

A transient modelling study in southern Norway that used a previous version of CryoGrid (Westermann et al., 2013), used static water/ice contents. They included a zone of lower soil moisture in the upper meters for the blockfield stratigraphy, but as permafrost degrades and the active layer deepens, water would pool up at the bottom of the active layer which strongly affects the thermal regime.

Our findings are within the range of the 1.3–2.0 ◦C lower temperatures that Juliussen and Humlum (2008) found in blockfields compared to till and bedrock in Central-eastern Norway. Our equilibrium model results show that, at Juvvasshøe, stable permafrost occurs in *blocks only, drained* conditions even at a snow cover of >2 m thickness. While the absolute ground temperatures differ greatly between the two sites, warming rates between 1951–1960 and 2010–2019 were similar for the runs that are not affected by latent heat effects of melting ice. The same is true between the different stratigraphies, that all experienced warming between 0.4 ◦C and 0.6 ◦C. An exception is the *blocks only* stratigraphy at Juvvasshøe with sf = 0.25, which only warmed 0.2 ◦C.

Thermal anomalies can be translated into elevation differences by assuming a temperature lapse rate, which influences altitudinal permafrost limits. If we assume a temperature lapse rate of 0.5 ◦C per 100 m (Farbrot et al., 2011), the lower limit of permafrost can be found up to 300 m lower in drained, blocky deposits compared to undrained, blocky deposits. This is a first-order approximation and does not factor in changes in precipitation and other changes with elevation. Gisnås et al. (2017) modelled a lower discontinuous permafrost limit in Finnmark at around 400 m, which is approximately 300 m above the Ivarsfjorden rock glacier.

Our results in Fig. 5 suggest that the Ivarsfjorden rock glacier underwent different stages of ground ice degradation depending on the (sub)surface material. A significant ice table remains in the *blocks only* and *sediment only* runs, which does not completely fit the observations from Lilleøren et al. (2022) that only a limited ice core might still be present under certain conditions. It should be noted that this system is described as 'complex creeping' and that the stratigraphies used in this study are idealized for means of comparison and investigating the effect of drainage in blocky deposits. This system is a degrading lower permafrost limit landform and thus sensitive around 0 ◦C. The idealized 1D model setup does not cover potential ponding of water or other spatial processes. Following the potential cold bias of our model setup, 0.5 ◦C higher ground temperatures

will lead to more ice loss in the *blocky* and *sediment only* runs and be more in line with observations from Lilleøren et al. (2022).

5.3 Implications for other work

The simulations in this study show the importance of ground ice when assessing the thermal state and evolution of permafrost. In permafrost areas with ground ice around the freezing point, atmospheric warming can lead to significant ground ice loss while temperature increases are limited. This is for example shown in the *blocks with sediment* simulation at the Ivarsfjorden rock glacier. The melting of ground ice has shaped many landscapes, related to excess ice and thaw subsidence (e.g. Schirrmeister et al., 2008) and has been simulated by Westermann et al. (2016). An accurate representation of the ground ice mass balance will be important for the prediction of thaw subsidence and the formation of thermokarst landforms.

While the rock glacier in this study is not used as a water source, rock glaciers in more arid regions are important water resources (e.g. Croce and Milana 2002). The global ratio of rock glacier-glacier water volume equivalent (WVEQ) is increasing due to differential warming of rock glaciers as compared to glaciers (Jones et al., 2019). Therefore, accurately simulating the transient development of ground ice in rock glaciers will be of value in water resource management. Further, rock glaciers are sensitive to climate change (Haeberli et al., 2010) and recent studies have linked rock glacier acceleration with increasing air temperatures (e.g. Käab et al., 2007; Hartl et al., 2016; Eriksen et al., 2018). Permafrost degradation might start a positive feedback of increasing deformation rates related to infiltrating meltwater that accesses the rock glacier interior, resulting in stretching of the permafrost body.

Ground ice plays an important role in slope stability in mountain permafrost environments. Degradation of mountain permafrost and ground ice can lead to slope instability (e.g. Gruber and Haeberli, 2007, Saemundsson et al. 2018, Nelson et al., 2001). In addition to long-term warming, the occurrence of single warm summers can strongly affect the ground ice content in mountain permafrost areas. A study from the Swiss Alps (Hilbich et al., 2008) described how the extremely warm summer of 2003 caused a substantial loss of ground ice which did not recover in following years, while ground temperatures did. This shows the sensitivity of these mountain environments to warming and the vital role of ground ice.

We show that inclusion of lateral drainage in porous blocky deposits with a low field capacity results in a significant negative thermal anomaly. In order to understand relative effects that cause thermal anomalies in blocky terrain at the lower limit of permafrost, a more sophisticated model setup is required. Future studies should include convective processes and the effect of protruding blocks through snow in addition to the drainage effect. This will improve the understanding of complex thermal systems with blocky deposits.

Harris and Pedersen (1998) already stated that the thermal anomaly in blocky terrain complicated the identification of the lower mountain permafrost limit. A suggestion for future mapping studies is to include different drainage regimes in grid cells depending on topography and choose a field capacity based on surface material. This would aid in capturing these lower permafrost limit landforms in maps.

6. Conclusions

In this study we used CryoGrid, a heat conduction model, with a bucket scheme and a lateral subsurface drainage component to simulate the effect of blocky terrain on the ground thermal regime and ground ice at two Norwegian mountain permafrost sites (Juvvasshøe and Ivarsfjorden). We used idealized stratigraphies to investigate thermal anomalies under different amounts of snowfall. Here, a ‘scenario’ is referred to a as a setup of the model with a defined subsurface stratigraphy, that is either well drained or poorly drained. From this study, the following conclusions can be drawn:

- Significantly lower ground temperatures are found in well drained blocky deposits compared to other scenarios. The thermal anomaly is up to 1.5 ◦C and is largest in simulations with a large amount of snowfall. Despite not including convective heat transfer and the effect of blocks protruding through the winter snow cover, the effect of a ground ice mass balance is isolated and shown to be significant.
- We find that stable permafrost can exist in well drained, blocky deposits under a mean annual ground surface temperature (MAGST) of 2.0–2.5 ◦C at location of the rock glacier in Ivarsfjorden. At the location of the PACE borehole in Juvvasshøe, southern Norway, we simulate stable permafrost for all snowfall amounts in well drained, blocky terrain. All other simulations feature positive ground temperatures at higher snowfall amounts.
- Transient simulations at the Ivarsfjorden rock glacier showed a completely or partially degraded ground ice table since 1951 for all scenarios except the blocky, well drained stratigraphy. The melting of ground ice strongly affects the warming rates in the ground. Warming rates of 5 m ground temperature are similar between the sites when ground ice persists.

This study suggests that the drainage effect can also reproduce the lower altitudinal limit of permafrost in blocky terrain, which has been found in many studies. Additionally, an accurate representation of the evolution of the ground ice table in mountain permafrost environments is important in relation to water resource management in arid regions, slope stability and future permafrost distribution mapping. The inclusion of the drainage effect is another step towards a better model representation of the complex thermal systems in permafrost environments.

Author contribution. CR performed the simulations, retrieved forcing data, wrote the draft manuscript and created all figures. SW helped design the study, developed the model and provided ideas throughout the entire study. KA developed code for retrieving and downscaling forcing data, assisted with this process and wrote text regarding the forcing data. KL and KI provided field measurements. RBZ and JA developed parts of the model. All authors contributed with text and suggestions.

Competing interests. The authors declare that they have no conflict of interest.

Code and data availability. The CryoGrid source code and model setup files are available under doi:10.18710/DSJ0BV. Measurement data used for evaluation of the model results available via k.s.lilleoren@geo.uio.no (Ivarsfjorden) and ketili@met.no (Juvvasshøe).

References

Aalstad, K., S. Westermann, T. V. Schuler, J. Boike, and L. Bertino (2018). “Ensemblebased assimilation of fractional snow-covered area satellite retrievals to estimate the snow distribution at Arctic sites”. In: The Cryosphere 12.1, pp. 247–270. url: https://doi. org/10.5194/tc-12-247-2018.

Arenson, L. U., Phillips, M., & Springman, S. M. (2009). Geotechnical considerations and technical solutions for infrastructure in mountain permafrost. In New permafrost and glacier research (pp. 3-50). Nova Science Publishers.

Azócar, G. and A. Brenning (2010). “Hydrological and geomorphological significance of rock glaciers in the dry Andes, Chile (27–33 S)”. In: Permafrost and Periglacial Processes 21.1, pp. 42–53. url: https://doi.org/10.1002/ppp.669.

Croce, F. A. and J. P. Milana (2002). “Internal structure and behaviour of a rock glacier in the arid Andes of Argentina”. In: Permafrost and Periglacial Processes 13.4, pp. 289–299. url: https://doi.org/10.1002/ppp.431.

Dall’Amico, M., S. Endrizzi, S. Gruber, and R. Rigon (2011). “A robust and energy-conserving model of freezing variably-saturated soil”. In: The Cryosphere 5.2, pp. 469–484. url: https://doi.org/10.5194/tc-5-469-2011.

Dahl, R. (1966). “Block fields, weathering pits and tor-like forms in the Narvik Mountains, Nordland, Norway”. In: Geografiska Annaler: Series A, Physical Geography 48.2, pp. 55– 85.

Eriksen, H., L. Rouyet, T. Lauknes, I. Berthling, K. Isaksen, H. Hindberg, Y. Larsen, and G. Corner (2018). “Recent acceleration of a rock glacier complex, Adjet, Norway, documented by 62 years of remote sensing observations”. In: Geophysical Research Letters 45.16, pp. 8314–8323. url: https://doi.o/rg/10.1029/2018GL077605.

Etzelmüller, B., I. Berthling, and J. L. Sollid (2003). “Aspects and concepts on the geomorphological significance of Holocene permafrost in southern Norway”. In: Geomorphology 52.1-2, pp. 87–104. url: https://doi.org/10.1016/S0169-555X(02)00250-7.

Etzelmüller, B., M. Guglielmin, C. Hauck, C. Hilbich, M. Hoelzle, K. Isaksen, J. Noetzli, M. Oliva, and M. Ramos (2020). “Twenty years of European mountain permafrost dynamics—the PACE legacy”. In: Environmental Research Letters 15.10, p. 104070. url: https://doi.org/10.1088/1748-9326/abae9d.

Farbrot, H., T. F. Hipp, B. Etzelmüller, K. Isaksen, R. S. Ødegård, T. V. Schuler, and O. Humlum (2011). “Air and ground temperature variations observed along elevation and continentality gradients in Southern Norway”. In: Permafrost and Periglacial Processes 22.4, pp. 343–360. url: https://doi.org/10.1002/ppp.733.

Fiddes, J., S. Endrizzi, and S. Gruber (2015). “Large-area land surface simulations in heterogeneous terrain driven by global data sets: application to mountain permafrost”. In: The Cryosphere 9.1, pp. 411–426. url: https://doi.org/10.5194/tc-9-411-2015.

Fiddes, J. and S. Gruber (2014). “TopoSCALE v. 1.0: downscaling gridded climate data in complex terrain”. In: Geoscientific Model Development 7.1, pp. 387–405. url: https://doi.org/10.5194/gmd-7-387-2014.

Fiddes, J., K. Aalstad, and M. Lehning (2022). “TopoCLIM: rapid topography-based downscaling of regional climate model output in complex terrain v1. 1”. In: Geoscientific Model Development 15.4, pp. 1753–1768. url: https://doi.org/10.5194/gmd-15-1753-2022.

Fiddes, J., K. Aalstad, and S. Westermann (2019). “Hyper-resolution ensemble-based snow reanalysis in mountain regions using clustering”. In: Hydrology and Earth System Sciences 23.11, pp. 4717–4736. url: https://doi.org/10.5194/hess-23-4717-2019.

Gisnås, K., B. Etzelmüller, C. Lussana, J. Hjort, A. B. K. Sannel, K. Isaksen, S. Westermann, P. Kuhry, H. H. Christiansen, A. Frampton, et al. (2017). “Permafrost map for Norway, Sweden and Finland”. In: Permafrost and periglacial processes 28.2, pp. 359–378. url: https://doi.org/10.1002/ppp.1922.

Gisnås, K., S. Westermann, T. V. Schuler, K. Melvold, and B. Etzelmüller (2016). “Smallscale variation of snow in a regional permafrost model”. In: The Cryosphere 10.3, pp. 1201–1215. url: https://doi.org/10.5194/tc-10-1201-2016.

Gruber, S. and W. Haeberli (2007). “Permafrost in steep bedrock slopes and its temperature related destabilization following climate change”. In: Journal of Geophysical Research:Earth Surface 112.F2. url: https://doi.org/10.1029/2006JF000547.

Gruber, S. and M. Hoelze (2008). “The cooling effect of coarse blocks revisited: a modeling study of a purely conductive mechanism”. In: Zurich Open Repository and Archive.

Haeberli, W., J. Noetzli, L. Arenson, R. Delaloye, I. Gärtner-Roer, S. Gruber, K. Isaksen, C. Kneisel, M. Krautblatter, and M. Phillips (2010). “Mountain permafrost: development and challenges of a young research field”. In: Journal of Glaciology 56.200, pp. 1043–1058. url: https://doi.org/10.3189/002214311796406121.

Hanson, S. and M. Hoelzle (2004). “The thermal regime of the active layer at the Murtèl rock glacier based on data from 2002”. In: Permafrost and Periglacial Processes 15.3, pp. 273–282. url: https://doi.org/10.1002/ppp.499.

Harris, C., W. Haeberli, D. Vonder Mühll, and L. King (2001). “Permafrost monitoring in the high mountains of Europe: the PACE project in its global context”. In: Permafrost and periglacial processes 12.1, pp. 3–11. url: https://doi.org/10.1002/ppp.377.

Harris, S. A. and D. E. Pedersen (1998). “Thermal regimes beneath coarse blocky materials”. In: Permafrost and periglacial processes 9.2, pp. 107–120. url: https://doi.org/10.1002/(SICI)1099-1530(199804/06)9:2%3C107::AID-PPP277%3E3.0.CO;2-G.

Hartl, L., A. Fischer, M. Stocker-waldhuber, and J. Abermann (2016). “Recent speed-up of an alpine rock glacier: an updated chronology of the kinematics of outer hochebenkar rock glacier based on geodetic measurements”. In: Geografiska Annaler: Series A, Physical Geography 98.2, pp. 129–141. url: https://doi.org/10.1111/geoa.12127.

Hersbach, H., B. Bell, P. Berrisford, S. Hirahara, A. Horányi, J. Muñoz-Sabater, J. Nicolas, C. Peubey, R. Radu, D. Schepers, et al. (2020). “The ERA5 global reanalysis”. In: Quarterly Journal of the Royal Meteorological Society 146.730, pp. 1999–2049. url: https://doi. org/10.1002/qj.3803.

Hilbich, C., C. Hauck, M. Hoelzle, M. Scherler, L. Schudel, I. Völksch, D. Vonder Mühll, and R. Mäusbacher (2008). "Monitoring mountain permafrost evolution using electrical resistivity tomography: A 7-year study of seasonal, annual, and long-term variations at Schilthorn, Swiss Alps". In: Journal of Geophysical Research: Earth Surface 113.F1. url: https://doi.org/10.1029/2007JF000799.
Hipp, T., B. Etzelmüller, H. Farbrot, T. Schuler, and S. Westermann (2012). "Modelling borehole temperatures in Southern Norway–insights into permafrost dynamics during the 20th and 21st century". In: The Cryosphere 6.3, pp. 553–571. url: https://doi.org/10.5194/tc-6-553-2012.
Humlum, O. (1997). "Active layer thermal regime at three rock glaciers in Greenland". In: Permafrost and Periglacial Processes 8.4, pp. 383–408. url: https://doi.org/10.1002/(SICI)1099-1530(199710/12)8:4%3C383::AID-PPP265%3E3.0.CO;2-V.
Isaksen, K., E. Heggem, S. Bakkehøi, R. Ødegård, T. Eiken, B. Etzelmüller, and J. Sollid (2003). "Mountain permafrost and energy balance on Juvvasshøe, southern Norway". In: 8th International Conference on Permafrost, Zurich, Switzerland, ISI: 000185049300083, pp. 467–472.
Isaksen, K., P. Holmlund, J. L. Sollid, and C. Harris (2001). "Three deep alpine-permafrost boreholes in Svalbard and Scandinavia". In: Permafrost and Periglacial Processes 12.1, pp. 13–25. url: https://doi.org/10.1002/ppp.380.
Isaksen, K., J. L. Sollid, P. Holmlund, and C. Harris (2007). "Recent warming of mountain permafrost in Svalbard and Scandinavia". In: Journal of Geophysical Research: Earth Surface 112.F2. url: https://doi.org/10.1029/2006JF000522.
Jones, D. B., S. Harrison, K. Anderson, and W. B. Whalley (2019). "Rock glaciers and mountain hydrology: A review". In: Earth-Science Reviews 193, pp. 66–90. url: https://doi.org/10.1016/j.earscirev.2019.04.001.
Juliussen, H. and O. Humlum (2008). "Thermal regime of openwork block fields on the mountains Elgåhogna and Sølen, central-eastern Norway". In: Permafrost and Periglacial Processes 19.1, pp. 1–18. url: https://doi.org/10.1002/ppp.607.
Kääb, A., R. Frauenfelder, and I. Roer (2007). "On the response of rockglacier creep to surface temperature increase". In: Global and Planetary Change 56.1-2, pp. 172–187. url: https://doi.org/10.1016/j.gloplacha.2006.07.005.
Langer, M., S. Westermann, J. Boike, G. Kirillin, G. Grosse, S. Peng, and G. Krinner (2016). "Rapid degradation of permafrost underneath waterbodies in tundra landscapes—toward a representation of thermokarst in land surface models". In: Journal of Geophysical Research: Earth Surface 121.12, pp. 2446–2470. url: https://doi.org/10.1002/2016JF003956.
Lilleøren, K. S. and B. Etzelmüller (2011). "A regional inventory of rock glaciers and icecored moraines in Norway". In: Geografiska Annaler: Series A, Physical Geography 93.3, pp. 175–191. url: https://doi.org/10.1111/j.1468-0459.2011.00430.x.
Lilleøren, K. S., B. Etzelmüller, L. Rouyet, T. Eiken, and C. Hilbich (2022). "Transitional rock glaciers at sea-level in Northern Norway". In: Earth Surface Dynamics Discussions, pp. 1–29. url: https://doi.org/10.5194/esurf-2022-6.
Liston, G. E. and M. Sturm (1998). "A snow-transport model for complex terrain". In: Journal of Glaciology 44.148, pp. 498–516. url: https://doi.org/10.3189/S0022143000002021. Martin, L. C. P., J. Nitzbon, K. S. Aas, B. Etzelmüller, H. Kristiansen, and S. Westermann (2019). "Stability conditions of peat plateaus and palsas in northern Norway". In: Journal of Geophysical Research: Earth Surface 124.3, pp. 705–719. url: https://doi.org/10.1029/2018JF004945.
Mittaz, C., M. Hoelzle, and W. Haeberli (2000). "First results and interpretation of energyflux measurements over Alpine permafrost". In: Annals of Glaciology 31, pp. 275–280. url: https://doi.org/10.3189/172756400781820363.
Nesje, A., Matthews, J. A., Linge, H., Bredal, M., Wilson, P., & Winkler, S. (2021). New evidence for active talus-foot rock glaciers at Øyberget, southern Norway, and their development during the Holocene. The Holocene, 31(11-12), 1786-1796.
Porter, C., P. Morin, I. Howat, M. Noh, B. Bates, K. Peterman, S. Keesey, M. Schlenk, J. Gardiner, K. Tomko, et al. (2018). ArcticDEM, Harvard Dataverse [data set], V1. url: https://doi.org/10.7910/DVN/OHHUKH.
Romundset, A., Bondevik, S., and Bennike, O.: Postglacial uplift and relative sea level changes in Finnmark, northern Norway, Quat. Sci.Rev., 30, 2398-2421, https://doi.org/10.1016/j.quascirev.2011.06.007, 2011
Saloranta, T. M. (2012). Simulating snow maps for Norway: description and statistical evaluation of the seNorge snow model. The Cryosphere, 6(6), 1323-1337.
Sæmundsson, Þ., C. Morino, J. K. Helgason, S. J. Conway, and H. G. Pétursson (2018). "The triggering factors of the Móafellshyrna debris slide in northern Iceland: Intense precipitation, earthquake activity and thawing of mountain permafrost". In: Science of the total environment 621, pp. 1163–1175. url: https://doi.org/10.1016/j.scitotenv.2017.10.111.
Schirrmeister, L., G. Grosse, V. Kunitsky, D. Magens, H. Meyer, A. Dereviagin, T. Kuznetsova, A. Andreev, O. Babiy, F. Kienast, et al. (2008). "Periglacial landscape evolution and environmental changes of Arctic lowland areas for the last 60 000 years (western Laptev Sea coast, Cape Mamontov Klyk)". In: Polar Research 27.2, pp. 249–272. url: https://doi.org/10.1111/j.1751-8369.2008.00067.x.
Vionnet, V., E. Brun, S. Morin, A. Boone, S. Faroux, P. Le Moigne, E. Martin, and J.-M. Willemet (2012). "The detailed snowpack scheme Crocus and its implementation in SURFEX v7. 2". In: Geoscientific Model Development 5.3, pp. 773–791. url: https://doi. org/10.5194/gmd-5-773-2012.
Westermann, S., T. Ingeman-Nielsen, J. Scheer, K. Aalstad, J. Aga, N. Chaudhary, B. Etzelmüller, S. Filhol, A. Kääb, C. Renette, L. S. Schmidt, T. V. Schuler, R. B. Zweigel, L. Martin, S. Morard, M. Ben-Asher, M. Angelopoulos, J. Boike, B. Groenke, F. Miesner, J. Nitzbon, P. Overduin, S. M. Stuenzi, and M. Langer (2022). The CryoGrid community model - a multi-physics toolbox for climate-driven simulations in the terrestrial cryosphere. submitted to Geoscientific Model Development.
Westermann, S., M. Langer, J. Boike, M. Heikenfeld, M. Peter, B. Etzelmüller, and G. Krinner (2016). "Simulating the thermal regime and thaw processes of ice-rich permafrost ground with the land-surface model CryoGrid 3". In: Geoscientific Model Development 9.2, pp. 523–546. url: https://doi.org/10.5194/gmd-9-523-2016.

Westermann, S., T. Schuler, K. Gisnås, and B. Etzelmüller (2013). “Transient thermal modeling of permafrost conditions in Southern Norway”. In: The Cryosphere 7.2, pp. 719–739. url: https://doi.org/10.5194/tc-7-719-2013.
Zweigel, R., S. Westermann, J. Nitzbon, M. Langer, J. Boike, B. Etzelmüller, and T. Vikhamar Schuler (2021). “Simulating snow redistribution and its effect on ground surface temperature at a high-Arctic site on Svalbard”. In: Journal of Geophysical Research: Earth Surface 126.3, e2020JF005673. url: https://doi.org/10.1029/2020JF005673.

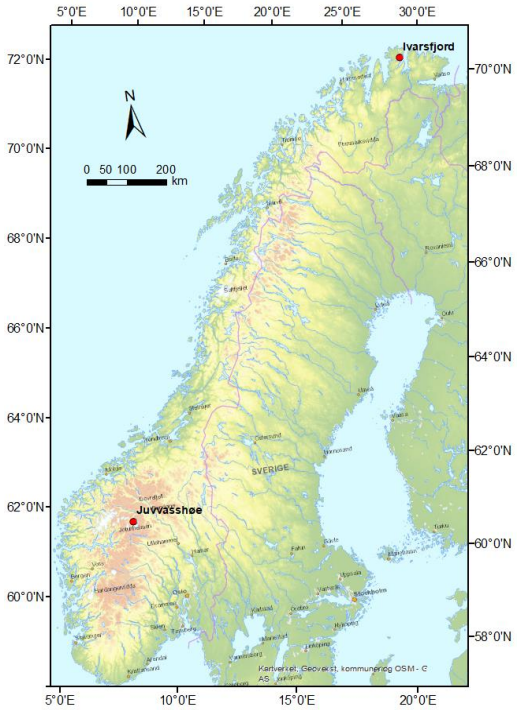

Figure 1: Location of the blockfield site at Juvvasshøe (1894 m.a.s.l.) and rock glacier site at Ivarsfjorden (60–160 m.a.s.l.) in Norway. All topographical background maps are the owned by the Norwegian Mapping Authority, Karteverket.

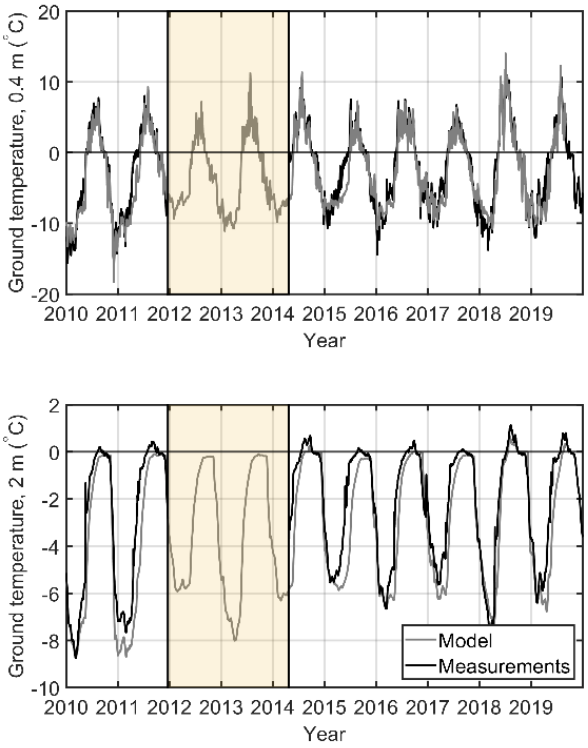

Figure 2: Modelled and measured ground temperature at the PACE borehole in Juvvasshøe at 0.4 m (upper) and 2.0 m (lower) depth. The shaded area indicates the period where no borehole data is available.

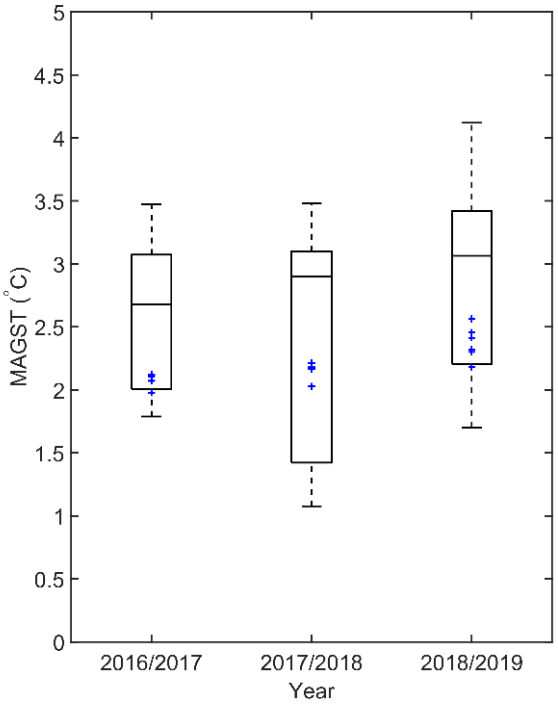

Figure 3: Modelled and measured MAGST in Ivarsfjorden during three years, from 13 July 2016 to 12 July 2019. The bars indicate the 25th and 75th percentile of measured MAGST and the whiskers represent the maximum and minimum temperatures. The blue indicators show modelled MAGST during the same period for a selected range of ground stratigraphies at sf = 1.

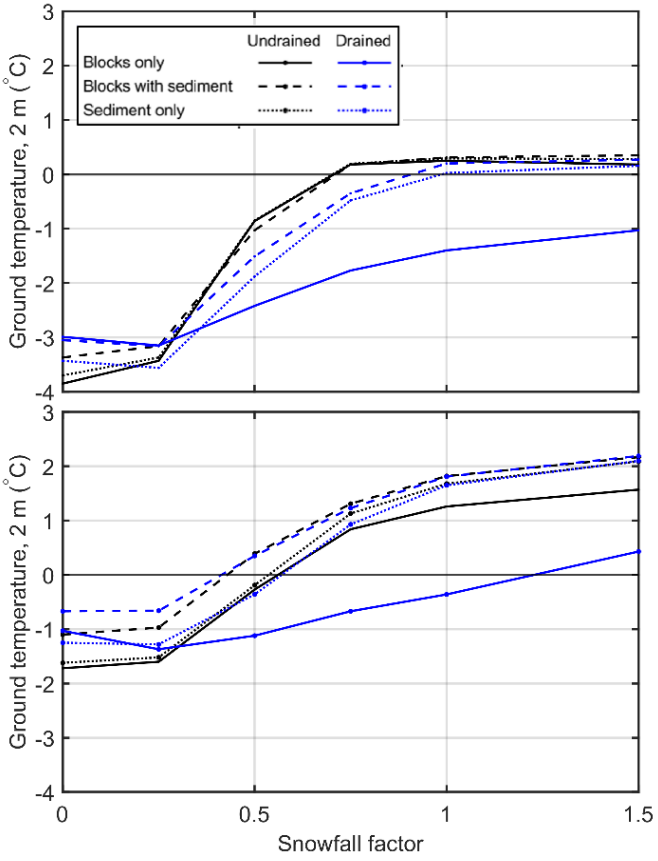

Figure 4: Equilibrium ground temperature at 2 m depth for three idealized stratigraphies (table 1).

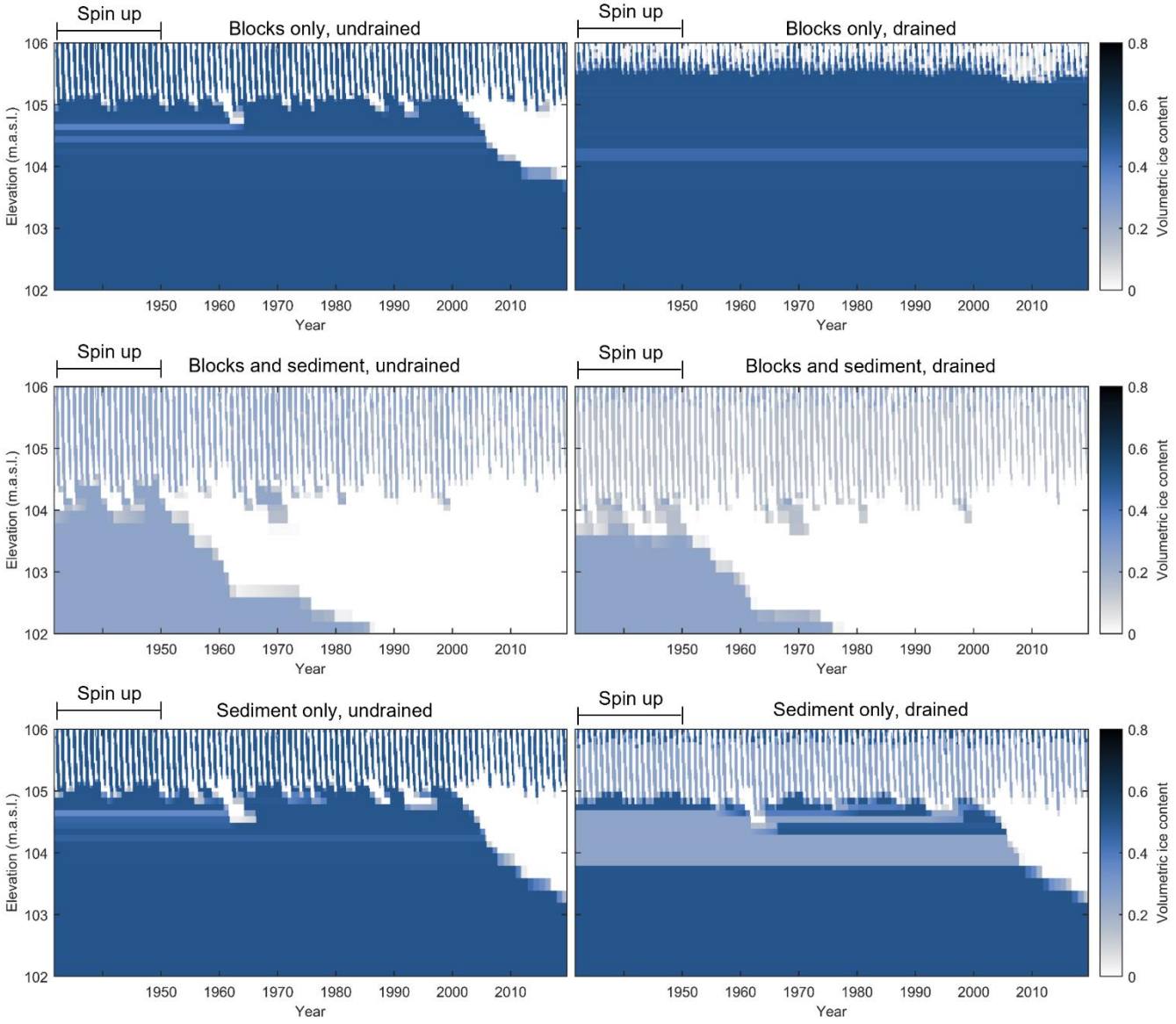

Figure 5: Modelled volumetric ground ice content at Ivarsfjorden for the idealized stratigraphies in *undrained* and *drained* conditions. The sf = 1.0 in all simulations.

625

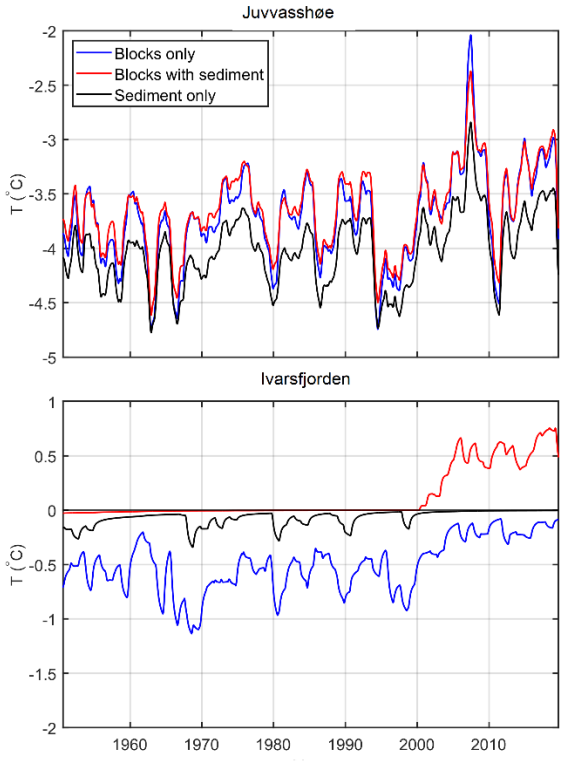

Figure 6: Ground temperature at 5 m depth for the idealized stratigraphies under *drained* conditions. sf = 1.0 for Ivarsfjorden and sf = 0.25 for Juvvasshøe.

Table 1: Idealized sediment stratigraphies used in validation, steady state and transient runs.

Depth (m)	Mineral	Organic	Porosity	Field capacity	Soil freezing
Blocks only					
0–5	0.5	0.0	0.5	0.01	Free water
Blocks with sediment					
0–5	0.75	0.0	0.25	0.15	Free water
Sediment only					
0–5	0.5	0.0	0.5	0.25	Sand

630

Table 2. Stratigraphy that results in the model that best fits measured ground temperatures at Juvvasshøe.

Depth (m)	Mineral	Organic	Porosity	Field capacity	Soil freezing
0–1	0.8	0.0	0.2	0.1	Free water
1–5	0.8	0.0	0.2	0.1	Free water